LIGHT HYDROCARBONS IN MARINE SEDIMENTS

A Dissertation

by

BERNIE BOYD BERNARD

Submitted to the Graduate College of
Texas A&M University
in partial fulfillment of the requirement for the degree of

DOCTOR OF PHILOSOPHY

May 1978

Major Subject: Oceanography

LIGHT HYDROCARBONS IN MARINE SEDIMENTS

A Dissertation

by

BERNIE BOYD BERNARD

Approved as to style and content by:

William M. Sackett
(Chairman of Committee)

Walter D. Hamlin, Jr.
(Head of Department)

Lela M. Jeffrey
(Member)

David R. Schink
(Member)

(Member)

(Member)

May 1978

ABSTRACT

Light Hydrocarbons in Marine Sediments (May 1978)

Bernie Boyd Bernard, B.S., Abilene Christian University

Chairman of Advisory Committee: Dr. William M. Sackett

Concentrations of the C_1-C_3 hydrocarbons and stable carbon isotope compositions of methane in recent sediments and seep gases of the Texas-Louisiana shelf-slope region were determined. These gases have been produced by both microbial and thermocatalytic processes. Microbially-produced gases consist almost exclusively of methane, having $C_1/(C_2+C_3)$ hydrocarbon ratios greater than 1000 and $\delta^{13}C_{PDB}$ values of methane more negative than $-60°/_{oo}$. Petroleum-related hydrocarbon gases generally have $C_1/(C_2+C_3)$ ratios smaller than 50 and isotopic ratios more positive than $-50°/_{oo}$. A geochemical model based on these two parameters is used to show that natural gas compositions can be altered due to mixing of gases from the two sources as well as by microbial action and migration through sediments.

Light hydrocarbons in the upper few meters of Gulf of Mexico sediments are almost entirely of microbial origin. In the Mississippi Delta region, interstitial sulfate is quickly depleted and extensive production of methane is observed within one or two meters of the seawater-sediment interface. This "horizon" of high methane concentration occurs progressively deeper in sediments in an offshore direction.

Bacterial production of methane is not restricted to the sulfate-free zone, however, but apparently also occurs within "microenvironments" in sediments having near-seawater interstitial sulfate concentrations. Two-meter long vertical methane profiles in near-shore Texas Shelf sediments exhibit maxima ranging from 100 to 500 µl/liter in the top 40 centimeters. Maxima in near-shore sediments are related to the large microbial population near the sediment surface. Disappearance of the maxima in the slope region is presumably due to inhibited microbial activity at lower temperatures, increased pressures, and decreased amounts of labile organic carbon.

Vertical methane concentration profiles in sediments fit a simple kinetic model. Relative rates of diffusion, production, and consumption of methane determine solutions to a steady-state diagenetic equation. These solutions express methane concentrations as a function of sediment depth in the sulfate-reducing zone. Fits of these solutions to observed methane profiles and changes in isotopic ratios of methane indicate that methane is consumed in the sulfate-reducing region at a first order rate with concentration. In the Mississippi Delta region, concentration profiles are controlled by methane consumption and upward diffusion from the relatively shallow methane horizon. On the outer shelf and slope, concentration profiles are controlled mainly by production and consumption. The effects of production and consumption balance to form "constant" concentrations of methane with depth. Rates of methane production and consumption, as well as minimum depths of the methane horizon and fluxes from sediment, vary with water depth and can be estimated from best-fit solutions to the

kinetic model.

Interstitial concentrations of ethene, ethane, propene, and propane are relatively constant with depth in the upper two meters of shelf, slope, and abyssal sediments, decreasing progressively from 160, 100, 110, and 60 nl/liter in near-shore sediments, to fairly uniform levels of 80, 25, 30, and 25 nl/liter downslope, respectively. As sulfate disappears, ethane and propane concentrations increase more than ten-fold but propane subsequently disappears. These patterns suggest that ethane and propane are also microbially produced to some extent in recent sediments and propane is subsequently consumed.

ACKNOWLEDGEMENTS

I sincerely thank Dr. William M. Sackett for the education I acquired from him as the chiarman of my advisory committee. He encouraged independent thinking and research and was always generous with his time. I feel fortunate to have developed under his direction.

I must also thank the other members of my committee: D. R. Schink, L. M. Jeffrey, R. R. Berg and C. S. Giam for their contributions to this work.

I thank Jim Brooks for all his help in sampling on cruises and his advice during analysis and writing. Part of this work is an extension of the study of light hydrocarbons in the Gulf of Mexico that he initiated.

I appreciate discussions with John Trefry, Norman Guinasso, Moses Chung, Bernard Boudreau, Denis Wiesenburg, and Ted Sauer, analytical help from Hussein Abd EL-Reheim and Keith Klatt, and typing of the first draft of this dissertation by Ginger Franks.

A special thanks goes to my wife Laura, who gave up her freedom for countless nights at home with the children and for the monotony of being the spouse of a graduate student.

This work was supported in part by National Science Foundation Grant No. OCE75-13299 and Bureau of Land Management Contract No. AA550-CT7-11.

TABLE OF CONTENTS

LIST OF TABLES

LIST OF FIGURES

LIST OF FIGURES (continued)

CHAPTER I

INTRODUCTION AND REVIEW

Objectives

Most of the energy produced by man in the world today is generated from the oxidation of naturally occurring carbonaceous material. An understanding of the diagenetic changes of organic matter from the time of deposition to the accumulation of petroleum is essential for future discovery and exploitation of the remaining reserves of these fuels. However, some of the oldest and most basic questions concerning the generation and accumulation of hydrocarbons have not been adequately answered. These questions include:

1. What is the source organic material for hydrocarbon generation?
2. What is the sediment depth limit of bacterial activity?
3. What is the nature of the transition from biologically to thermocatalytically produced hydrocarbons?
4. Is temperature or time more important in the generation of hydrocarbons and to the "liquid window" concept? What is minimum temperature for initiation of significant thermal cracking?
5. What is the role of catalysis by clay minerals in the maturation of organic matter?
6. What are the isotopic limits of methane produced by thermocatalysis and by microorganisms?

Format from *Journal of Geophysical Research*

7. Can accumulated hydrocarbons in the subsurface be detected by surface "prospecting"? If so, how?

8. How are hydrocarbon gases altered as they migrate?

For over two decades, stable carbon isotope and molecular compositions of natural organic compounds have been used in an attempt to answer these questions. As the state of knowledge in these areas advances, answers to the seemingly basic questions become more and more complex. Studies of recent sediments as well as the deep subsurface have become important in understanding the biogeochemistry of hydrocarbons. The sources, concentrations, and fates of the light hydrocarbons in the upper few meters of marine sediments have not been adequately investigated to date, however, and previous work has concentrated on estuarine sediments.

Little quantitative work has been done on light hydrocarbons in sediments deposited in open marine environments, and identification of gas sources (either bacteriogenic or petroleum-related) has hardly been attempted. Most geochemical prospecting has consisted of "sniffing" the bottom waters of continental shelf regions for methane or other hydrocarbon anomalies. Attempts have also been made to identify sediment gas origins by hydrocarbon molar compositions or isotopic ratios of methane, but alterations of gas compositions in the sediments have hindered interpretations and in some cases induced false conclusions. For accurate interpretations of these measurements, the investigator must first understand the biological and physical processes involved in light hydrocarbon generation and in the alteration of their compositions. The processes of carbon isotope fractionation

in nature are discussed first.

Natural Carbon Isotope Compositions

Introduction

Natural carbon is comprised of about 98.9% ^{12}C and 1.1% ^{13}C (Nier, 1950). However, ^{13}C in naturally occurring carbon varies about 0.11%, with the "lightest" carbon containing about 1.02% and the "heaviest" about 1.13% ^{13}C. Isotopic compositions are generally expressed in terms of parts-per-mil deviations from a standard $^{13}C/^{12}C$ ratio and reported as δ values. The definition for the δ value for carbon ($\delta^{13}C$) is:

$$\delta^{13}C = \left[\frac{(^{13}C/^{12}C)_{sample}}{(^{13}C/^{12}C)_{standard}} - 1 \right] \times 1000 \qquad (1)$$

Values reported in this study will always be referenced to the standard introduced by Craig (1953), a belemnite from the Peedee Formation of South Carolina termed PDB.

Figure 1, taken from Fuex (1977), shows isotopic ranges for various types of carbonaceous material found in nature. Marine limestones are typically the most enriched, and methane the most depleted in ^{13}C of all the natural carbon compounds found on earth.

Methane is present in marine sediments generally as the product of one of two major processes. It can originate from the microbial decomposition of organic matter in reducing environments at temperatures below 50°C (microbial gas), and it can be produced by the abiotic processes of clay mineral catalysis acting for millions of years at elevated temperatures and pressures on more refractory organic material (thermocatalytic gas). Because of different produc-

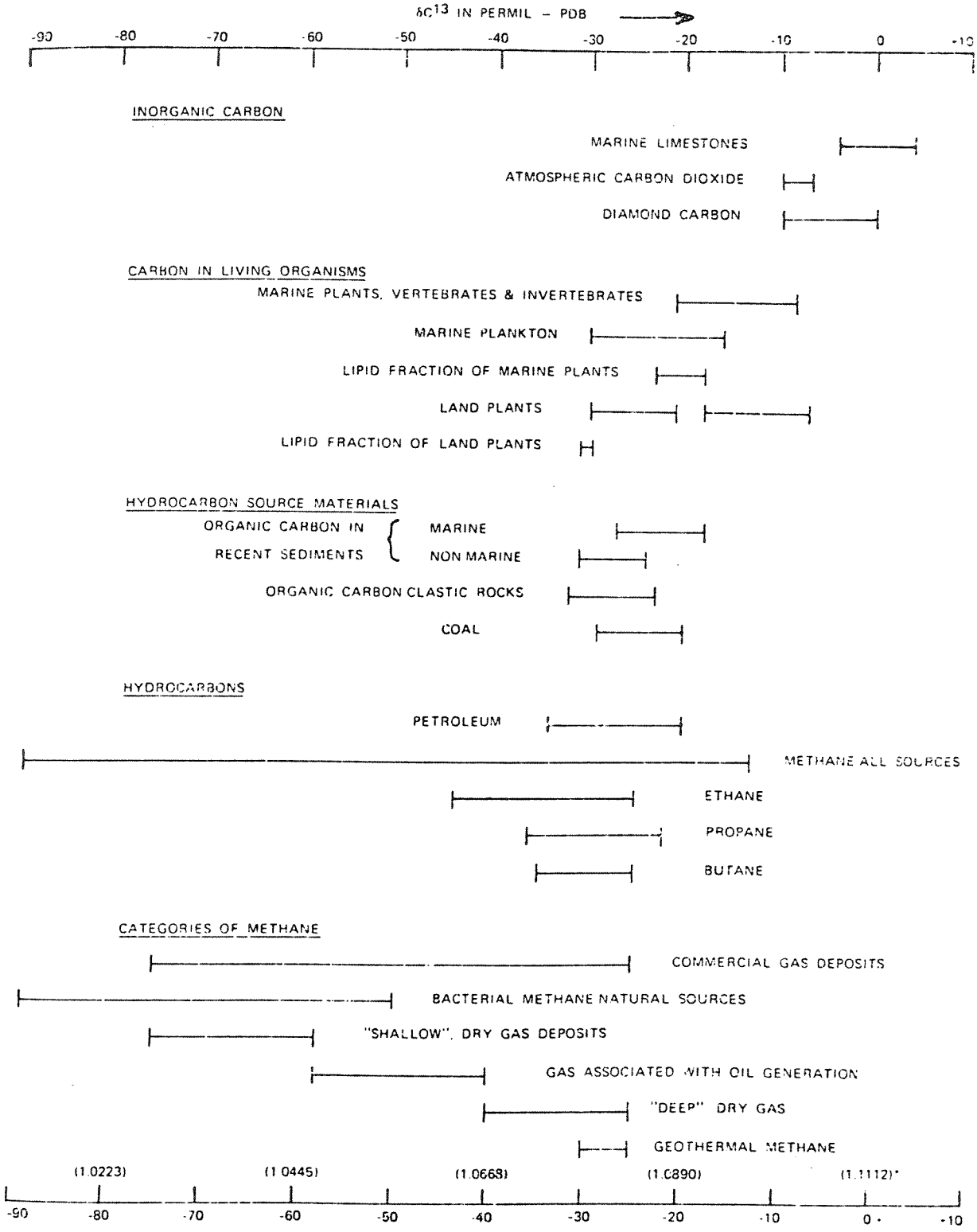

Fig. 1. Carbon isotope ranges of carbonaceous materials (after Fuex, 1977).

tion mechanisms, methane has the largest $\delta^{13}C$ range of any naturally occurring material. Over the past 20 years, very distinct differences in the isotopic composition of microbial and thermocatalytic methane have been observed. These measurements and their application to the development of theories of fractionation mechanisms are discussed next.

Isotopic Composition of Thermocatalytic Methane

An initial study by West (1945) demonstrated a 10 permil depletion of ^{13}C in a few natural gases relative to associated crude oils. Silverman and Epstein (1958) also observed that carbon in natural gases from petroliferous areas was isotopically lighter than petroleum. They concluded from measured values of $-33.4°/_{oo}$ and $-49.3°/_{oo}$ that methane formation from petroleum involves a relatively large isotope fractionation, but did not postulate a formation mechanism. Similarly, Zartman *et al.* (1961) and Wasserburg *et al.* (1963) reported carbon isotopic compositions of methane for several natural gases associated with petroleum ranging from $-29.2°/_{oo}$ to $-51.6°/_{oo}$, but stated that the exact mechanism by which methane is produced was unknown.

Silverman (1964) separated the light components of a crude oil into narrow boiling range fractions to examine the isotopic character of the individual C_1-C_3 hydrocarbons and C_4-C_6 isomeric mixtures. Analyses of the separated fractions indicated that the $^{13}C/^{12}C$ ratio was lowest for methane and increased progressively in the higher hydrocarbons up to C_6. Higher boiling components showed a gradual decrease in $^{13}C/^{12}C$ ratios with increasing boiling range.

Silverman also observed from a mild thermal cracking experiment with topped crude oil that the newly generated gas components were almost 10°/₀₀ lighter, and the gasoline-range components slightly heavier, than the residual stock. He concluded from these experiments that the lowest molecular-weight components in petroleum are formed by the decomposition of higher molecular-weight parent compounds and should be isotopically lighter than their parents because of the slightly greater reactivity of ^{12}C-^{12}C bonds over ^{13}C-^{12}C bonds. In support of this hypothesis, Stephenson *et al.* (1948) observed during the thermal decomposition of propane-1-^{13}C that ^{12}C-^{12}C bonds are ruptured about 8% more frequently than are ^{13}C-^{12}C bonds.

From measured isotope ratios of several Italian natural gases, Colombo *et al.* (1965, 1966) suggested two alternative hypotheses explaining the isotopic distribution in petroleum-related methanes: (1) the methane in any given natural gas has an isotopic composition which results from the admixture of an isotopically lighter bacterial methane and of a heavier methane formed together with higher hydrocarbons in chemical processes; and (2) the observed isotopic distribution is the result of fractionation processes occurring during the migration of gases. According to hypothesis 2, diffusive effects through clay mineral beds could presumably selectively deplete ^{13}C in methane during migration so that gases accumulating in reservoirs would be isotopically lighter than when initially produced. The authors concluded that the two hypotheses represent limiting conditions, and both hypotheses should be considered in the framework of the complex process involving the origin, migration, and accumulation of

natural gases.

Studies by Sackett (1968) and Sackett *et al.* (1970) indicate that neither of the above hypotheses was needed to explain the range of isotopic compositions of natural methanes. Rather, temperature of formation, maturity, and strength of terminal carbon-carbon bonds in the parent materials are the primary factors influencing the isotopic composition of petroleum-related methanes. Sackett's pyrolysis experiments show that methane produced from various hydrocarbons is initially considerably lighter than the carbon in parent molecules, in agreement with Silverman (1964). His results further indicate that carbon isotope fractionation associated with the generation of methane is proportional to the temperature of cracking and to the number of carbon atoms in the parent hydrocarbon materials. As an explanation for the observed fractionation effect, Sackett (1968) suggested the following:

> Presumably the carbon number relation is a result of decreasing terminal bond dissociation energies in the rearrangement products formed during the pyrolysis of straight chain hydrocarbons. The relation between dissociation energies and isotope fractionation may be explained by considering that the substitution of a heavy for a light isotope, *i.e.*, ^{13}C for ^{12}C, lowers the vibrational frequency and the zero-point energy of a chemical bond, and thus more energy is required to break a ^{13}C-^{12}C than a ^{12}C-^{12}C bond. It therefore follows that the energy difference between these two types of isotopic bonds is more significant in organic molecules having a low relative to a high carbon-carbon bond dissociation energy and that for the one series ethane, propane, butane and for another series propane, isobutane, neopentane, with decreasing terminal bond dissociation energies, carbon isotope fractionation should increase proportionally.

Subsequently, Frank and Sackett (1969) and Frank *et al.* (1974) reported the results of further cracking experiments on neopentane and n-octadecane. The ^{13}C depletion in methane initially generated

during thermal cracking of neopentane remained within ±1°/₀₀ at temperatures ranging from 500° to 600°C, implying that the temperature dependence of kinetic fractionations in this temperature range is relatively unimportant. Similarly, a series of long-term thermal cracking experiments performed on n-octadecone at 400°C and higher established that temperature effects for 400°C and above are unimportant relative to the nature of the bonds being broken in determining the carbon isotope composition of resulting methane. These findings along with previous studies suggest that the multiplicity of carbon-carbon bond types and isotope fractionation during the further cracking of decomposition products are the primary factors that determine the isotopic composition of the methane produced.

In defense of their dual-genesis hypothesis previously discussed, Colombo *et al.* (1969) presented compositions of about 100 additional gas samples from southern Italy. They observed a decreasing ethane/methane ratio and an increasing amount of ^{12}C in methane in an upward sediment direction for the gas fields studied. They argue that the hypotheses advanced by Sackett would predict the opposite of their observation, *i.e.*, initial stages of thermal cracking should produce isotopically light methane with relatively large fractions of ethane rather than decreasing fractions of ethane. Furthermore, they propose that preferential diffusion in the order of $^{12}CH_4 > {}^{13}CH_4 > C_2H_6$ will result in an enrichment of $^{12}CH_4$ and a depletion of C_2H_6 in natural gases which migrate upward through the fine-grained clay minerals.

After measuring the isotopic compositions of several Russian natural gases, Galimov (1969) addressed the hypotheses discussed

previously. He concluded that methane in natural gas has a different geochemical history than that of the associated petroleum. Galimov first suggested that the organic matter rather than petroleum in sedimentary rocks is the most likely source material for methane generation. He also argued from theoretical and experimental exidence that methane should be enriched (rather than depleted) in ^{13}C during migration through clay minerals, refuting the migration hypothesis of Columbo *et al.* (1965, 1966). Finally, he postulated that isotope exchange equilibria between methane and carbon dioxide controls the isotopic composition of bacterially-produced gases and of very deep gases existing at temperatures greater than 200°C, but the isotopic character of methane produced between these zones (including most petroleum-related gases) is controlled by temperature-dependent kinetic isotopic effects.

In light of the findings of previous investigators and their own observations, Alekseyev *et al.* (1972) discussed the mechanisms of isotopic fractionation during migration and their possible significance in relation to fractionation during thermocatalysis. The authors suggest that isotopic fractionation during migration is affacted by the processes of diffusion, filtration, adsorption, solution and degassing, and by phase transitions. Due to these different mechanisms, migrational effects do not provide a uni-directional isotope fractionation, but depending on the predominant process, can significantly after the carbon isotopic composition of natural gases.

More recently, Coleman (1976) has discussed the significance of

isotope fractionation during migration. He concludes from a detailed examination of the literature that isotopic changes can occur during migration of natural gas, but since the nature of these changes is dependent on the minerals through which the gas migrates, unambiguous predictions about the directions and magnitudes of changes in isotopic composition cannot be made.

Fuex (1977) has also discussed the factors controlling the isotopic composition of thermocatalytically-produced methane. He considers the kinetic isotope effect in which ^{12}C-^{12}C bonds are more easily broken than ^{13}C-^{12}C bonds and the non-uniform intramolecular distribution of the carbon isotopes to be the primary fractionation factors in the formation of methane. Also, he suggests some secondary effects which may occasionally become significant. These include migration processes, isotopic exchange between methane and carbon dioxide, and bacterial oxidation of methane. Fuex admits that migration fractionation is certainly possible in the migrating front, but suggests that it is precluded in steady-state migration unless there is a significant loss of the fractionated gas. He agrees with Sackett that the process of migration should not be viewed as a mechanism of isotopic fractionation, but simply as a means of transporting gases formed at different stages of source maturation with correspondingly different isotopic compositions.

Most recently, Sackett (1978) has concluded from extensive laboratory cracking experiments on n-octadecane that the extent of fractionation of initially-formed methane is dependent on temperature. Assuming a linear temperature effect of -2.5‰ per 100°C decrease

in temperature, he postulates that isotopic differences between methane and the parent carbon are -30.4°/₀₀ at 300°C, -32.9°/₀₀ at 200°C, and -35.4°/₀₀ at 100°C. If the source rock parent carbon is assumed to be heavier than -30°/₀₀ vs. PDB, initial cracking of this lipid or kerogen material at 100°C should produce methane no lighter than about -65°/₀₀ vs. PDB. This limit on the isotopic character of natural thermocatalytic gas is extremely conservative considering that (1) n-octadecane gives the greatest fractionation of any of the materials pyrolyzed by Sackett, (2) thermocatalytic gas accumulations existing in the subsurface are probably mixtures of both the initial gas produced by cracking and heavier gas produced subsequently, and (3) experiments have shown that clay mineral catalysis acts to reduce rather than enhance carbon isotope fractionation.

The argument often arises that since laboratory cracking experiments are generally conducted at temperatures greater than 200°C and most natural thermocatalytic gas is produced at subsurface temperatures below 200°C, laboratory experiments may not simulate natural gas production. Investigators are limited in the temperature range they can examine since temperatures lower than 200°C will not generate sufficient gas for isotopic analysis even over several months. Nature, however, has millions of years to generate gas from thermocatalytic cracking of organic material. As Sackett (1978) points out, the temperature dependence of fractionation may not be linear and cannot be accurately extrapolated to 100°C. Certainly more work on the structure of petroleum precursors, fractionation mechanisms, and the role of clay mineral catalysis needs to be done.

Isotopic Composition of Microbial Methane

Previous to publication of isotopic compositions of naturally-occurring bacterially-produced gases, Rosenfeld and Silverman (1959) reported and 80°/$_{oo}$ enrichment of ^{12}C in laboratory-produced methane relative to a methanol substrate. Methanogenic bacteria from Pacific Ocean mud cultured at 23°C produced methane having an initial $\delta^{13}C$ value of ∿-90°/$_{oo}$. As ^{12}C-enriched methane was produced during fermentation, residual methanol necessarily became enriched in ^{13}C, and this enrichment was reflected in an increasing ^{13}C content in subsequent methane of ∿140°/$_{oo}$ after 25 days. Rosenfeld and Silverman noted that the observed 80°/$_{oo}$ ^{12}C enrichment over the parent carbon represented the highest natural carbon isotope fractionation yet reported. The next year, Oana and Deevey (1960) reported compositions of 12 bacterially-produced gases from 5 dimictic lakes in Connecticut. $\delta^{13}C$ values of methane ranged from -57.2 to -80.2°/$_{oo}$, the latter value being considered "the lightest natural carbonaceous substance yet analyzed". These two studies were the first to establish that microbially-produced methane is depleted in ^{13}C to a larger degree than thermocatalytically-produced natural gases, but neither addressed the question of why the large fractionations occur.

Shortly after, Nakai (1960) published carbon isotope ratios of microbially-produced methane and carbon dioxide from natural gas fields in Japan. He found that methane was enriched in ^{12}C whereas carbon dioxide was enriched in ^{13}C, as compared to source organic material. Nakai suggested that the extremely light isotopic composition of methane could be explained by an isotopic equilibrium

between methane and CO_2. In theory, the isotopes of carbon, like those of other elements, partition between available molecular sites to favor the most thermodynamically stable arrangements. This thermodynamic equilibrium in the methane-carbon dioxide system can be expressed by:

$$^{13}CH_4 + {}^{12}CO_2 \rightleftarrows {}^{12}CH_4 + {}^{13}CO_2 \qquad (2)$$

The equilibrium constant for this type of reaction is commonly represented by the symbol α, and is given by:

$$\alpha = \frac{(^{13}C/^{12}C)_{CO_2}}{(^{13}C/^{12}C)_{CH_4}} \qquad (3)$$

Craig (1953) calculated values of α for the methane-carbon dioxide system at several temperatures using differences in vibrational frequences of the isotopic species. More recently, Bottinga (1969) calculated more accurate values of α from better spectroscopic data for temperatures from 0° to 700°C. For more detailed discussions of the isotope equilibrium constant, the reader is referred to these reports as well as the recent work of Coleman (1976). Using Craig's values of α, Nakai (1960) showed that methane and carbon dioxide in most of the microbially-produced natural gases he examined could be in isotopic equilibrium at temperatures between 0° and 53°C, whereas the measured temperatures ranged from 7° to 31°C.

Wasserburg *et al.* (1963) compared the compositions of several bedrock gases of thermocatalytic origin to five glacial-drift gases from Illinois. Glacial-drift gases are produced from the decomposition of buried peats, soils, and organic-rich silts which were deposited

during interglacial stages. The authors observed that the $\delta^{13}C$ values of methane in these gases were distinctly more negative, by 20 to 30°/₀₀ than the values for methane from bedrock gases associated with oil. The isotopic composition of the drift gases, ranging from -71.7 to -84.4°/₀₀, revealed "their carbon to be the lightest found in nature to date." The authors calculated that the equilibrium temperatures based on isotopic compositions of methane and carbon dioxide range from 3° to 24°C. Since no rapid exchange mechanism at low temperatures can be invoked for isotopic equilibration of methane and carbon dioxide subsequent to production, the authors suggested that the gases either were generated essentially in equilibrium or were produced by independent processes which happened to yield a reasonable range of temperatures.

Ovsyannikov and Lebedev (1967) reported isotopic compositions of methane and carbon dioxide in several Russian biogenic natural gases, generated mainly from marsh and estuarine deposits. $\delta^{13}C$ values of methane ranged from -52°/₀₀ to -69°/₀₀, whereas carbon dioxide was always much heavier. In the authors' opinion:

> Under the nearsurface conditions, where bacterial generation of methane is most intensive, the attainment of isotope exchange equilibrium is difficult because of low temperatures and continuous escape of one of the components (CO_2) from the system. It is possible the isotope exchange does occur, but at the time of bacterial metabolism, *i.e.*, with the bacteria serving as the catalyst.

Colombo *et al.* (1966) reported $\delta^{13}C$ values of methane for 52 samples from Italian natural gas wells ranging from -37.8°/₀₀ to -71.5°/₀₀. The lighter gases were assumed to be of microbial origin and the authors observed that methane was isotopically lightest in

those samples which had the highest methane/total hydrocarbon molar ratios. They emphasized the existence of two distinct mechanisms (bacteriogenic and thermocatalytic) of methane formation in natural gases, one of which would give rise to exclusively light methane, whereas the other would generate isotopically heavier methane along with higher hydrocarbons. Generally, the $\delta^{13}C$ of any given sample would be some combination of gases generated by both mechanisms.

Galimov (1969) measured the isotopic and molecular compositions of 64 Russian natural gases, several of which were of microbial origin. He concluded that in the sediment depth range of 0-500 meters, where the methane exhibited the isotopically lightest carbon, enrichment of ^{12}C in methane could be attributed to isotopic exchange effected by bacteria between methane and carbon dioxide. Below this "biochemical zone" he postulated that isotopic exchange is excluded because of the absence of bacteria, and methane is generated thermocatalytically without reflecting any thermodynamic equilibrium process.

Another Russian group, Alekseyev *et al.* (1972) presented more isotopic compositions of natural gas samples, including one $\delta^{13}C$ value as light as $-95.0^{o}/_{oo}$. The authors agreed with previous investigators that "the bacteria probably serve as a catalyst in an isotope-exchange reaction between CO_2 and CH_4, which leads to enrichment of the methane in isotope ^{12}C, and the carbon dioxide in ^{13}C."

After further work on natural gas fields in Japan, Nakai *et al.* (1974) reported that gases from Quaternary to Tertiary beds consisted mainly of methane, carbon dioxide, nitrogen, and argon and had $\delta^{13}C$

values of methane ranging from -64°/₀₀ to -75°/₀₀. Isotopic equilibration temperatures calculated using Bottinga's (1969) fractionation factors agreed well with measured temperatures of associated water (from 13° to 59°C). The authors concluded that "CH_4 and co-existing CO_2 produced by unidirectional reactions have reached an isotopic exchange equilibrium through enzyme reactions."

Several more recent publications report $\delta^{13}C$ values of dozens of microbially-produced natural gases from all over the world ranging from about -60°/₀₀ to -95°/₀₀. These analyses include Cariaco Trench sediment gases by Lyon (1973), Deep Sea Drilling Project borehole gases by Claypool *et al.* (1973), marine seep gases by Brooks *et al.* (1974) and Bernard *et al.* (1976), Illinois natural gas by Coleman (1976) and German natural gas by Schoell (1977). Recently, our group has reported an extraordinary $\delta^{13}C$ value of methane in the hypersaline Orca Basin on the Louisiana slope of -105°/₀₀, certainly the lightest carbon yet found on earth (Sackett *et al.*, 1977a).

In his comprehensive study, Coleman (1976) reports compositions of over 100 natural gas samples and addresses the question of whether microbially-produced methane is generated in thermodynamic equilibrium with co-existing carbon dioxide. He develops a series of models describing the kinetics of isotope fractionation during bacteriogenic gas generation, the most complex of which he demonstrates to be in accord with existing laboratory data and some natural systems. Briefly, the model predicts that the isotopic compositions of bacteriogenic methane and carbon dioxide approach steady-state values, with the only subsequent change being an increase in the CH_4/CO_2 ratio with

time. The model also indicates that "CH_4 and CO_2 are not generated in isotopic equilibrium and that the apparent thermodynamic equilibrium in many cases may only be coincidental." So while it is generally agreed that methane and carbon dioxide in natural gases do not come to thermodynamic equilibrium at low temperatures subsequent to their generation, there is still disagreement as to whether bacteria "catalyze" the equilibrium reaction during gas production.

Models of Gas Origin

Over the past 20 years, investigators have observed that trends in the isotopic and molecular compositions of natural gases with age or depth in the sediment are very similar throughout the world. For instance, Sackett (1968) plotted most of the existing isotopic data of natural methane occurrences against age of formation to demonstrate a rapid initial increase in ^{13}C content of methane with age until mid-tertiary, then a more constant isotopic composition of older gases. Another prominent trend is that methane in natural gases is isotopically lightest in samples which have a higher methane/total hydrocarbon ratio (for example, Colombo *et al.*, 1966). These natural compositions can generally be explained by the transition with increasing depth from microbially-produced gas to gas of predominantly thermocatalytic origin. This concept has evolved from models developed over the past decade.

Galimov's Model

Galimov (1969) distinguished several zones of methane generation in the sediment, as shown in Figure 2. The dashed line represents the theoretical curve corresponding to isotopic equilibrium of the methane-

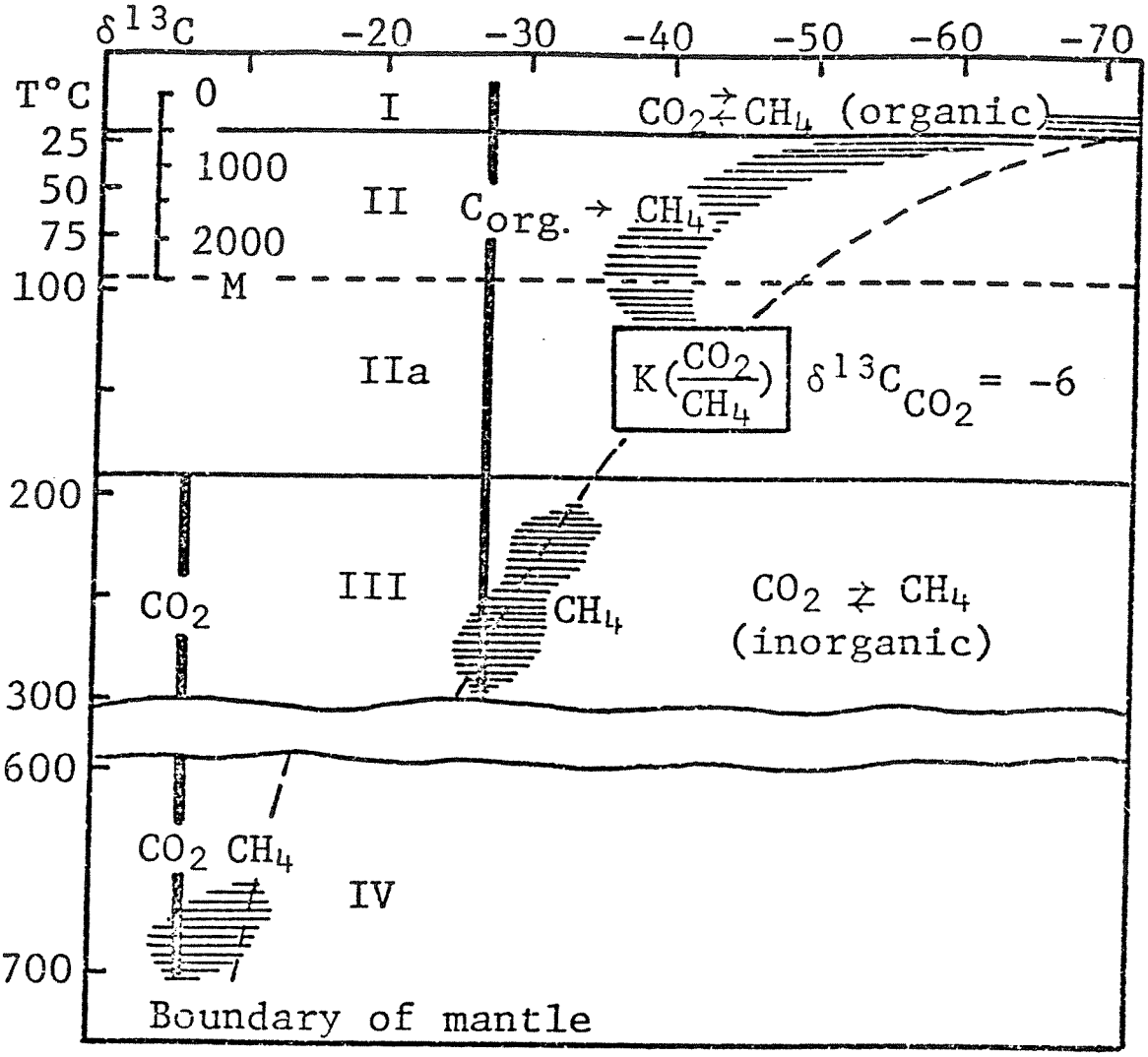

ZONES:

I - biochemical
II - catalytic
IIa - transitional
III - thermal
IV - abyssal

Fig. 2. Zonality of distribution of the carbon of methane in the temperature field of the earth (after Galimov, 1969).

carbon dioxide system at the given temperature. Descriptions of the zones are as follows:

I. Biochemical zone: In the depth range of 0-500 meters methane exhibits maximum enrichment of ^{12}C and $\delta^{13}C$ values of natural gases lie on the theoretical equilibrium line. Isotopic values in this zone are attributed to carbon exchange processes brought to equilibrium by bacteria.

II. Catalytic zone: The biochemical zone is underlain by a zone of catalytic generation of methane. Microbial processes are assumed to be inactive, and the abiotic mechanism of isotope exchange is precluded by relatively low temperatures in this region. Therefore, the isotopic compositions of natural gases do not fall on the theoretical curve for equilibrium. The observed enrichment of ^{12}C in methane compared to organic matter is due to temperature-dependent kinetic isotope fractionations. Galimov indicates a zone of transition (IIa) between zones II and III but makes no comment about it.

III. Thermal zone: The third region of gas distribution is the zone of thermal metamorphism and volcanism. At temperatures of 200°C or more, isotope exchange equilibrium can theoretically be established by physical processes over long periods of time. Natural methane compositions fall on the theoretical curve for equilibrium and, indeed, investigators have used methane-carbon dioxide pairs from hydrothermal springs as geothermometers in calculating geothermal temperatures (Craig, 1953; Hulston and McCabe, 1962).

Stahl's Model

From the studies of Nakai (1960), Müller and Wienholz (1967),

Colombo *et al.* (1969), Stahl and Tang (1971), and Stahl and Carey (1975), Stahl (1974a) developed a model explaining the isotopic and molecular compositions of natural gases (Figure 3). The model demonstrates trends in $\delta^{13}C$ values and $C_1/\Sigma C_n$ ratios (methane divided by the sum of all saturated gaseous hydrocarbons) with increasing age and maturity of sediments. The gases plotted lowest in Figure 3 represent those found in most recent sediments. These gases are very light isotopically and have very high $C_1/\Sigma C_n$ ratios, indicative of a microbial origin. Further sedimentation places the organic material into zones of higher temperature where chemical processes such as hydrolysis, cracking, and hydrogen disproportion become increasingly important. Isotopic fractionation occurs mainly as a result of effects associated with the different binding energies of the isotopes. Stahl explains:

> The methane emerging from the first stages of thermocatalytic alteration of source material is therefore rich in the light isotopes. Consequently the 'young' gases from Japan (Nakai, 1960) and Southern Italy (Colombo *et al.*, 1969) are characterized by large amounts of methane ($C_1/\Sigma C_n > 0.99$) with low concentrations of ^{13}C ($\delta^{13}C < -60°/_{oo}$). With deeper burial, as the thermal stress on carbon complexes increases, more ^{13}C-^{12}C bonds are broken and the gas becomes isotopically heavier. Increasing thermocatalysis also causes the ratio of methane to all saturated gaseous hydrocarbons ($C_1/\Sigma C_n$) to change in favour of the higher hydrocarbons.

By these statements Stahl attempts to explain the increase in ethane-and-heavier (C_2+) hydrocarbons with $\delta^{13}C$ increases from $-70°/_{oo}$ to $-45°/_{oo}$ in Figure 3. This zone of diagenesis is of concern because it represents the transition of natural gases from microbial origin to predominantly thermocatalytic origin. Stahl implies that as the processes of thermocatalysis contribute an increasingly greater

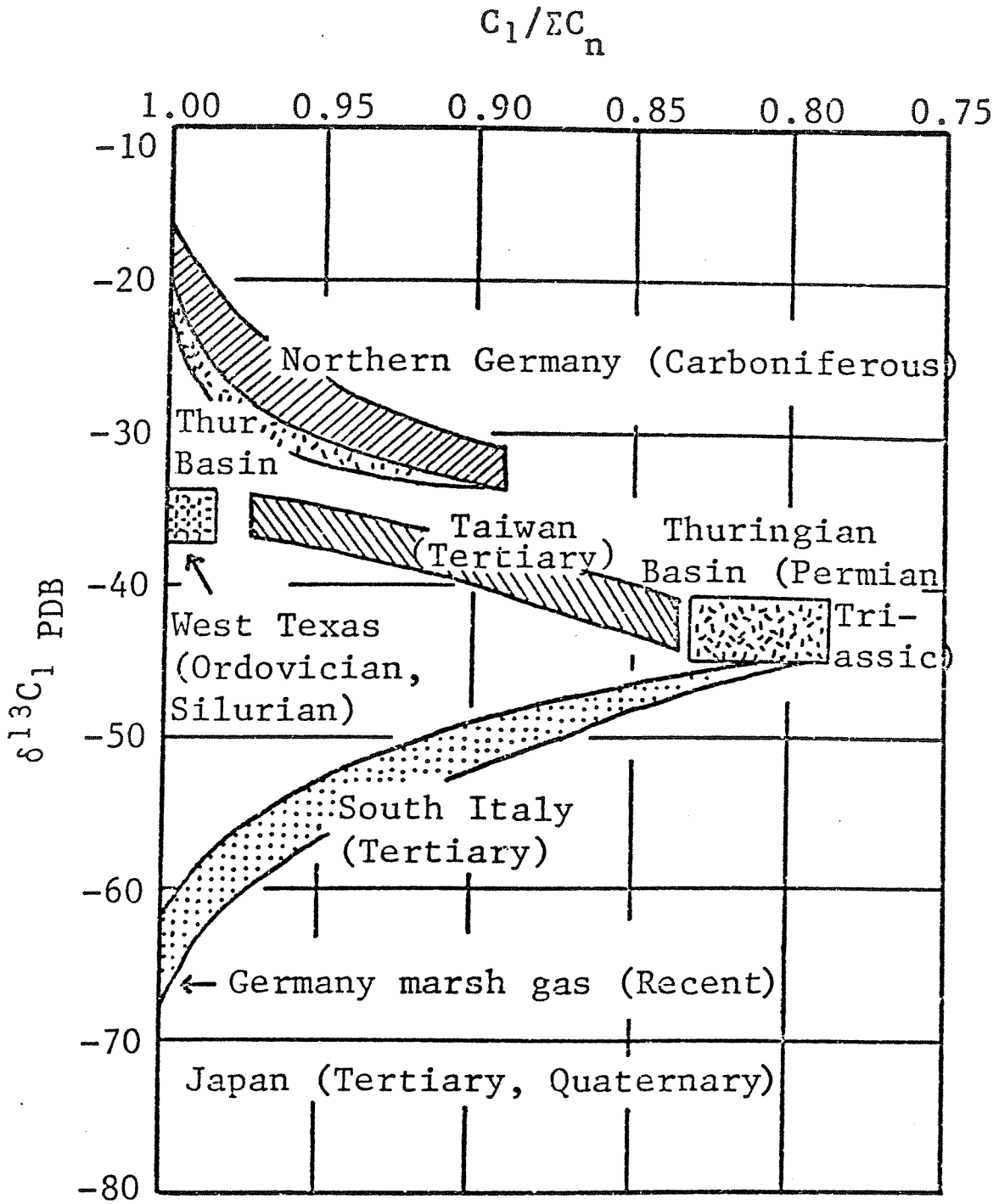

Fig. 3. Isotopic variations in methane in natural gases (after Stahl, 1974a).

fraction of natural gas, isotopic values of methane become heavier, and ethane, propane, and the butanes are produced in increasingly greater quantities. However, Sackett (1978) and recent experiments in our laboratory indicate that the primary initial products of simulated thermocatalysis are ethane and propane, with only relatively small amounts of methane produced. Cracking for longer periods results in a decrease in the C_2+ hydrocarbons and a predominance of methane. These results argue against the postulations of Stahl (1974a) that immature thermocatalytic gases are characterized by greater than 99% methane and that increasing thermocatalysis causes the hydrocarbon ratio to change in favour of the higher hydrocarbons. It should be noted that laboratory cracking experiments must be conducted at much higher than "natural" temperatures in order to generate gases in a reasonable length of time so the experiments may not accurately represent natural systems.

According to Stahl, as organic source material is further altered, hydrocarbons are increasingly cracked and a turning point or "minimum" in $C_1/\Sigma C_n$ ratio is observed. The ^{13}C content of methane continues to increase, but two distinct trends are apparent. Thermocatalytic methane from predominantly terrestrial source material is significantly richer in ^{13}C than methane produced from marine organics. Terrestrial sources are comprised mainly of relatively mature coal-like material which has undergone more thermal stress than the lipid-like marine source material. Remaining terminal carbons are bonded more strongly and consist of a relatively larger fraction of ^{13}C. Methane produced from these terminal carbons is necessarily more enriched in ^{13}C and

isotopic fractionation relative to the source material is not as great. These differences are discussed in more detail by Sackett *et al.* (1970), Sackett and Menendez (1972), and Stahl (1974b).

Finally, with extreme maturity an "overcooked" stage of methane formation is described by Stahl, where virtually all of the available carbon has been converted to methane. These gases have only trace quantities of higher hydrocarbons as shown by $C_1/\Sigma C_n$ ratios greater than 0.99, and their isotopic compositions reflect that of the source material, ranging from -15°/$_{oo}$ to -35°/$_{oo}$ vs. PDB.

This Work

Two parameters which can be used to characterize the origins of natural gases are $\delta^{13}C$ values of methane and $C_1/(C_2+C_3)$ molar ratios (methane divided by the sum of ethane plus propane). Molar ratios of the light hydrocarbons expressed in this manner yield values which vary over 4 orders of magnitude, and are more distinctive than Stahl's $C_1/\Sigma C_n$ values. The previous discussions indicate that gases of thermocatalytic origin have isotopic values ranging from -35 to -50°/$_{oo}$, and $C_1/(C_2+C_3)$ ratios generally greater than 1000. Figure 4 illustrates that two distinct zones of origin can be delineated by these two parameters. Mixing of gases of both origins is represented by the dashed lines connecting the two source zones. The two mixing lines were generated by hypothetically mixing a typical thermocatalytic gas ($\delta^{13}C$ value of -45°/$_{oo}$; $C_1/(C_2+C_3)$ ratio of 10) with two separate microbial gases having $\delta^{13}C$ values of -60°/$_{oo}$ and -80°/$_{oo}$, respectively, and $C_1/(C_2+C_3)$ ratios of 10,000.

Most gas compositions in the literature which fall outside the two

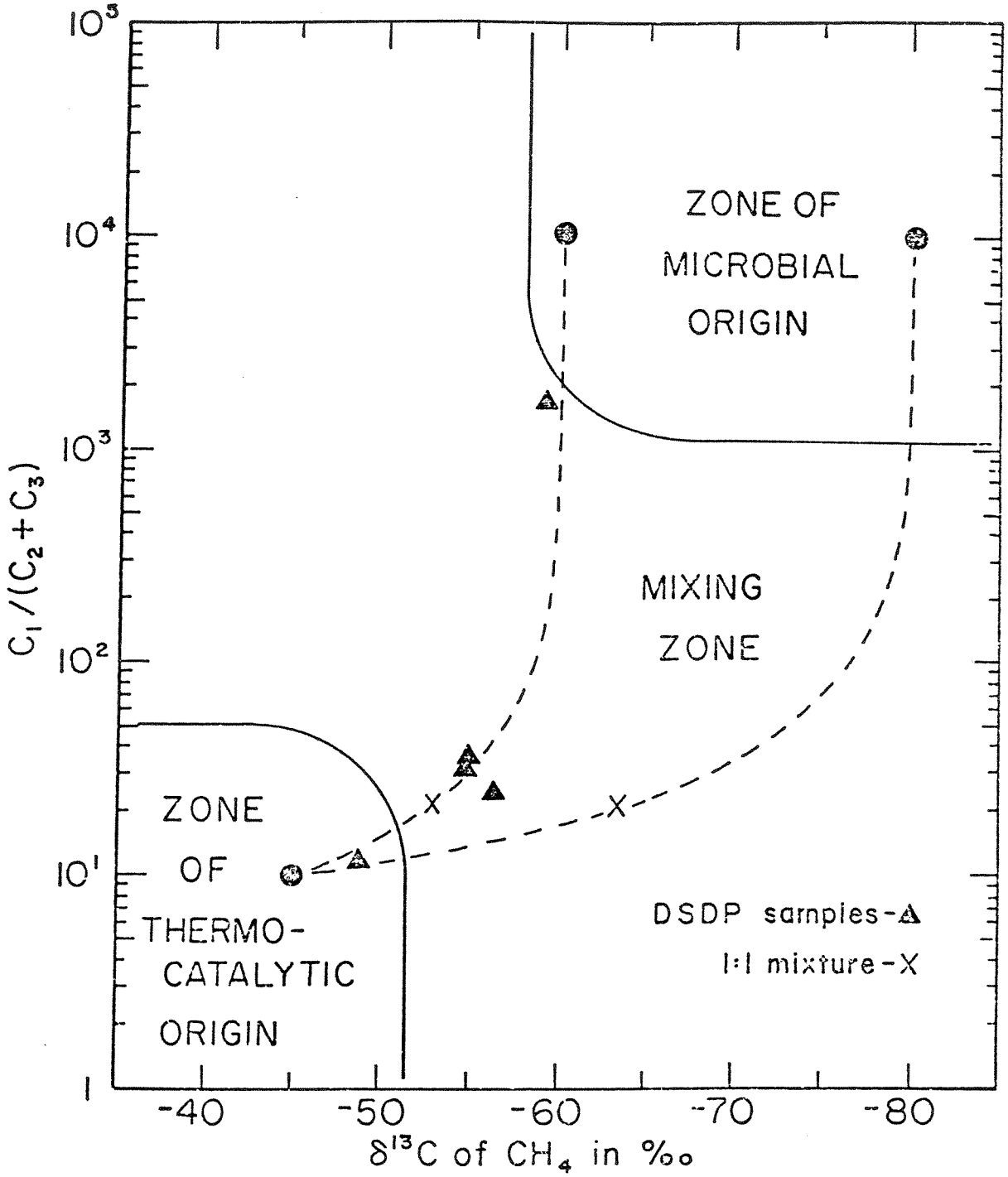

Fig. 4. Model for source characterization of marine hydrocarbon gases.

zones of origin can be attributed to mixing in various ratios of gases from the two sources. For example, the isotopic and molecular ratios of five samples from a Deep Sea Drilling Project borehole (marked by triangles on Figure 4) reported by Claypool *et al.* (1973) fall close to one of the hypothetical mixing curves, and can be interpreted as the result of mixing various fractions of thermocatalytic and microbial gas.

Positions corresponding to a mixture of equal (1:1) fractions from the two sources are marked on the mixing lines. It is clear from Figure 4 that petroleum-related gas can be diluted with biogenic gas as much as 1:1 without shifting the resulting $C_1/(C_2+C_3)$ ratio out of the thermocatalytic region. On the other hand, isotopic values of methane in mixtures are shifted almost linearly with mixing ratios. Thus, only small fractions of biogenic gas are required to cause a significant isotopic change in a predominantly petroleum-related mixture. Similarly, only small fractions of thermocatalytic gas can cause a predominantly biogenic gas to appear related to petroleum in hydrocarbon composition. The mixing model indicates that four of the five DSDP samples consist mostly of biogenic gas, regardless of low $C_1/(C_2+C_3)$ ratios.

CHAPTER II

MARINE SEEP GASES

Introduction

Gas generated in sediments by microbial or thermocatalytic processes may accumulate, migrate upward through the sediment, and eventually seep into the overlying water column. Early work reported by Ohle (1959), McCartney and Bary (1965), and Pickwell (1967) indicated that bubbles rising from gas seeps can be readily detected at sea by standard sonar equipment. Over the past few years more than one hundred seeps have been located along the continental shelf of the northern Gulf of Mexico (Albright, 1973; Geyer and Sweet, 1973; Sweet, 1973; Tinkle *et al.*, 1973). If a large proportion of naturally occurring seepage were indicative of underlying petroleum and natural gas reservoirs, acoustical gas seep detection would provide an almost ideal method for offshore hydrocarbon exploration. However, in a preliminary study, Brooks *et al.* (1974) reported collecting two seep gases having hydrocarbon compositions (99.98% methane) and isotopic ratios of methane ($\delta^{13}C \sim -60°/_{oo}$) highly indicative of a biogenic origin. Since a better knowledge of the compositions of naturally occurring seep gases is extremely important from an oil exploration stand-point as well as for an understanding of the geochemistry of natural hydrocarbon gases, an effort was made over the past three years to collect additional seep gas samples. The compositions reported here suggest that only a relatively small fraction of seepage in the Gulf of Mexico has a significant thermocatalytic component.

Methods of Sample Collection and Analysis

Twenty-one gas samples from seepage in the northwestern Gulf of Mexico have been collected since May 1974 as part of this study. Two were reported earlier by Brooks *et al.* (1974) and another 12 by Bernard *et al.* (1976). The bubbling gas seeps were detected by 12 KHz acoustical reflection techniques and the gas samples were collected under the sea surface by snorkel divers using inverted glass jars. The seeps were located mainly over topographic highs between the 50 and 100 fathom contours on the upper Texas-Louisiana shelf (Figure 5), so the bottom depths from which most sample gases emerged were shallower than would be indicated by the general contour lines on Figure 5. At site 3, East Flower Garden Bank, gas samples were collected by scuba divers at the surface, at 15 meters depth, and at 30 meters depth as the bubbles emerged from the bottom. Sample 7 was collected from the bottom by a scuba diver at 21 meters depth and samples 15 and 18 were collected by a submersible as they seeped from the bottom. All other samples were collected within 3 meters of the sea surface. The gas seepage to the surface varied in volume from sporadic, single-stream bubbles of less than a milliliter per minute to plumes with seepage rates of over 50 liters per minute, so that the amount of gas collected at a given seepage site varied from less than ten milliliters to several liters. After collection the jars containing the samples were sealed while still immersed in the ocean, returned to the ship, and stored inverted with a sea water seal until analyzed.

The molecular compositions of the seep gases were determined using a Hewlett-Packard 5710A gas chromatograph with a flame ion-

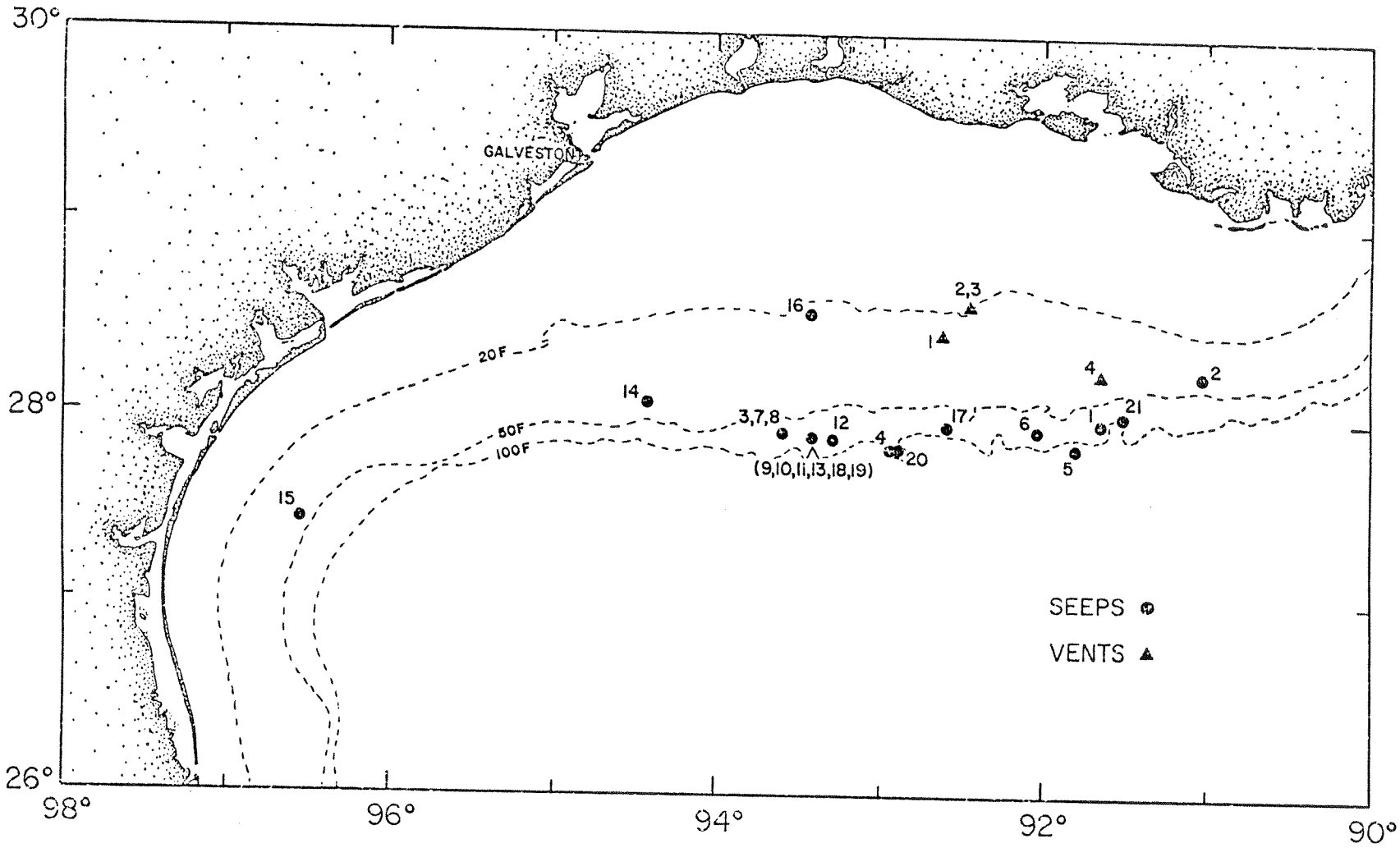

Fig. 5. Gulf of Mexico gas seepage collection sites.

ization detector in conjunction with a Hewlett-Packard 3380A electronic integrator. Hundred-microliter samples were injected into the chromatographic stream and separated on a 3.0-meter Porapak Q column thermostated at 60°C. Carbon isotope ratios were determined by combustion of aliquots of the methane samples to CO_2 at 800°C and subsequent analysis on a dual collecting Nuclide mass spectrometer (Sackett *et al.*, 1970).

Results and Discussion

Locations, bottom depths, and molecular and isotopic compositions of the seep gases collected in this study are listed in Table 1. Also tabulated are the compositions of gas samples collected from four underwater vents. These gas vents are noncommercial by-products of offshore petroleum production operations.

It should be noted that there were considerable amounts of atmospheric gas in most samples and the compositions reported in Table 1 are for only the hydrocarbon fraction. Most of the atmospheric fraction is the result of dissolved air diffusing into the hydrocarbon bubbles during their ascent through the water column or during storage. The carbon dioxide contents determined by infrared techniques on the samples in greatest quantity were less than 0.1%.

As illustrated in Table 1, all of the natural seep gases analyzed were composed primarily of methane with 18 of 21 samples having $C_1/(C_2+C_3)$ ratios greater than 1000, two between 100 and 1000, and one less than 100. Isotopic values of methane in the samples ranged from -39.0°/$_{oo}$ to -66.5°/$_{oo}$ with all samples more negative than -53°/$_{oo}$ having $C_1/(C_2+C_3)$ ratios greater than 1000, and the more positive $\delta^{13}C$

TABLE 1. Composition of Gas Seepage in the Northern Gulf of Mexico

Seep Number	Location (°N)	Location (°W)	Depth (m)	$[CH_4]$ (%)	$[C_2H_6]$ (%)	$[C_3H_8]$ (ppm)	$C_1/(C_2+C_3)$	$\delta^{13}C_{CH_4}$
1	27°59.0'	91°39.0'	62	98.05	0.88	5600	68	-39.9
2	28°14.6'	91°02.0'	55	99.79	0.20	130	470	-44.7
3	27°55.4'	93°35.5'	30	99.86	0.14	12	710	-51.3
4	27°51.9'	92°55.0'	75	99.95	0.05	nd	2000	-44.8
5	27°50.4'	91°50.5'	81	99.98	0.02	nd	5000	-45.9
6	27°56.5'	92°01.8'	57	99.95	0.05	5.0	2000	-50.9
7	27°54.5'	93°35.8'	21	99.95	0.046	4.0	2173	-56.6
8	27°54.5'	93°35.8'	21	99.97	0.031	7.4	3225	-53.8
9	27°55.2'	93°25.8'	60	99.97	0.031	1.7	3225	-56.5
10	27°54.4'	93°26.0'	50	99.98	0.02	nd	5000	-58.0
11	27°55.2'	93°25.8'	52	99.98	0.019	3.0	5262	-58.1
12	27°53.0'	93°18.0'	48	99.99	0.002	nd	50000	-59.1
13	27°54.5'	93°26.0'	48	99.97	0.03	nd	3333	-60.4
14	28°03.0'	94°23.0'	70	99.96	0.04	nd	2500	-61.0
15	27°26.0'	96°31.0'	60	99.97	0.025	nd	4000	-60.6
16	28°32.3'	93°24.5'	40	99.98	0.02	nd	5000	-61.0
17	27°57.8'	92°36.5'	33	99.98	0.02	nd	5000	-65.5
18	27°55.2'	93°25.8'	52	99.96	0.041	2.0	2440	-60.3
19	27°55.2'	93°25.8'	52	99.97	0.034	2.8	2940	-66.5
20	27°49.4'	92°53.5'	100	99.93	0.07	44	1427	-63.3
21	28°02.9'	91°31.0'	44	99.92	0.08	nd	1250	-65.5
Vents								
1	28°25.5'	92°37.8'	-	96.8	1.6	1.1%	36	-50.8
2	28°35.0'	92°28.0'	-	95.3	2.4	1.0%	28	-43.9
3	28°35.0'	92°28.0'	-	94.6	2.9	1.4%	22	-46.8
4	28°13.4'	91°41.1'	-	84.1	7.0	4.8%	7	-42.0

values generally associated with larger fractions of ethane and propane. The hydrocarbon compositions, isotopic values of methane, and trends between the two parameters are similar to those reported on hydrocarbon gases found in several Deep Sea Drilling Project (DSDP) cores by Claypool *et al.* (1973). Figure 6 shows a plot of $C_1/(C_2+C_3)$ ratios versus $\delta^{13}C$ values for the seep samples listed in Table 1 on the schematic model outlined earlier.

There appears to be a major contradiction between the inferences drawn from the molecular and isotopic compositions of several of the samples plotted in Figure 6. $\delta^{13}C$ values between -39.9 and -51.3°/$_{oo}$ for seep numbers 1 through 6 suggest a thermocatalytic origin, but the $C_1/(C_2+C_3)$ ratios are considerably greater than expected for thermocatalytic products. These compositions cannot be explained by mixing processes, as seen from Figure 6.

There are several possible explanations for the contradiction. First, methane produced by methanogenic bacteria acting on substrates such as carbon dioxide, formate, acetate and methanol may change in isotopic composition as the substrate is depleted. For example, Rosenfeld and Silverman (1959) showed that during bacterial fermentation of methanol, the methane changed in isotopic composition from about a 70°/$_{oo}$ enrichment in $^{12}CH_4$ relative to the substrate carbon at the beginning of an experiment to about a 70°/$_{oo}$ depletion in $^{12}CH_4$ near the end of the experiment when the methanol was almost completely utilized by the bacteria. Other evidence for isotopically heavy microbial methane is a $\delta^{13}C$ value of -45°/$_{oo}$ for methane in Lake Kivu, reported by Deuser *et al.* (1973). This methane is certainly biogenic

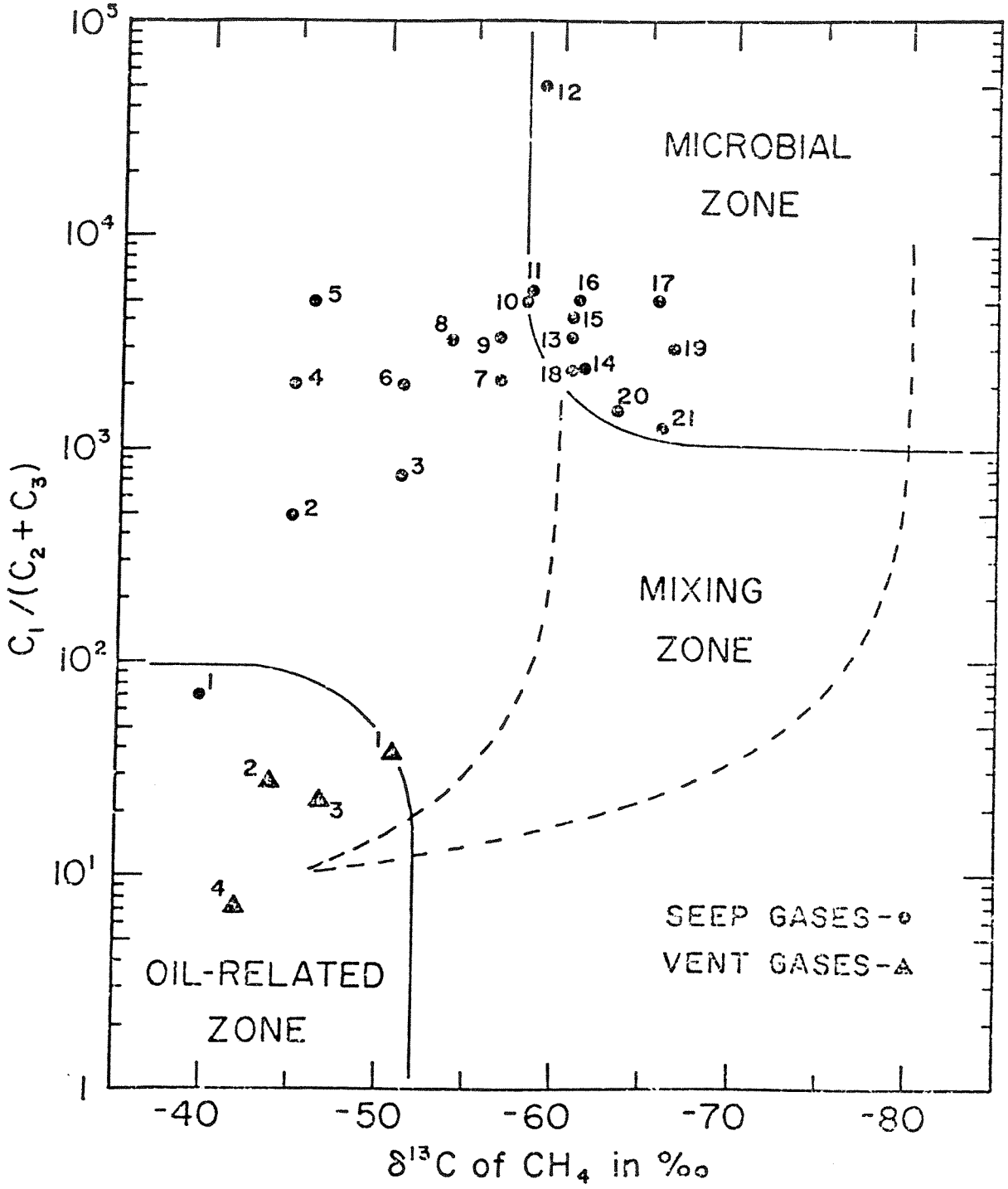

Fig. 6. $C_1/(C_2+C_3)$ vs. $\delta^{13}C$ for seep gas samples listed in Table 1.

and the authors conclude that a volcanic source of heavy CO_2 may be responsible for an anomalously heavy methane composition. (It is probable, however, that this reported value may simply be incorrect.) Without knowledge of the isotope fractionation associated with other methane-producing microbial processes, the isotopic composition of the CO_2 and other possible substrates, or the degree of utilization of the substrate reservoir, isotopically heavy methanes produced by microbial processes cannot be eliminated as an explanation. Indeed, they may be represented by sample numbers 4, 5, and 6, with relatively heavy isotopic compositions -44.3, -45.9, and -50.9°/$_{oo}$, respectively, but with very small amounts of ethane and higher hydrocarbons.

Samples 1, 2, and 3 contain larger fractions of higher hydrocarbons than microbial degradation can produce (hydrocarbons as high as heptane were detected in sample 1), but their $C_1/(C_2+C_3)$ ratios are still higher than the oil-related vent gases. The vent gas samples are representative of light hydrocarbon concentrations normally associated with oil and gas reservoirs located in Texas and Louisiana, as over 95% of the wells examined in these regions have $C_1/(C_2+C_3)$ ratios smaller than 50 (Moore *et al.*, 1966). Seep 1 has isotopic and molecular compositions comparable to the thermocatalytic vent gases, but if gases 2 and 3 are also seeping from thermocatalytic sources they have been depleted in ethane and higher hydrocarbons before analysis.

One explanation of low ethane and higher hydrocarbon concentrations in gas produced by thermocatalytic processes involves a molecular fractionation of the light hydrocarbons due to differences in water solubilities. According to McAuliffe (1966), the Bunsen

solubility coefficients of methane, ethane, and propane in water at 20°C are 34.2, 45.1, and 31.8 ml_{STP}/liter, respectively, with solubility decreasing for the butanes and higher alkanes. Changes in temperature and salinity affect the solubilities of the individual hydrocarbons and deviations from single component solubilities are caused by mixtures of two or more soluble components, so solubilities for hydrocarbon gas mixtures in seawater are not accurately known. Due to the high solubility of ethane, however, a gas bubble containing a mixture of the light hydrocarbons should be depleted in ethane while rising through the water column. The solubility of propane is so similar to that of methane that the concentration ratio (C_1/C_3) should remain fairly constant. These predictions have been confirmed in this study by laboratory experiments which showed that hydrocarbon mixtures similar in composition to oil-related gas, when equilibrated with hydrocarbon free water, gave a greater C_1/C_2 ratio in the remnant bubble than in the initial gas mixture. The C_1/C_2 ratio of that gas dissolved in the solvent water was correspondingly smaller than that of the initial gas mixture. No differences in the C_1/C_3 ratio between the initial gas, the remnant gas, or the gas dissolved in the water were observed.

Whereas solubility differences resulting in the depletion of ethane could possibly explain small discrepancies in ethane concentration between the vent gases and gas seeps 1, 2, and 3, it is not likely that ethane is preferentially removed from hydrocarbon bubbles by solution to the extent observed. For example, at seep site 3 (East Flower Garden Bank), where samples were collected at 1, 15, and

30 meters below the surface, no ethane concentration differences were detected between samples. It should be noted, however, that these gas bubbles were extremely large and rose rapidly, allowing relatively little surface area to be exposed to the water. At a later time, seepage was collected from another site directly off of the bottom at the East Flower Garden (21 meters deep), then the very smallest (<2 mm diameter) bubbles were collected at the water surface above the site. The former is sample 7 and the latter is sample 8. Repeated analyses of the two samples demonstrated that the surface bubbles were indeed slightly depleted in ethane, illustrating the extent of this alteration phenomenon (Table 1).

Another explanation for the relatively low ethane and propane concentrations observed in presumed thermocatalytic gas seepage is that of molecular fractionation during migration through the sediments. As gases migrate upward from their source region, the sediments may act as a fractionating "chromatographic" column, retarding the higher hydrocarbons. Any subsequent gas seepage from the sediment could be deficient in the higher hydrocarbons relative to the initial composition in the reservoir. Thus, higher hydrocarbons may be removed to a greater extent than propane, which in turn may be depleted more than ethane, as observed for samples 1, 2, and 3. This relationship has been reported for light hydrocarbon concentration differences between a natural gas reservoir and gases dissolved in overlying well water by Coleman (1976). His study found that gas which had migrated vertically over 400 meters from a gas injection into an underground storage reservoir into an overlying water well retained its isotopic compo-

sition of $-42°/_{oo}$ within $0.2°/_{oo}$. The $C_1/(C_2+C_3)$ ratio of the gas changed from 19 to greater than 1000, however, indicating that the C_2+ hydrocarbons were removed during migration. It should be noted that this type of separation only occurs at a migration front and that eventually the gas composition should change in favor of the higher hydrocarbons. Indeed, Coleman (personal communication) has indicated that subsequent measurements of the water well gas showed a relative increase in ethane and propane several months later and predominantly propane over a year later.

The possibility of carbon isotope fractionation of methane should also be discussed. It is indicated above that fractionation effects are only very slight during migration. Also, since the solubilities of $^{13}CH_4$ and $^{12}CH_4$ are almost identical, only a very slight fractionation between the two should ever be observed as methane bubbles rise through a water column. At seep site 3, where samples were taken at 1, 15, and 30 meters below the surface, no isotope fractionation between methane samples could be detected within $\pm 0.1°/_{oo}$. When samples of methane were equilibrated with water in the laboratory so as to dissolve over 75% of the gas, a fractionation of only $0.3°/_{oo}$ was observed. The isotopic change during ascent of very small bubbles represented by samples 7 (bottom) and 8 (surface) was less than $3°/_{oo}$, indicating that methane in most natural gas seepage does not undergo significant isotope fractionation during ascent of the bubble or during storage before analysis.

Model Revision and Conclusions

Three processes which apparently alter natural gas compositions,

then, are mixing, substrate depletion during microbial gas production, and C_2+ hydrocarbon depletion during thermocatalytic gas migration. these phenomena are shown on the revised model in Figure 7. The depletion of ^{12}C in older microbial gas is illustrated by a shift to the left in the Zone of Microbial Origin, corresponding to an increase in $\delta^{13}C$ values of methane with no significant change in $C_1/(C_2+C_3)$ ratios. (The limiting extent of this isotopic alteration is not resolved). The depletion of higher hydrocarbons during migration of petroleum-related gas is illustrated by an upward shift in the Zone of Thermocatalytic Origin, corresponding to an increase in $C_1/(C_2+C_3)$ ratios with no significant change in $\delta^{13}C$ values of methane. This model, showing gas source zones, mixing curves, and alteration trends, has been used by Bernard *et al.* (1977) to characterize both sediment and seep gases occurring naturally in the marine environment.

These results should be of interest to exploration geochemists who consider hydrocarbon compositions or isotopic ratios in surface sediments or dissolved methane concentrations from bottom water in the evaluation of the reservoir potential of a region. If the 21 gas seep compositions reported here are representative of gas seepage in general, the use of hydrocarbon "sniffing" in offshore petroleum exploration must be reevaluated. High concentrations of dissolved methane in near-bottom waters produced from microbial processes could be misinterpreted as the result of seepage from petroleum-related sources. In addition, dissolved higher hydrocarbons may not be detected near existing oil-related seepage due to their depletion during migration from the reservoir.

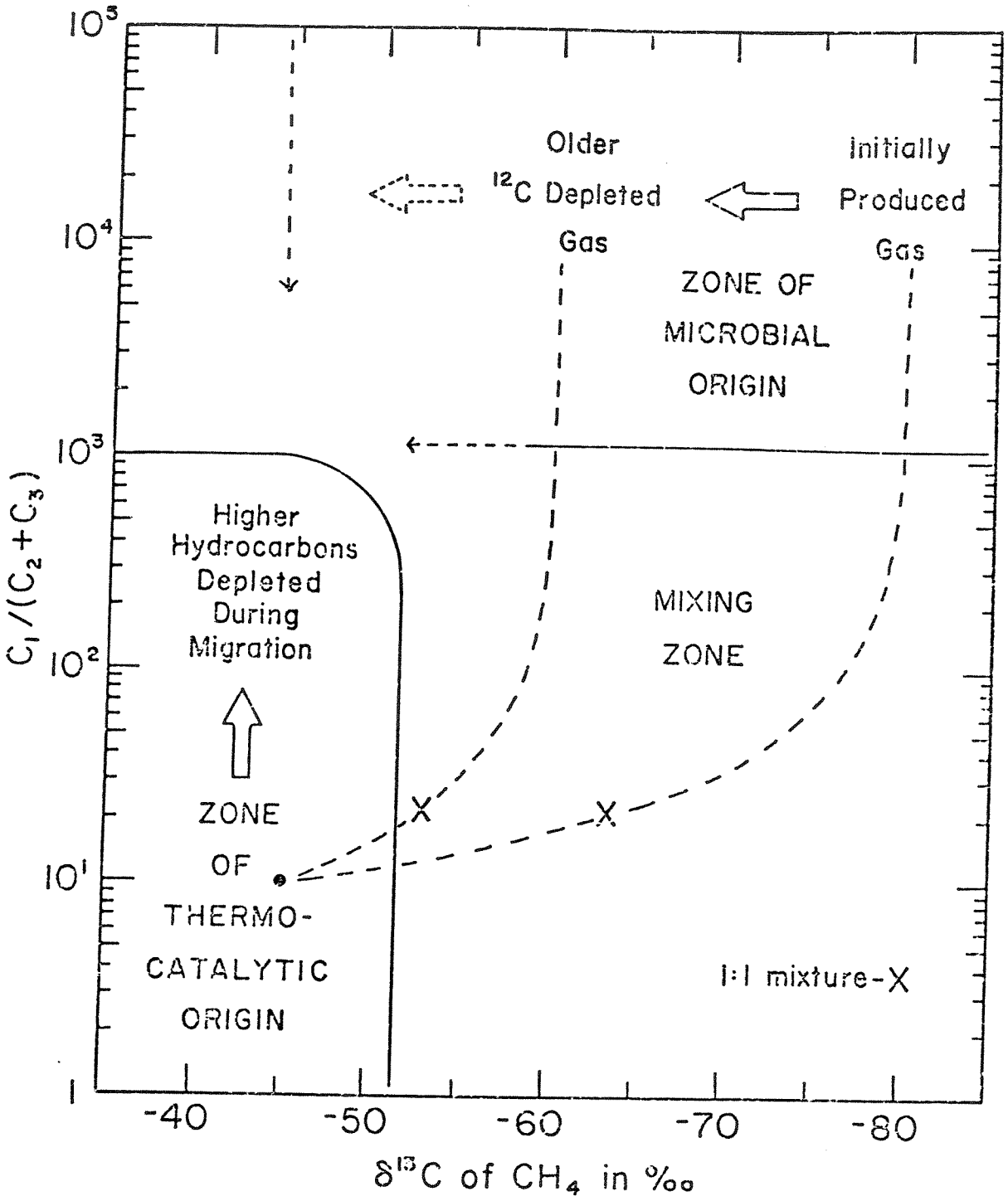

Fig. 7. Revised model for source characterization of marine hydrocarbon gases (after Bernard *et al.*, 1977).

of microorganisms which use dissolved interstitial oxygen for respiration (aerobes). The processes which control interstitial oxygen concentrations are consumption by these bacteria, sediment deposition rate, and diffusion from overlying water. Oxygen concentrations necessarily approach zero at some sediment depth when diffusive processes can no longer replace the oxygen consumed by the aerobes. The depth of the aerobic-anaerobic boundary varies with sediment accumulation rates, organic content, and temperature. Sediments quickly become anoxic in near-shore and delta environments, and may contain no oxygen even at the surface. In continental shelf and slope regions, the oxidation of remobilized manganese demonstrated by bands of precipitated manganese dioxide illustrates the penetration of oxygen to depths of 20-40 cm (Trefry, 1977). In the deep-sea, oxygen may exist at several meters depth, as indicated by high Eh values in several Deep Sea Drilling Project cores (Presley *et al.*, 1970). These data are suspect, however, as recent measurements using O_2 microprobes have shown oxygen to essentially disappear at less than a meter depth even in abyssal sediments (C. Bowser, personal communication).

Anaerobic sulfate-reducing zone: The minute nitrate concentration in marine sediments is rapidly consumed by denitrifying bacteria, so sulfate-reducing bacteria quickly become dominant with the depletion of oxygen. Sulfate is present in marine interstitial waters at relatively high concentrations (28mM at the sediment surface) and H_2S, an end product of sulfate reduction, is tolerated by very few microorganisms. Sulfate-reducing bacteria are able to assimilate only a limited number of organic compounds, chiefly lactic acid and four-

The origin of hydrocarbon gas in marine sediments is more accurately determined by comparison of the isotopic and molecular compositions of the sample gas using the proposed model. In this regard, prospecting for reservoired hydrocarbons should include coring on or near geologic features such as unconformities, faults, bedding planes, or distinct gas seepage, to first establish the source of emanating gases in the region. If the gas is of microbial origin, as are most of the gas samples analyzed from the northwest shelf of the Gulf of Mexico, reconsideration can be given to the petroleum potential of the area.

CHAPTER III

MARINE SEDIMENT GASES

Introduction

In addition to the seep gases, 58 sediment cores have been sectioned and analyzed for interstitial light hydrocarbons. Carbon isotope ratios were also measured on samples containing sufficient methane (>0.1 ml_{STP}). The gases in these cores were analyzed in order to evaluate the relative contributions of microbially-produced and thermocatalytic gases in near-surface marine sediments. The South Texas continental shelf was cored extensively in an attempt to locate areas of seepage of oil-related gas through faulting or bedding planes. Except for one area, no anomalously high concentrations of thermocatalytic natural gas were discovered on the Texas shelf. Therefore, this chapter on sediment gases will focus on the mechanisms of production and concentrations of microbial gas in marine sediments.

Mechanisms of Microbial Methane Production

Introduction

Microorganisms produce methane in a variety of environments such as dung heaps and anaerobic sewage digestors (Smith, 1966), digestive tracts of animals (Beijer, 1952; Bryant, 1965), landfills (Games and Hayes, 1974), glacial drift (Meents, 1960; Wassarburg *et al.*, 1963; Coleman, 1976), marshes (Teal and Kanwisher, 1966; Whelan, 1974a), paddy fields (Koyama, 1955; 1963; 1964a; Takai, 1970), freshwater lakes (Koyama, 1953; 1964b; Oana and Deevey, 1960; Cappenburg, 1972; 1974a,b; Koyama *et al.*, 1973), anoxic marine waters (Atkinson and Richards, 1967; Deuser *et al.*, 1973; Lamontagne *et al.*, 1973; Hunt, 1974; Reeburgh,

1976), and marine sediments (Emery and Hoggan, 1958; Reeburgh, 1969; Nissenbaum *et al.*, 1972; Claypool and Kaplan, 1974; Hammond, 1974; Lyon, 1974; Martens and Berner, 1974; Reeburgh and Heggie, 1974; Whelan, 1974b; Oremland, 1975; Barnes and Goldberg, 1976; Bernard *et al.*, 1977; Martens and Berner, 1977).

Physiological and ecological constraints limit the extent of biogenic methane production, however, so these environments of methane production have distinct similarities. Methane-producing bacteria are strict anaerobes (Brock, 1974) and apparently will not proliferate even in the presence of dissolved sulfate. Because each group of microorganisms in the sediment occupies a special ecological niche depending on substrate availability and restriction of the physical environment, the species that are best able to adapt to the conditions of that environment are favored and become dominant. This selectivity results in a succession of bacterial types downward through the sediment column.

Bacterial Succession in Sediments

Bacteria obtain energy for growth and cell maintenance from a series of dehydrogenation, or coupled oxidation-reduction reactions. The uniqueness of each microorganism is based upon the type of molecule that can be used as the oxidizing agent or terminal electron acceptor. Two general types of metabolic processes are present in the decomposition of organic matter. One process uses inorganic compounds such as O_2, NO_3^-, $SO_4^=$, and HCO_3^- as electron acceptors (respiratory processes), and the second process involves organic intermediates produced in the decomposition itself (fermentative processes). Although fermentations

yield relatively little energy compared to aerobic and anaerobic respiration, they are not competitive and can occur simultaneously. In fact, fermentation processes can be preparatory steps for some respiration processes as they break down large organic molecules to small organic acids and alcohols.

The most efficient oxidizing agent is dissolved oxygen. During aerobic assimilation oxygen is consumed by microorganisms until it is depleted. The bacteria then use other compounds capable of releasing energy when reactively coupled as oxidizing agents with organic matter. Table 2 (from Claypool and Kaplan, 1974) demonstrates the relative energy yields when glucose (representing organic matter) is oxidized by various agents. Actual free energy changes under natural conditions may vary but the advantage to organisms capable of utilizing the higher energy yield process is illustrated. When two or more physiologically different organisms compete for the same organic substrate, those capable of generating the greatest metabolic energy will dominate.

The result of the oxidation efficiency succession of sediment ecosystems has been illustrated by Claypool and Kaplan (1974) in Figure 8 by a schematic cross section of an organic-rich marine sedimentary column. The ecological factors form three distinct biochemical environments, each characterized by the dominant form of respitory metabolism. The three zones distinguished by the authors are: the aerobic zone, the anaerobic sulfate-reducing zone, and the anaerobic carbonate-reducing zone.

Aerobic zone: The aerobic zone is characterized by the dominance

TABLE 2. Energy-Yielding Metabolic Processes as Coupled Oxidation-Reduction Reactions (after Claypool and Kaplan, 1974).

	$\Delta G^{o'}$ (kcal per mole of glucose equivalent oxidized)
a. Aerobic respiration	
$CH_2O + H_2O \rightarrow CO_2 + 2H_2$	
$2H_2 + O_2 \rightarrow 2H_2O$	
$CH_2O + O_2 \rightarrow CO_2 + H_2O$	-686
b. Nitrate reduction	
$5CH_2O + 5H_2O \rightarrow 5CO_2 + 10H_2$	
$10H_2 + 4NO_3^- + 4H^+ \rightarrow 2N_2 + 12H_2O$	
$5CH_2O + 4NO_3^- + 4H^+ \rightarrow 2N_2 + 5CO_2 + 7H_2O$	-579
c. Sulfate reduction	
$2CH_2O + 2H_2O \rightarrow 2CO_2 + 4H_2$	
$4H_2 + SO_4^= \rightarrow S^= + 4H_2O$	
$2CH_2O + SO_4^= \rightarrow S^= + 2CO_2 + 2H_2O$	-220
d. Carbonate reduction	
$2CH_2O + 2H_2O \rightarrow 2CO_2 + 4H_2$	
$4H_2 + HCO_3^- + H^+ \rightarrow CH_4 + 3H_2O$	
$CO_2 + H_2O \rightarrow HCO_3^- + H^+$	
$2CH_2O \rightarrow CH_4 + CO_2$	- 99
e. Nitrogen fixation	
$3CH_2O + 3H_2O \rightarrow 3CO_2 + 6H_2$	
$6H_2 + 2N_2 \rightarrow 4NH_3$	
$3CH_2O + 2N_2 + 3H_2O \rightarrow 4NH_3 + 3CO_2$	- 57
f. Fermentation: heterolactic	
glucose $\rightarrow$ acetaldehyde + CO_2 + lactate + H_2	
H_2 + acetaldehyde $\rightarrow$ ethanol	
glucose $\rightarrow$ lactate + ethanol + CO_2	- 49
g. Fermentation: Stickland reaction	
alanine + $2H_2O \rightarrow NH_3$ + acetate + CO_2 + $2H_2$	
$2H_2$ + 2 glycine $\rightarrow 2NH_3$ + 2 acetate	
alanine + 2 glycine + $2H_2O \rightarrow$ 3 acetate + CO_2 + $3NH_3$	-17

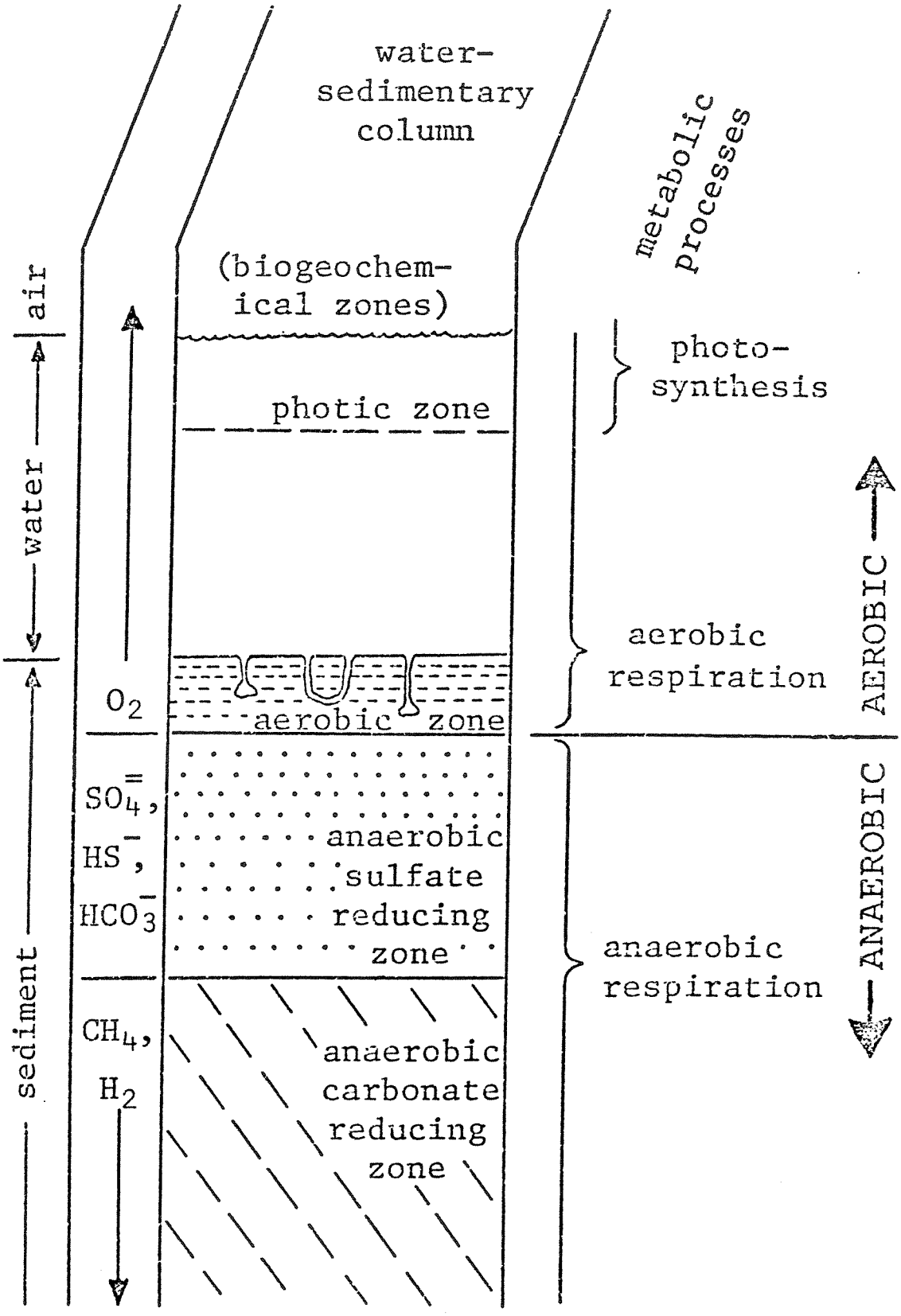

Fig. 8. An idealized cross section of an open marine organic-rich (reducing) sedimentary environment (after Claypool and Kaplan, 1974).

carbon carboxylic acids (Postgate, 1965), so these organisms require a symbiotic association with fermenting bacteria to provide these short-chain organic intermediates.

The processes affecting interstitial sulfate have been described by several investigators (Kaplan *et al.*, 1963; Berner, 1964a,b; Presley and Kaplan, 1968; Berner, 1974; Goldhaber and Kaplan, 1975; Shokes, 1976; Goldhaber *et al.*, 1977). Observed distributions have been explained mathematically by kinetic modeling in which relative rates of sediment deposition and diffusion and consumption of sulfate determine solutions to the steady-state diagenetic equation. These solutions fit well to measured interstitial sulfate concentrations in the reducing sediments of nearshore, estuarine, and delta areas.

Sulfate concentrations are not significantly depleted in deep-sea sediments within the depth range sampled by gravity or piston coring due to low sediment temperature and organic content. Interstitial waters of several Deep Sea Drilling Project borehole cores contain near-seawater sulfate concentrations hundreds of meters deep (Presley and Kaplan, 1970; Broecker, 1973), implying that sulfate may never be completely consumed in some areas.

These observations indicate that the depth of complete sulfate depletion is very near the sediment surface in estuarine and nearshore areas and exists increasingly deeper in the sediment in an offshore direction. This trend is attributed to the high bacterial activity of warm, organic-rich, rapidly depositing, nearshore sediments being inhibited by decreasing temperatures and organic input with increasing water depth.

Anaerobic carbonate-reducing zone: This environment could more properly be termed the CO_2-reducing zone. When interstitial sulfate is depleted, microorganisms use the next most efficient electron acceptor available in marine sediments for respiration, CO_2. The dominant bacteria, called methanogens (Zeikus, 1977), produce methane by reduction of carbon dioxide, causing extensive accumulations of methane below the depth of sulfate disappearance.

Whether the zones of sulfate reduction and methane production overlap, or are mutually exclusive, has not been clearly established. Claypool and Kaplan (1974) demonstrated by relative energy yield calculations (Table 2) that methane-producing bacteria should not be active in the presence of dissolved sulfate. Martens and Berner (1977) support this view using measured methane and sulfate distributions, concluding that methane is most likely produced only in the absence of dissolved sulfate and is consumed by sulfate-reducing bacteria upon diffusing upward. In contrast, Barnes and Goldberg (1976) suggest that methane generation and sulfate reduction are not not mutually exclusive processes, rather that low concentrations of methane in sulfate-reducing pore water represent a balance between production by methanogens and consumption by sulfate-reducers. This conflict is discussed further in a later section..

Stages of Methane Formation

The overall conversion of complex organic matter to methane is not brought about by a single group of microorganisms, but is considered to be a two-stage process including at least two large, physiologically distinct bacterial populations (McCarty, 1964; Wolfe, 1971).

Non-methanogenic stage: In the first stage a heterogeneous group of bacteria convert proteins, carbohydrates, polysaccharides, fatty acids, lipids, alcohols, and nitrogenous compounds into acetate, formate, methanol, hydrogen, and carbon dioxide by fermentation and hydrolysis. The mechanisms of these conversions are explained in detail by Toerien and Hattingh (1969) and Kotze' *et al.* (1969).

The metabolism of the non-methanogenic organisms involves the degradation of complex organic matter to substrates which can be used by them for the synthesis of cell material and also by the methanogenic bacteria for the production of methane. Considering the many different organic compounds which must be broken down, a variety of microorganisms must be present to catalyze the various reactions. Although this group includes aerobic and facultative anaerobic species, the total non-methanogenic bacterial population consists mainly of obligate anaerobes (Kotze' *et al.*, 1968). In addition to bacteria, protozoa have frequently been observed in anaerobic environments, but do not occur in large numbers. A wide range of fungi, molds, and yeasts have also been reported by Cooke (1954).

Along with the different microorganisms in the group, the presence of several extracellular enzymes such as cellobiase, protease, amylase, and lipase has been established (Kotze' *et al.*, 1968). Extracellular enzymes are secreted by various microorganisms to degrade complex organic molecules to smaller units before being ingested.

Methanogenic stage: In the second stage, the end-products of the first stage metabolism are converted to methane and carbon dioxide by

a physiologically unique group of strict obligate anaerobes which are the terminal organisms in the microbial food chain (Wolfe, 1971). These methanogens are not completely understood and are difficult to obtain in pure cultures. Excellent reviews on the isolation and culturing of these bacteria are given by Wolfe (1971) and Zeikus (1977). There is strong evidence that methanogens are unable to assimilate substrates other than formate, acetate, methanol, carbon dioxide, and hydrogen (Toerien and Hattingh, 1969), so the higher order acids and alcohols must be degraded to these compounds before being consumed. It was initially thought that *Methanobacterium omelianskii* oxidized ethyl alcohol to acetate by the reaction:

$$2CH_3CH_2OH + CO_2 \rightarrow 2CH_3COOH + CH_4 \qquad (4)$$

implying that some bacteria can directly produce methane from ethyl alcohol (Barker, 1941). The conversion of ethanol to methane was later shown to be the product of the reaction of two bacterial species by Bryant *et al.* (1967), and may be represented by:

$$\text{Bacterium A} \quad 2CH_3CH_2OH + 2H_2O \rightarrow 2CH_3COOH + 4H_2 \qquad (5)$$

$$\text{Bacterium B} \quad CO_2 + 4H_2 \rightarrow CH_4 + 2H_2O \qquad (6)$$

The growth of Bacterium A is inhibited by the production of hydrogen. Thus, the process of methane formation removes hydrogen and permits the continued anaerobic degradation of small organic molecules.

Methanogens were initially thought to ferment propionic acid by the following reactions (Stadtman and Barker, 1951a):

$$4CH_3CH_2\overset{*}{C}OOH + 8H_2O \rightarrow 4CH_3COOH + 4\overset{*}{C}O_2 + 24H \qquad (7)$$

$$3CO_2 + 24H \rightarrow 3CH_4 + 6H_2O \qquad (8)$$

Tracer experiments indicated that the number 2 and 3 carbons of

propionic acid ended up as the carboxyl and methyl carbons of acetic acid, respectively. The fermentation of propionic acid is important since significant quantities have been found to result from the fermentation of complex organics (McCarty, 1964). As with the fermentation of ethanol, the true methanogenic species probably do not utilize propionic acid but live symbiotically with a non-methanogenic strain that does.

Other higher-order lipids and fatty acids must first be degraded by β-oxidation to a corresponding number of acetate units if the acid is even-carbon numbered, or acetates and one propionate if it is odd-carbon numbered. For butyric acid:

$$\overset{*}{C}H_3CH_2\overset{*}{C}H_2COOH + 2H_2O \rightarrow 2\overset{*}{C}H_3COOH + 8H \qquad (9)$$

It is most likely then, that organic matter is completely degraded to acetic acid, formic acid, methanol, carbon dioxide, or hydrogen before being used by true methanogens.

Acetate fermentation: Stadtman and Barker (1949, 1951b) used tracers to show that methane is formed directly and entirely from the methyl moiety, and carbon dioxide exclusively from the carboxyl carbon, of the acetic acid molecule:

$$\overset{*}{C}H_3COOH \rightarrow \overset{*}{C}H_4 + CO_2 \qquad (10)$$

Using acetic acid labelled with deuterium, Pine and Barker (1956) confirmed the reaction:

$$CD_3COOH \xrightarrow{H_2O} CD_3H + CO_2 \qquad (11)$$

and with normal acetate in deuterated water they showed:

$$CH_3COOH \overset{D_2O}{\rightarrow} CH_3D + CO_2 \qquad (12)$$

These reactions further demonstrate the exclusivity of methane form-

ation from the number two carbon of acetate. From the mechanisms of β-oxidation of fatty acids to acetate units, it follows that the even-numbered carbons of a long chain fatty acid will eventually be converted to methane while the odd carbons are oxidized to CO_2. In the case of odd-number carbon acids such as pentanoic and heptanoic, the final degradable segment is not acetate but propionate as mentioned earlier. By reactions (7) and (10), the first and second carbons of propionate should be converted to CO_2 and the third to methane, but tracer studies by Buswell *et al.* (1951) indicate that all three carbon atoms of propionate are converted to methane or carbon dioxide in varying degrees. They suggest that the formation of a symmetrical 4-carbon intermediate such as succinate from propionate could allow randomization of the first and second carbons of propionate and would account for their similarity of reduction.

Methanol fermentation: Tracer studies by Stadtman and Barker (1951b) demonstrated the fermentation path for methanol by showing that methane is formed from the methyl moiety of the methanol molecule. Deuterium isotope studies by Pine and Vishniac (1957) confirmed the reaction:

$$4CH_3OH \xrightarrow{D_2O} 3CH_3D + CO_2 + H_2O + DOH \qquad (13)$$

which implies that methane can be produced directly from methanol without being oxidized. The CO_2 produced by the reaction may be reduced to methane by other bacteria.

Formate fermentation: Methane production from formate is not well understood. Formate-decomposing methanogens were first isolated by Stadtman and Barker (1951c). Tracer experiments by Fina *et al.*

(1960) show that some methanogenic bacteria produce methane by direct reduction of formate. Direct reduction accounts for only a part of the total methane, however, and a large proportion is formed by reduction carbon dioxide.

CO_2 reduction: A simple carbon dioxide reduction theory was developed by van Niel (Barker, 1936) which suggests the reaction:

$$CO_2 + 4H_2 \rightarrow CH_4 + 2H_2O \qquad (14)$$

It is now agreed that a significant amount of methane is generated by methanogenic bacteria according to this reaction. Hydrogen is produced by a large group of fermenting bacteria, but apparently does not accumulate in sediments due to consumption by hydrogen-utilizing species. Carbon dioxide is generated by the non-methanogenic bacteria as well as in aerobic decomposition and sulfate-reduction processes (existing mainly as HCO_3^- and CO_2) and is abundant in anaerobic sediments.

Natural systems: Smith and Mah (1966) estimated that as much as 70% of the methane from methanogenic bacteria in natural systems originates from acetate, while the remaining 30% originates mainly from carbon dioxide reduction. In contrast, Claypool and Kaplan (1974) state that CO_2 reduction probably accounts for most of the methane produced in marine environments. They argue that the free energy change due to the conversion of hydrogen and carbon dioxide to methane is about three times as great as the change due to the fermentation of acetic acid so the former substrates could provide more energy for growth of methanogenic bacteria.

Carbon isotope fractionation effects could help in understanding

the predominant substrates of methanogenesis in various natural systems. Since the mechanism of acetate fermentation is different from that of CO_2 reduction, the isotopic character of resulting methane could change with the varying proportions of acetate or CO_2 contributions. Investigations in this regard might explain the wide variation in microbially-produced methane demonstrated in Figure 1.

Methods of Sample Collection and Analysis

Sediment samples were obtained using standard gravity coring techniques. Upon retrieval, the sediment contained in a plastic liner was removed from the core barrel and sectioned at specific depths. Five-centimeter sections were immediately extruded into 0.5-liter containers containing 125 milliliters of sodium azide poisoned, hydrocarbon-free seawater. The containers were capped and the headspaces flushed with helium or nitrogen through septa in the lids. The light hydrocarbons dissolved in the interstitial water were equilibrated with the gas phase by agitation for five minutes with a high speed shaker. The shaker also dispersed the sodium azide throughout the sediment to inhibit microbial activity. The head space gases were then analyzed or the containers inverted to form liquid seals around the lids and stored in darkness at near-freezing temperatures until analysis.

The system for analysis of the light hydrocarbons is shown schematically in Figure 9. Trap A contains activated charcoal maintained at liquid nitrogen temperature for removal of hydrocarbon impurities in the purge helium stream. The system is flushed by opening all valves and heating trap B to $\sim$90°C with a boiling water

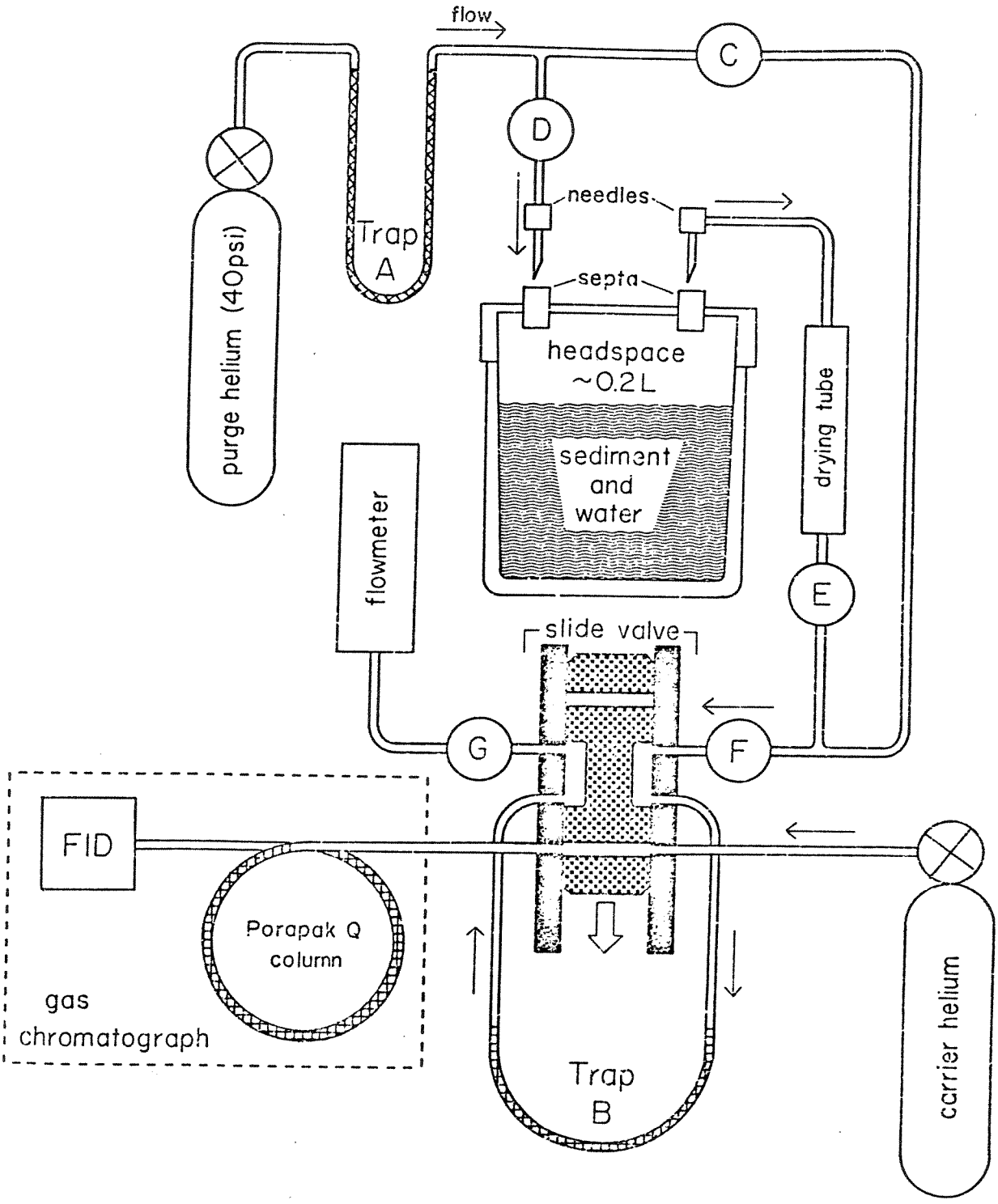

Fig. 9. Schematic of the system used for analysis of sediment light hydrocarbons.

bath. Trap B contains Porapak Q as a substrate to collect the hydrocarbons. Liquid nitrogen is placed around the trap and valve C is closed before the container is coupled to the system by inserting 20-guage needles into the septa (outflow line first). Helium enters the sample container through valve D, purges the headspace gases through an anhydrous magnesium perchlorate drying tube, and carries the light hydrocarbons into trap B where they are quantitatively collected.

The flush rate is adjusted by valve D to one liter per minute so that the hydrocarbons in the 0.2 liter headspace are quantitatively removed in 2 minutes. The trap is then isolated by closing valves F and G, and the container removed from the system. The trap is then heated, injected into the carrier stream by a pneumatic slide valve, and the hydrocarbons separated on a 3 meter, 1.5-mm I.D. Porapak Q column thermostated at 60°C. A flame ionization detector (HP 5710A Gas Chromatograph) is used in conjunction with an electronic integrator (HP3380) for the analysis of hydrocarbon concentrations. A typical chromatogram showing separation of the gases is shown in Figure 10.

Due to the solubility differences of the light hydrocarbons in seawater, the partition coefficients between the water-sediment mixture and headspace vary for each hydrocarbon. Partition coefficients for the individual hydrocarbons were determined by repeated equilibrations of samples after replacement of the headspace gas with helium. After purging, the sample container was re-agitated and the analysis procedure repeated. The individual partition coefficients were calculated by the equation:

$$K_i = 1 - (X_2/X_1)_i \qquad (15)$$

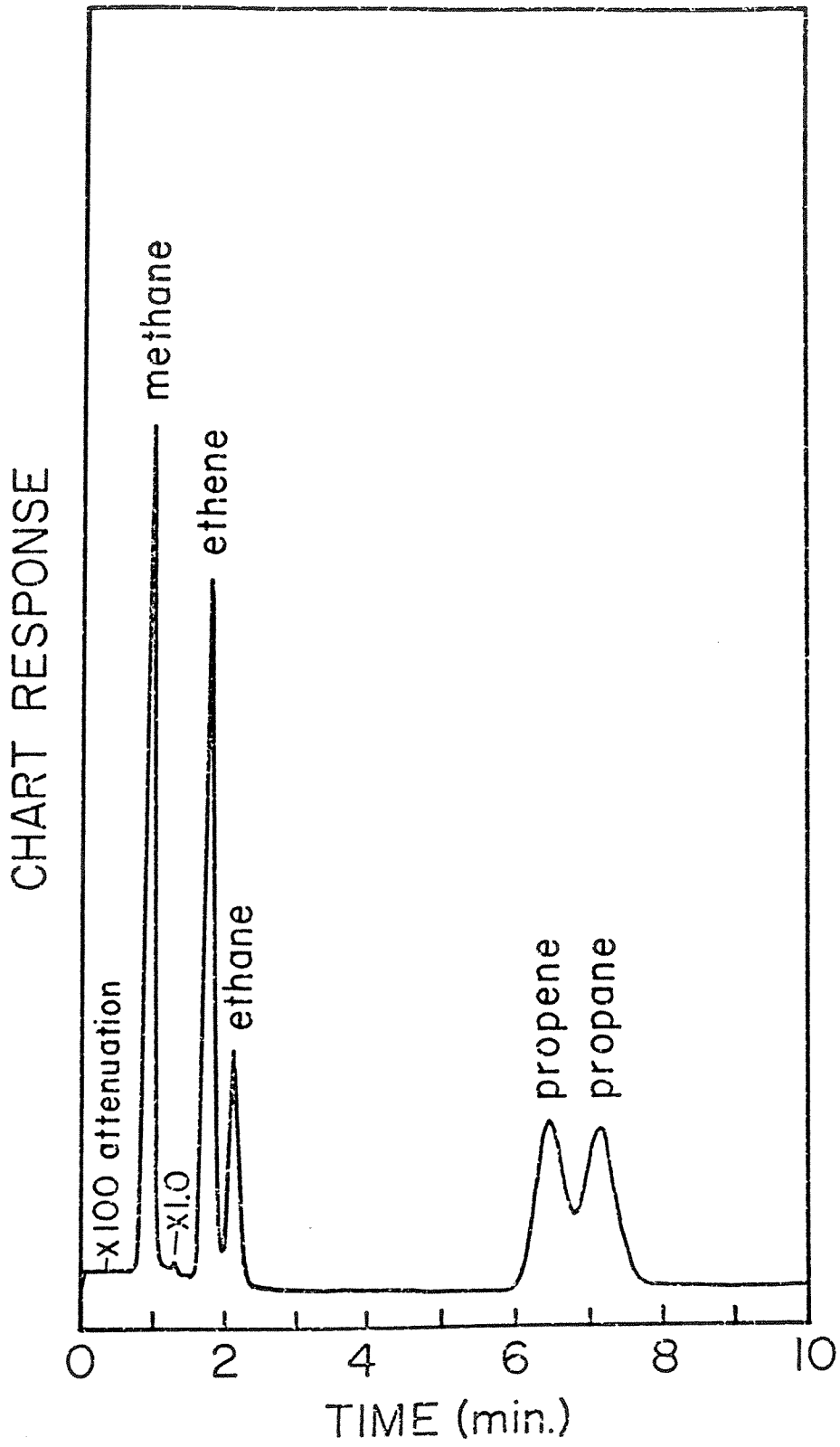

Fig. 10. Chromatogram of sediment light hydrocarbons.

where K is the partition coefficient for a particular hydrocarbon, and $(X_2/X_1)_i$ is the ratio of the detector response generated by component i from the first (X_1) and second (X_2) equilibrations.

These partition coefficients represent the fraction of total gas in a sample container that is present in the gas phase after an equilibration. Since at least 80% of every light hydrocarbon gas is removed from the sediment by each equilibration, simply summing the response from the first two equilibrations would represent at least 96% recovery of each gas from the sediment samples. Since coefficients for a group of cores taken and analyzed under similar conditions are quite repetitive, it is faster and more accurate to establish standard partition coefficients of each gas in a group of core samples by performing second equilibrations only on selected samples. The total response of a gas in a sample (T_i) can then be calculated using the equation:

$$T_i = (X_1/K)_i \tag{16}$$

After a volume of a standard gas mixture is trapped and injected into the gas chromatograph for calibration, concentrations of each gas can be calculated by the equation:

$$C_i = (C_{std}/X_{std})_i \times (V_{std}/V_{mud}) \times T_i \tag{17}$$

where gas concentration (C_i) is in microliters per liter wet sediment, C_{std} is the concentration of component i in a standard gas mixture in parts-per-million, X_{std} represents detector response generated by standard component i, V_{std} is the volume of standard gas in milliliters, and V_{mud} is the volume in milliliters of sediment placed in the sampling container.

TABLE 3. Integrator Units Obtained in Gas Partitioning Experiments

	Methane	Ethene	Ethane	Propene	Propane
Nanoliters of gas injected	380	16	17	15	18
Response, first equilibration (X_1)*	619.8	51.57	60.51	72.09	91.89
Response, second equilibration (X_2)	37.25	7.425	4.039	9.313	3.966
Calculated partition coefficient (K)	0.940	0.856	0.933	0.871	0.957
Calculated total units in sample (T)	659.4	60.2	64.9	82.8	96.0
Response, calibration standard (X_{std})	666.5	59.2	65.3	81.7	96.5
Percent deviation of T from X_{std}	-1.1	1.7	-0.6	1.3	-0.5

*Symbols are explained in text.

Table 4. Partition Coefficients of Two Groups of Samples

	Methane	Ethene	Ethane	Propene	Propane
Group A (20°C)	.944	.840	.897	.835	.950
Group B (40°C)	.955	.848	.919	.902	.960
*Solubility @ 20°C (ml/l)	34	105	45	107	32

*Calculated from data of McAuliffe (1966)

whereas Group B was heated to about 40°C in a hot water bath. The gas solubilities in 20°C distilled water calculated from the data of McAuliffe (1966) are also tabulated for comparison. Solubilities of most of these gases in seawater are not accurately known but should follow the same trend as in distilled water. Partition coefficients are a function of the solubilities of gases which, in turn, depend on temperature. The coefficients listed in Table 4 reflect the relative gas solubilities, decreasing with increasing solubility, etc. Group B partition coefficients were noticeably higher than those of Group A, indicating the negative effect of higher temperature on gas solubilities. Higher partition coefficients decrease the chance of error in the calculation of total gas in the samples because relatively more gas is removed from the sample during the first equilibration, so warming the samples to 40°C is now the preferred procedure.

It was also discovered after the majority of the samples for this work were analyzed that the glass containers containing the sediment-water mixture would not break if frozen. All subsequent samples were frozen before analysis for two reasons: (1) microbial activity should be completely inhibited and (2) the crystallization and expansion of the water during freezing tends to break up the structure of the clay particles, thus helping expose any light hydrocarbons occluded on or trapped inside the clay lattice. Indeed, higher apparent partition coefficients for all the light hydrocarbons, especially ethane and propane, were observed from analysis of frozen samples.

For each section of sediment sampled for light hydrocarbons, an adjacent sample of sediment was collected, weighed, freeze-dried, and

reweighed for the determination of weight percent interstitial water. From this percentage, porosity can be calculated and concentrations of light hydrocarbons are reported per liter interstitial water rather than wet sediment.

For measuring methane concentrations in excess of saturation at one atmosphere pressure such as are typically found in sulfate-free reducing sediments, the sampling method outlined here is inferior to the so-called *in situ* pore water samplers (or gas harpoons) developed by other investigators because of the possibility of outgassing during core retrieval. However, existing *in situ* samplers cannot collect enough pore water for precise determinations of light hydrocarbons other than methane. The sediment depth which can be reached and the sampling intervals are also limited with the *in situ* technique. Concentrations of hydrocarbon gas existing in the top few meters of the Texas continental shelf and slope sediments are far below saturation so that the escape of gas during handling by our sampling method is driven only by the processes of molecular diffusion from the core material. The time period that the core material is exposed to conditions causing loss of gas due to outward diffusion after extrusion is generally less than one minute. The depth within the core section to which significant gas loss occurs during this time can be estimated using a diffusion coefficient of 2×10^{-6} cm^2/sec (Martens and Berner, 1977) to be about 0.1 millimeter. In effect then, in one minute diffusive processes skim the outer 0.1 millimeter from the surface of the exposed core section, introducing a maximum reduction of one percent in total gas content of a sample.

Natural Interstitial Methane Variations

Introduction

Two basic questions arise from investigations of natural variations of methane in marine sediments. These are:

1. Is methane produced in the sulfate-reducing zone?
2. Is methane consumed in the sulfate-reducing zone?

Large accumulations of methane are generally observed in sediments only below the depth of microbial sulfate depletion. Claypool and Kaplan (1974) concluded from relative-energy-yield calculations that methane-producing bacteria should not be active in the presence of dissolved sulfate. Martens and Berner (1977) support this view using measured methane and sulfate distributions, concluding that methane is most likely produced only in the absence of dissolved sulfate and is consumed in the sulfate-reducing region upon diffusing upward.

Several other investigators have also observed this apparent consumption. The upward-concave methane profiles in sediments observed by Barnes and Goldberg (1976) and Reeburgh and Heggie (1977) as well as methane distributions in the Cariaco Trench (Reeburgh, 1976) can best be explained by the postulation of a methane sink in these anaerobic, sulfate-reducing environments. The most likely removal process is oxidation by the sulfate-reducing bacteria. Sulfate-reducers capable of oxidizing methane and other hydrocarbons using lactate as the principle carbon source have been cultured by Davis and Yarbrough (1966). In contrast, Sorokin (1957) could not detect methane consumption by sulfate-reducers when methane was the sole carbon source. This is not surprising, however, since there are no

known anaerobic microorganisms capable of using methane as the sole carbon source (Quayle, 1972). Martens and Berner (1977) showed that methane could not be the chief carbon substrate for the sulfate reducers in anoxic marine sediments because too much sulfate is reduced per mole of methane consumed. Apparently, sulfate reducers prefer other organic compounds, but methane may be used as a secondary carbon source.

On the question of methane production in the sulfate-reducing zone, Barnes and Goldberg (1976) have suggested that methane generation and sulfate reduction are not mutually exclusive processes. Rather, low concentrations of methane in sulfate-reducing pore water represent a balance between production by methanogenic bacteria and consumption by sulfate reducers. This hypothesis implies that methane is produced in the sulfate-reducing zone at a rate comparable to that below the depth of sulfate depletion. Nearly all of the methane produced in the sulfate-reducing zone must then be oxidized to CO_2 to account for the observed low concentration. However, preliminary studies in our laboratory indicate that there is insufficient isotopic change in ΣCO_2 in this region for methane to be produced and consumed at such a high rate. Instead, methane may be produced to a limited extent in the sulfate-reducing zone, but at a much smaller rate. As an example, Martens and Berner (1974) suggested that methane could be produced in the presence of interstitial sulfate within organic-rich, sulfate-free microenvironments such as the interior portions of decaying organisms.

Cappenberg has demonstrated an ecological relationship and an

overlap in distributions of the sulfate reducers and methanogens from field observations in lake muds (Cappenburg, 1974a), inhibition experiments (Cappenburg, 1974b), ^{14}C-labeled substrate experiments (Cappenburg and Prins, 1974), and mixed continuous culture studies (Cappenburg, 1975). Recently, Oremland and Taylor (1978) have found that the sulfate reducers and methanogens compete for available hydrogen so that when interstitial sulfate is reduced to a concentration low enough that it, rather than hydrogen, limits growth of sulfate reducers, methanogens can then use the available hydrogen for their growth. In other words, sulfate reducers dominate when sulfate is abundant and they effectively consume all available hydrogen produced in the sediments. When sulfate is no longer present in sufficient concentration to support cell growth of sulfate reducers, hydrogen becomes available to the methane producers.

Texas Shelf Sediments

Light hydrocarbon concentrations measured in sediments taken at 53 stations of the Texas continental shelf and slope are listed in Appendix A. Most of the stations are located on transects either progressing seaward from the shoreline or tangent to the coast. Methane concentrations are reported as microliters (NTP) per liter interstitial water and the other gases as nanoliters (NTP) per liter interstitial water. Estimated errors for dissolved gas determinations are less than ±3%.

Two transects comprised of 12 of the stations are illustrated in Figure 11. Transect I was sampled in March and Transect II in July. Interstitial methane concentrations along the two transects

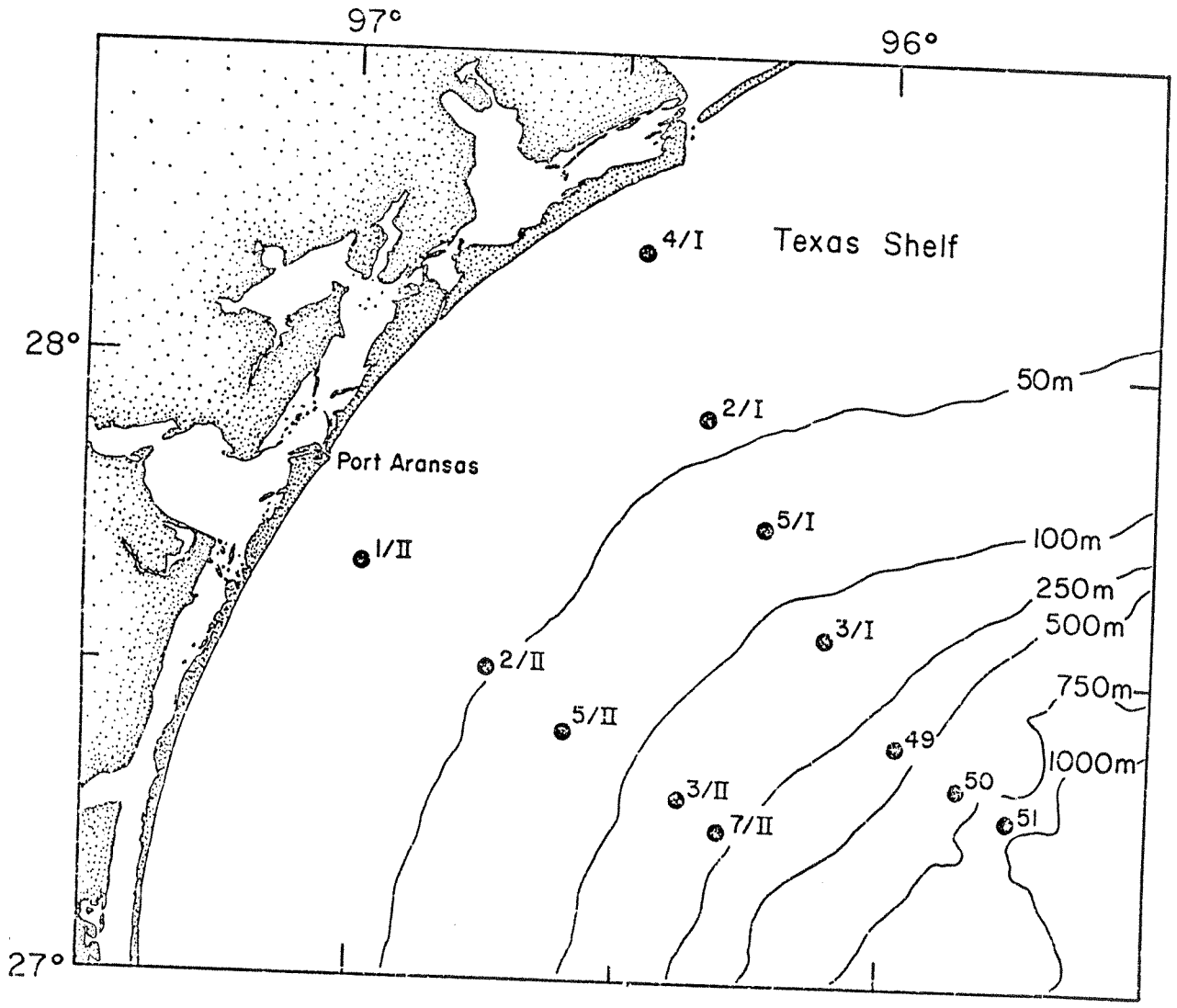

Fig. 11. Locations of cores along Transects I and II on the Texas continental shelf.

are plotted against sediment depth in Figures 12 and 13. Stations 4/I, 2/I, 5/I, 3/I, 49, 50, and 51 (Transect I) are shown in Figure 12 and Figure 13 contains Stations 1/II, 2/II, 5/II, 3/II, and 7/II (Transect II). Concentration profiles are positioned on the figures relative to the sea floor depth where the cores were taken (dashed lines represent sea floor contours). Water depths and distances from shore to the stations are written along the axes of the profiles. Concentration and sediment depth scales are identical in all profiles. The profiles are plotted in this manner to illustrate the change in methane concentration profiles with increasing water depth. Methane levels are generally higher at nearshore stations, and show very discernible maxima within the top 30 to 40 centimeters of sediment. Vertical concentration profiles of the other stations taken of the Texas shelf (Appendix A) generally show similar trends to the stations comprising Transects I and II and are not presented here.

Interstitial sulfate in the top few meters of these shelf sediments has not been significantly depleted, and in this area of the South Texas shelf sulfate is found down to several meters below the sediment surface, so methane should not produced so extensively in the surface sulfate-rich sediments.

Sackett *et al.* (1977b) have measured water column methane concentrations monthly over the last two years in the South Texas shelf area. Methane maxima in near-bottom waters have been consistently observed in some areas, but few concentrations above 0.4 microliters per liter have been observed. Therefore, methane concentrations in surface sediments as high as several hundred microliters per liter

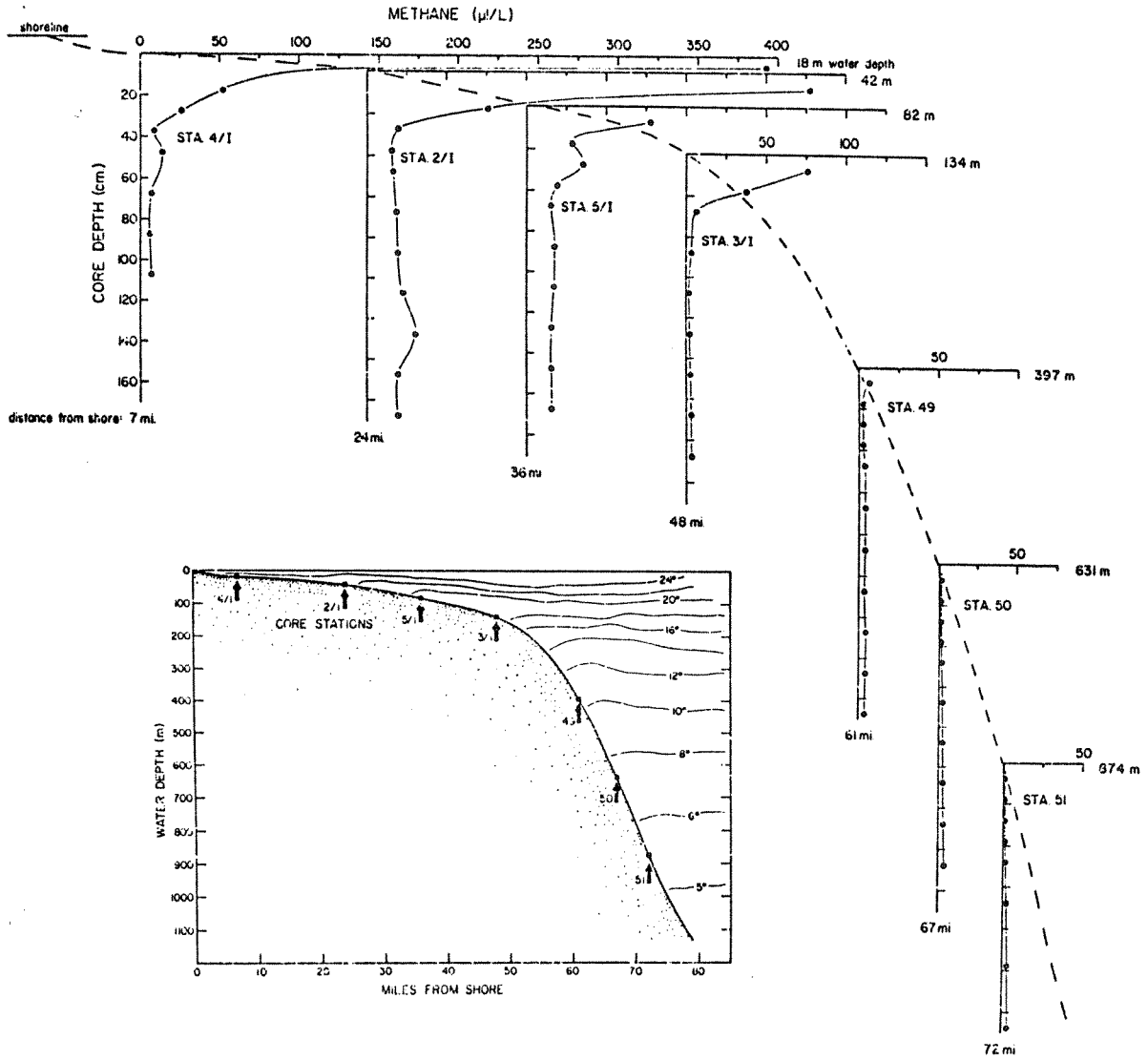

Fig. 12. Interstitial methane along Transect I, positioned on the sea floor contour. Inset shows the general temperature structure of the area in spring.

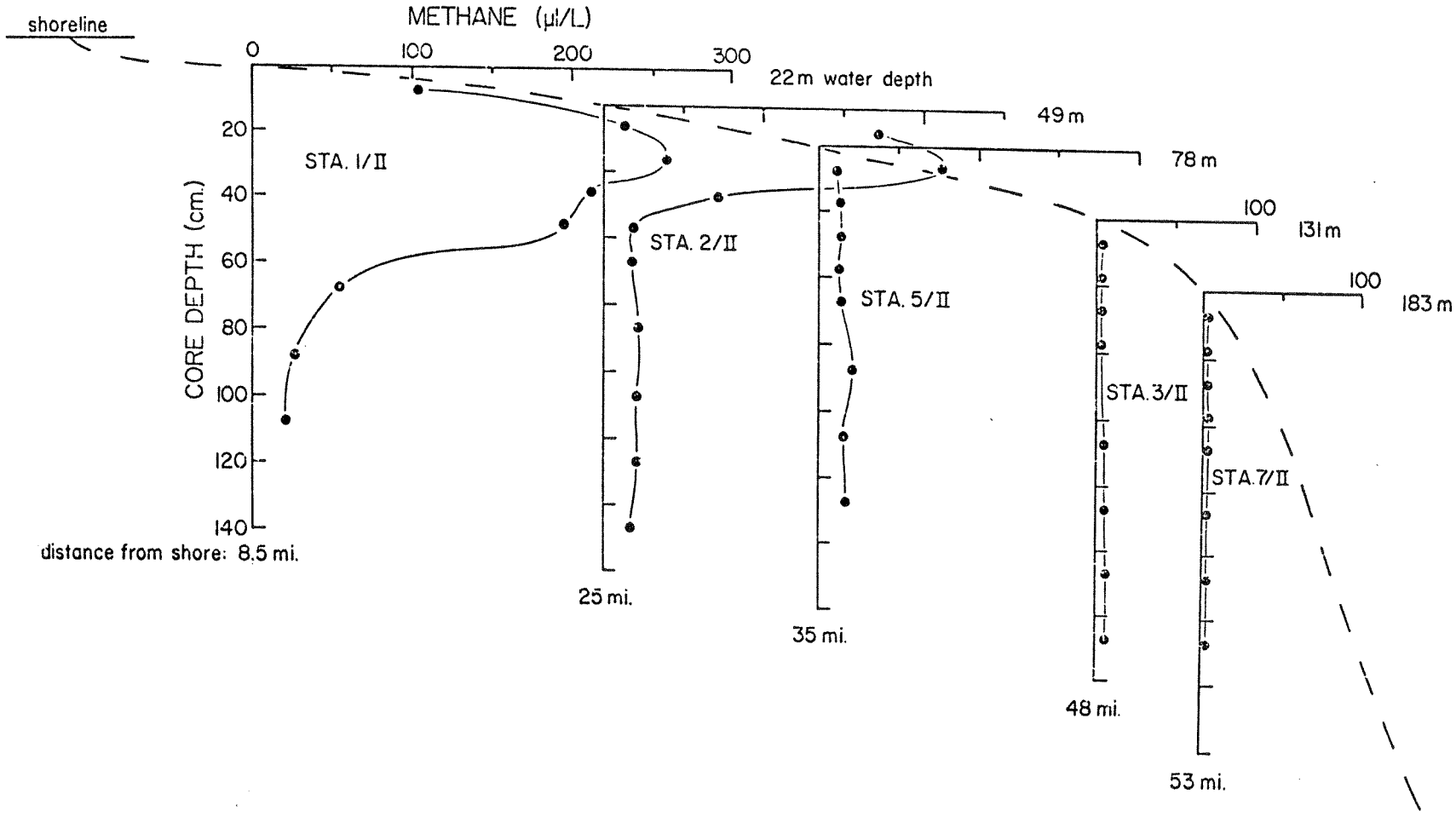

Fig. 13. Interstitial methane along Transect II, positioned on the sea floor contour.

cannot be a result of diffusion downward from the water column, but result rather from *in situ* production.

That microbial populations are most extensive and physiologically versatile in the top layers of sediment has been known for some time (Certes, 1884; Russell, 1892; Drew, 1912; Lloyd, 1931; Reuszer, 1933; Zobell and Anderson, 1936; Kaplan and Rittenburg, 1963). Wherever vertical profiles of bacterial populations have been examined in marine sediments, a progressive decrease in the bacterial populations with increasing sediment depth has been observed (Zobell, 1946). The decrease is most rapid in the top few centimeters of sediment, and generally slows, becoming erratic with increasing depth, as illustrated by Table 5 taken from Zobell (1942). The vertical distribution of bacteria in sediments can be directly correlated with available organic matter and nutrient material. Much of the organic matter of marine sediments consists of material which is fairly refractory to bacterial decomposition, so changes in total organic matter with sediment depth due solely to microbial activity are seldom observable. The surface sediment is subject to a constant rain of organic detritus, however, including the more labile material which is rapidly consumed by bacteria before burial. As available organic matter and nutrients disappear with depth in the sediment, bacterial populations decrease.

There are obvious similarities between vertical bacterial distributions and the vertical methane profiles of nearshore stations illustrated in Figures 12 and 13. The two figures suggest that the methanogenic bacteria exist in large numbers near the sediment surface, and are possibly active inside small, sulfate-free microenvironments

Table 5. Bacteria Per Gram Sediment at Three Core Sites off the California Coast (from Zobell, 1942)

Core Depth (cm)	Bacteria per gram	Bacteria per gram	Bacteria per gram
0-2	840,000	38,000,000	7,500,000
3-5	102,000	940,000	250,000
10-12	63,000	88,000	160,000
23-25	19,000	36,000	23,000
36-38	1,500	2,400	8,700
48-50	2,200	400	2,100
74-76	370	180	600
99-101	190	330	200
150-152	210	250	300
201-203	140	130	100
252-254	140	290	150
Water depth	430m	950m	1090m

in the sediment after reduction of ambient sulfate has occurred. These micro-niches could take the form of fecal pellets, decaying organic matter, shell fragments, or flocculent clay particules. Methane produced in the microenvironments apparently diffuses into the surrounding sediment where it is bacterially oxidized, and upward into the overlying bottom water where it is removed by advection.

The shelf stations taken along Transects I and II (Figures 12 and 13) are at similar water depths and distances from shore, so if only these factors affect methane concentrations, corresponding profiles in the two figures should ideally be identical. This is not the case since the profiles along Transect I show methane increasing upward to the 5-10 cm interval, whereas the profiles of Transect II indicate a methane maximum at the 25-30 cm interval (concentrations in the 0-5 cm interval are unknown). The lack of uniformity in the distribution of bacteria among the various sediment types observed on the Texas shelf might explain these differences. Bacterial distributions are intimately associated with the physical consistency and organic content of the sedimentary deposits. In some areas, submarine topography has a greater influence on the median particle size and organic content of the sediments than the depth of water or distance from shore. Zobell (1946) states that bacterial populations are more closely related to the character of the sediments than to their distance from land and, as a rule, sand contains fewer bacteria than sediments consisting of smaller particles. The greater abundance of bacteria found in finer sediments is attributed primarily to a higher organic content.

The absence of high surface methane concentrations along Transect II could also be attributed to seasonal influences. Transect II was sampled in July, whereas Transect I was sampled in March. Nearshore water temperatures approaching 30°C in the summer months may be above the temperature range for optimum growth of the methanogens, effectively inhibiting methane production. Other possible seasonal effects include changes in fluxes of organic detritus and nutrients to the surface sediments.

Figures 12 and 13 also illustrate the disappearance of the surface methane maximum in cores taken progressively further offshore. In Figure 12, the methane maximum decreases significantly at Station 3/I, is barely visible at Station 49, and disappears at Stations 50 and 51. The decrease of the near-surface methane with increasing distance from shore can be explained by changes in microbial activity rather than changes in populations. Bacterial numbers generally decrease outward on the Texas continental shelf (J. Schwarz, personal communication), although millions of bacteria per gram of sediment are still found in sediments several thousands of meters deep, so the observed decrease of the methane maximum cannot be explained on the basis of bacterial numbers alone. In some areas there are actually more bacteria in sediments from deep water where the temperatures are 3-7°C than in those from shallow waters where bottom temperatures are considerably higher (Zobell and Anderson, 1936). The optimum temperatures for the multiplication of marine bacteria probably range from 20-25°C, but while lower temperatures retard reproduction, survival of the bacteria is prolonged.

General water temperature contours at the study area are shown in the insert of Figure 12. These temperatures are representative of late spring but do not change significantly below 200 meters throughout the year. Stations are marked on the insert and surface methane concentrations correlate well with the temperature contours. Temperatures below ∿15°C and decreased labile organic inputs beyond the shelf break apparently inhibit microbial activity and methane production to an extent that methane diffuses out of the sediment before it can accumulate as it does nearer shore. The increase in hydrostatic pressure may also suppress production of methane in these slope sediments. For example, Jannasch *et al.* (1971) found that rates of microbial activity were 10 to 100 times slower in the deep-sea than in controls at comparable temperatures.

Changes in production with temperature again imply that surface methane concentrations in Texas shelf sediments are seasonally influenced. Low temperatures nearshore in winter (∿12°C) could inhibit microbial activity and slow methane production. Warming of the sediments in the spring, enhanced by increased detrital input from phytoplankton blooms and runoff, might accelerate methane production in the microenvironments, causing methane oscillations at the tops of nearshore sediments. These oscillations, if real, could provide and excellent means of evaluating the magnitude of the effective diffusion coefficient of methane in porous sediments.

Sediment methane concentrations below the surface maxima also vary with distance from shore. On the upper continental shelf, methane levels in this layer generally range from 15 to 20 microliters per

liter pore water and showed no trends with depth in the upper 1.5 meters of sediment. In the slope region, concentrations decreased progressively in an offshore direction to less than 5 microliters methane per liter pore water, and slight increases in methane concentration were observed with depth in the sediment. Higher methane concentrations in the shelf region are attributed to greater microbial activity in the sediments as a result of higher temperatures and greater amounts of available organic material than in sediments deposited further offshore.

In contrast to the erratic shelf profiles, the relatively well-behaved gradients on the slope lend themselves more readily to the application of simple mathematical models describing the kinetics of methane production. These slope concentrations are apparently the result of an equilibrium between diminished methane production within microenvironments, methane oxidation by sulfate-reducing bacteria, and diffusion of methane from the top layer of sediment into the overlying water. A discussion of methane profiles in slope sediments follows.

Slope Sediments

The behavior of a chemical species dissolved in pore water can be described by the equation:

$$(\partial C/\partial t)_x = dC/dt - \omega \partial c/\partial x \qquad (13)$$

where C is the concentration of the dissolved species, t is time, x is sediment depth measured positively downward from the moving sediment-water interface, and ω is the net rate of sediment accumulation (Berner, 1974). The total derivative dC/dt includes all processes affecting the

concentration of the dissolved species except those due to advection (sediment accumulation). For methane, changes due to mineral precipitation, dissolution and sorption reactions can be ignored and only diffusive and biological effects need be considered. Mathematically:

$$dC/dt = D\partial^2C/\partial x^2 + dC/dt_{biol} \quad (19)$$

where D is the effective diffusion coefficient for methane in the pore water-sediment system and dC/dt_{biol} describes effects due to biological production and consumption of the gas.

Strictly speaking, the effects of porosity changes and compaction on the advective and diffusive terms should be included in equations 18 and 19 (Berner, 1975), but the assumptions that pore water velocity is equal to sediment grain velocity and that D is constant with depth greatly simplify solutions. Likewise, no attempt is made here to correct for possible mixing by bioturbation (Schink and Guinasso, 1977), a phenomenon restricted to the upper tens of centimeters in slope and abyssal sediments.

The kinetics of biological methane production and consumption have not been well described. Bacterial consumption or production of a chemical species in the sediment is assumed to be first order with respect to the material undergoing decomposition (Berner, 1974; Lerman, 1977). The assumption that methane is microbially consumed following first order kinetics has been used to explain methane profiles in anoxic marine sediments (Martens and Berner, 1977). It is postulated here that methane is consumed in the zone of active sulfate reduction at a rate proportional to its concentration and is concurrently produced in this zone within sulfate-free microenviron-

ments. Methane consumption can be represented mathematically by:

$$\partial C/\partial t_{cons} = -KC \tag{20}$$

and production by:

$$\partial C/\partial t_{prod} = K'G \tag{21}$$

where K and K' are the respective rate constants for methane production and consumption (sec^{-1}), and G represents the concentration of substrate decomposed for its production.

In this case, G is not the concentration of total organic material or even the labile fraction consumed by all bacteria, but only the compounds used for the production of methane. The compounds in recent sediments represented by G are apparently not significantly depleted by methane production in microenvironments above the sulfate-free zone, since activities of methanogenic bacteria increase drastically below this interval. The assumption that G is effectively constant throughout sediments above the sulfate-free depth simplifies the microbial production term (equation 21) to:

$$\partial C/\partial t_{prod} = J \tag{22}$$

where J represents a constant production of methane with time.

Assuming steady-state conditions for the distribution of methane with time in marine sediments yields:

$$(\partial C/\partial t)_x = D\partial^2 C/\partial x^2 - \omega \partial C/\partial x - KC + J = 0 \tag{23}$$

If the concentration of the species approaches a constant value with "infinite" depth, the solution to equation 23 is given by Lerman (1977), who demonstrates that the rate of sedimentation (advective term) can be neglected if $\omega^2/4D << K$ in equation 23. This simplification is valid for methane diagenesis in slope and abyssal sediments (as will

be shown) so equation 23 reduces to:

$$D(d^2C/dx^2) - KC + J = 0 \qquad (24)$$

If $C=C_o$ at the sediment-seawater interface (x=0) and $C \to C_x$ as $x \to \infty$, the solution to equation 24 is given by:

$$C = J/K + (C_o - J/K)\exp[-x(K/D)^{\frac{1}{2}}] \qquad (25)$$

The ratio J/K has units of concentration and represents the constant level of methane (C_x) resulting from the balance of production and consumption as diffusive effects disappear with increasing sediment depth. The reciprocal of $(K/D)^{\frac{1}{2}}$ has units of length and represents the scale length (1/e length) set by diffusion and consumption. The scale length represents the depth at which methane concentrations are within ~37% (e^{-1} x 100) of the asymptotic value, C_x. Methane concentration profiles with depth in the top few meters of marine sediments should agree with the function described by equation 25 if effects of a deeper zone of extensive methane production can be neglected and biological production and consumption actually occur according to the assumptions of the model.

The exact depth of sulfate depletion and accompanying zone of extensive methane production is unknown for most areas of the Gulf of Mexico but the existence of a methane "horizon" at some sediment depth has been commonly observed by seismic techniques on the Texas-Louisiana shelf (Roemer, 1976) and in the abyssal region by Deep Sea Drilling Project borehole cores (Claypool *et al.*, 1973). In the highly reducing, rapidly accumulating Mississippi Delta sediments, interstitial sulfate is quickly depleted and extensive microbial production of methane occurs a few centimeters below the seawater-

sediment interface. This methane horizon exists progressively deeper in the sediment in an offshore direction, the depth being a function of sedimentation rate, temperature, organic input, and oxygen availability from overlying water.

The existence of this drastic increase in methane concentration due to extensive microbial production at some sediment depth contradicts the assumption made for the solution of equation 24 that concentrations approach a constant value with infinite depth. The methane horizon is deep enough in slope and abyssal sediments of the Gulf, however, that the effects of upward diffusion of methane from the horizon are negligible in the top few meters and vertical profiles can be approximated by equation 25. The more general solution of equation 24, incorporating the effects of the methane horizon, will be discussed later.

Sediment samples from six Gulf of Mexico locations (Figure 14) were analyzed and modeled using the previously described procedures. Figure 15 shows interstitial methane and sulfate concentrations (measured every 20 centimeters in a 9 meter piston core) for Station 54 plotted against sediment depth. A profile generated by equation 25 is shown on the figure using $C_o=0$ (the overlying water methane concentration in this region was about 0.05 µl/L) and best-fit values for $(D/K)^{\frac{1}{2}}$ and J/K. The slight change in the profile due to the inclusion of the advective term of equation 23 using a sedimentation rate of 0.05 cm y^{-1} (Shokes, 1976) is illustrated by the dashed line. Because the solution profile of Figure 15 is only slightly shifted by the advective term, precision indicated by data scatter does not

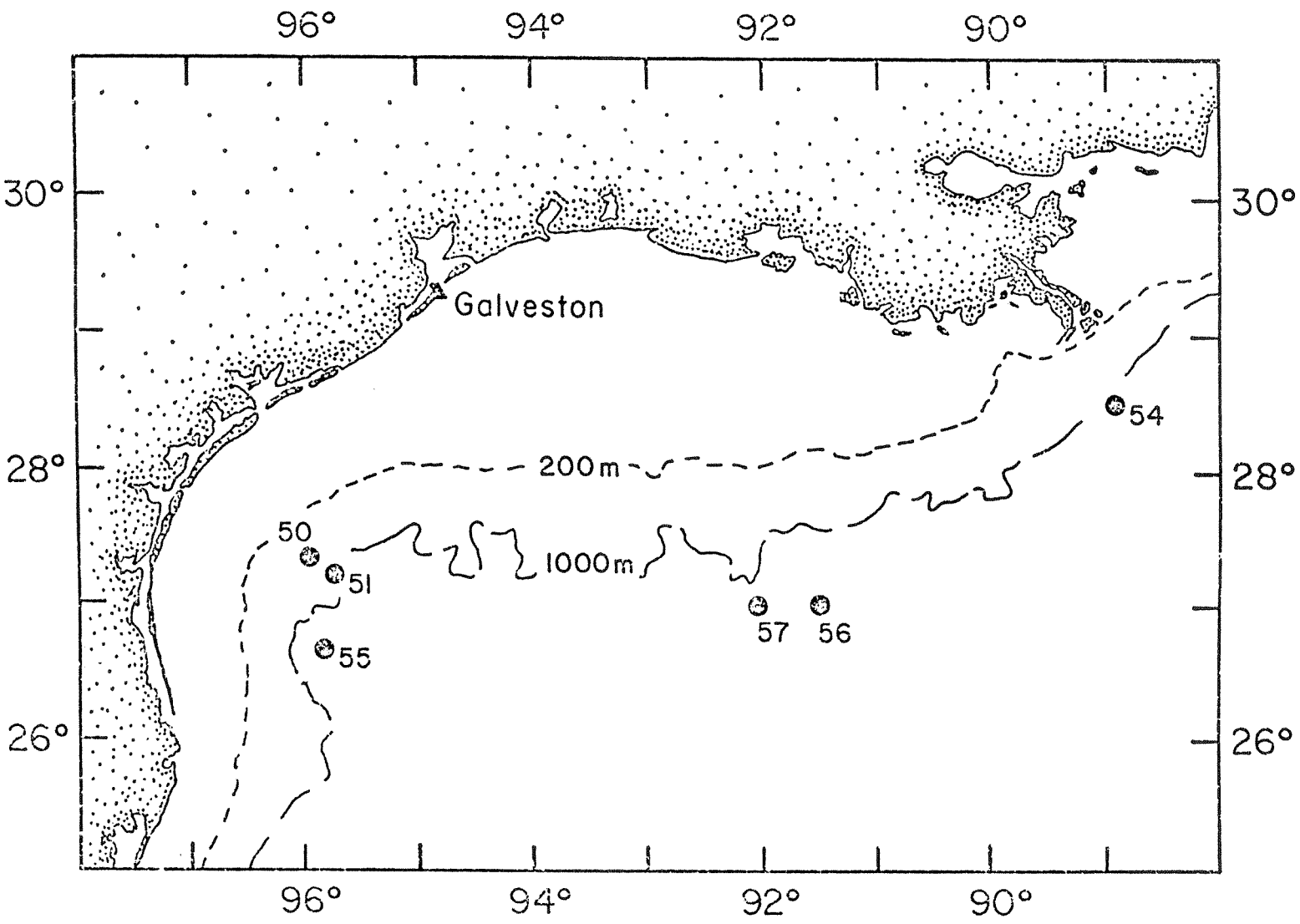

Fig. 14. Locations of cores taken off the shelf in the northern Gulf of Mexico.

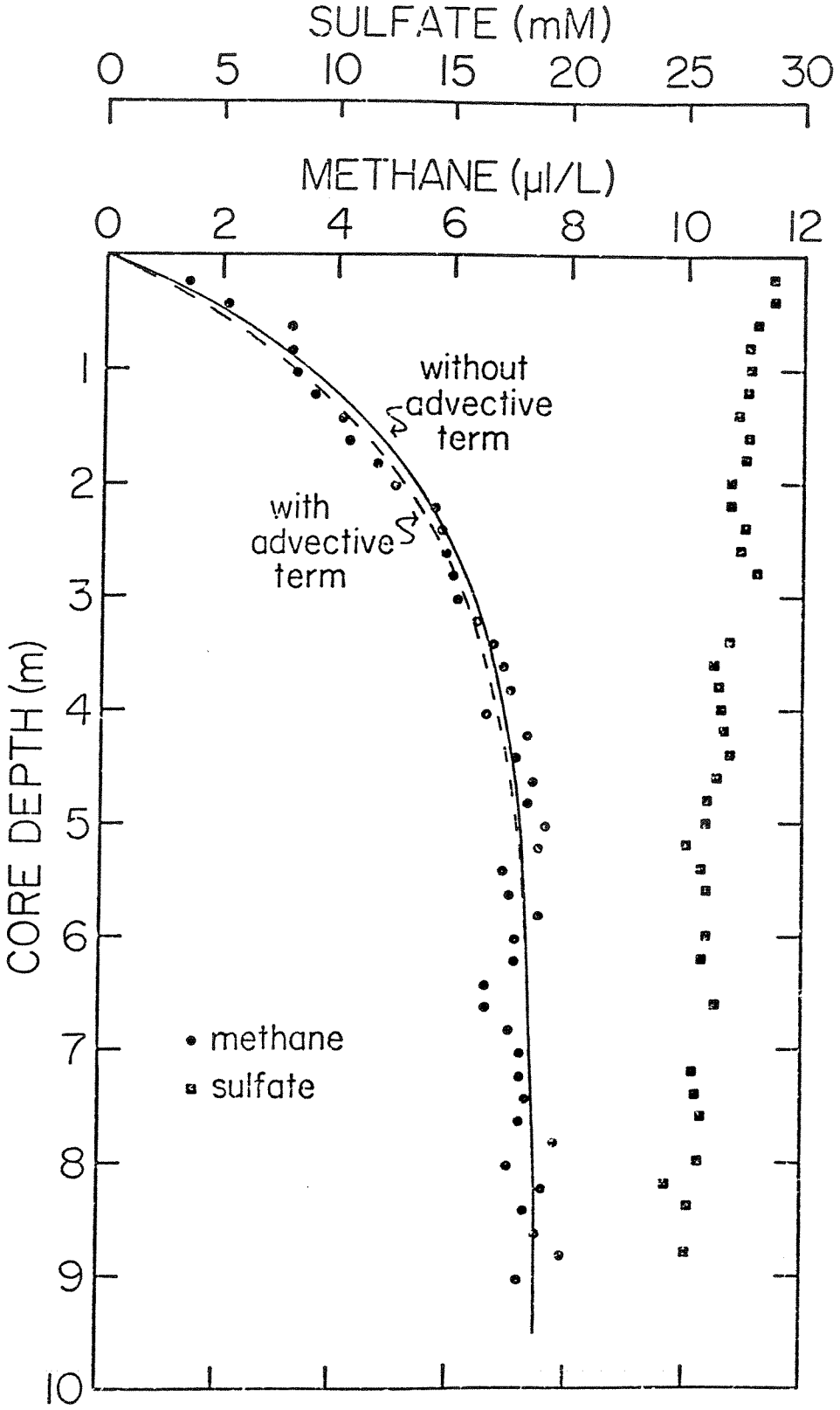

Fig. 15. Interstitial methane and sulfate at Station 54.

justify the inclusion of this complicating term. For the data presented here, advective effects due to sedimentation will be ignored since the data can be adequately described without them, and the simpler equation 24 can be used.

The measured methane concentrations at Station 54 level off at 7.5 µl/L at depth, indicating that a balance between production and consumption is established. Because interstitial sulfate remains greater than 25mM throughout the core (although there is a decrease with depth), methane production is probably limited to sulfate-free microenvironments. The gradual decrease in sulfate is indicative of microbial activity to 9 meters depth. In equation 25, the ratio of production to consumption, J/K, is demonstrated by the constant methane concentration of 7.5 µl/L as the effects of diffusion out of the sediment disappear with increasing sediment depth. The scale length $(D/K)^{\frac{1}{2}}$ can be estimated by a best-fit curve of equation 25 to the data to be 160 cm and if a reasonable value of D is assumed, values for K and J can be established.

The diffusion coefficient of methane at infinite dilution in water at various temperatures is given by Sahores and Whitherspoon (1970). Assuming a pore water temperature of 4.5°C and salinity of $35°/_{oo}$ results in a value of 8.3×10^{-6} cm^2/sec. Correcting for the effects of porosity and tortuosity of the sediments (Li and Gregory, 1974) yields and effective diffusion coefficient of methane through sediments of 4.6×10^{-6} cm^2/sec. Estimates of J and K are in error proportionally to any error introduced by this estimate of D.

Using a value of 4.6×10^{-6} cm^2/sec for D, values for J and K

are calculated to be 1.3×10^{-9} µl/L-sec and 1.8×10^{-10} sec^{-1}, respectively. Although no estimates of methane production rates in microenvironments are reported in the literature, Martens and Berner (1977) estimate a consumption rate of $K = 8 \times 10^{-9}$ sec^{-1} for the anoxic sediments of Long Island Sound. The consumption rate reported here, 40 times slower than in Long Island Sound, is reasonable considering the lower sediment temperature, sedimentation rate, organic carbon input and slower sulfate reduction rate. A comparison of the decrease in sulfate with depth at Station 54 to that of Martens and Berner (1977) indicates that interstitial sulfate is apparently reduced at a rate more than 100 times faster in Long Island Sound sediments, supporting the forty-fold discrepancy in methane consumption rates. (Note that K is indeed much larger than $\omega^2/4D$ and advective effects can be neglected.)

Methane and sulfate concentrations from gravity cores taken at Stations 50, 51, and 55 are presented in Figure 16. These cores do not extend to sediment depths where methane concentrations presumably become constant. In these cases, asymptotic methane concentrations representing J/K values as well as estimates of D/K can still be projected using best-fit curves generated by equation 25. These theoretical curves are plotted on Figure 16 for comparison with the data, and estimates of J and K are listed in Table 6. At Station 50, C_o is apparently not near zero as observed for the other stations, but rather about 0.75 µl/L. This station is located on the outer Texas shelf and the observed near-surface methane concentration can be attributed to enhanced microbial production at the sediment surface

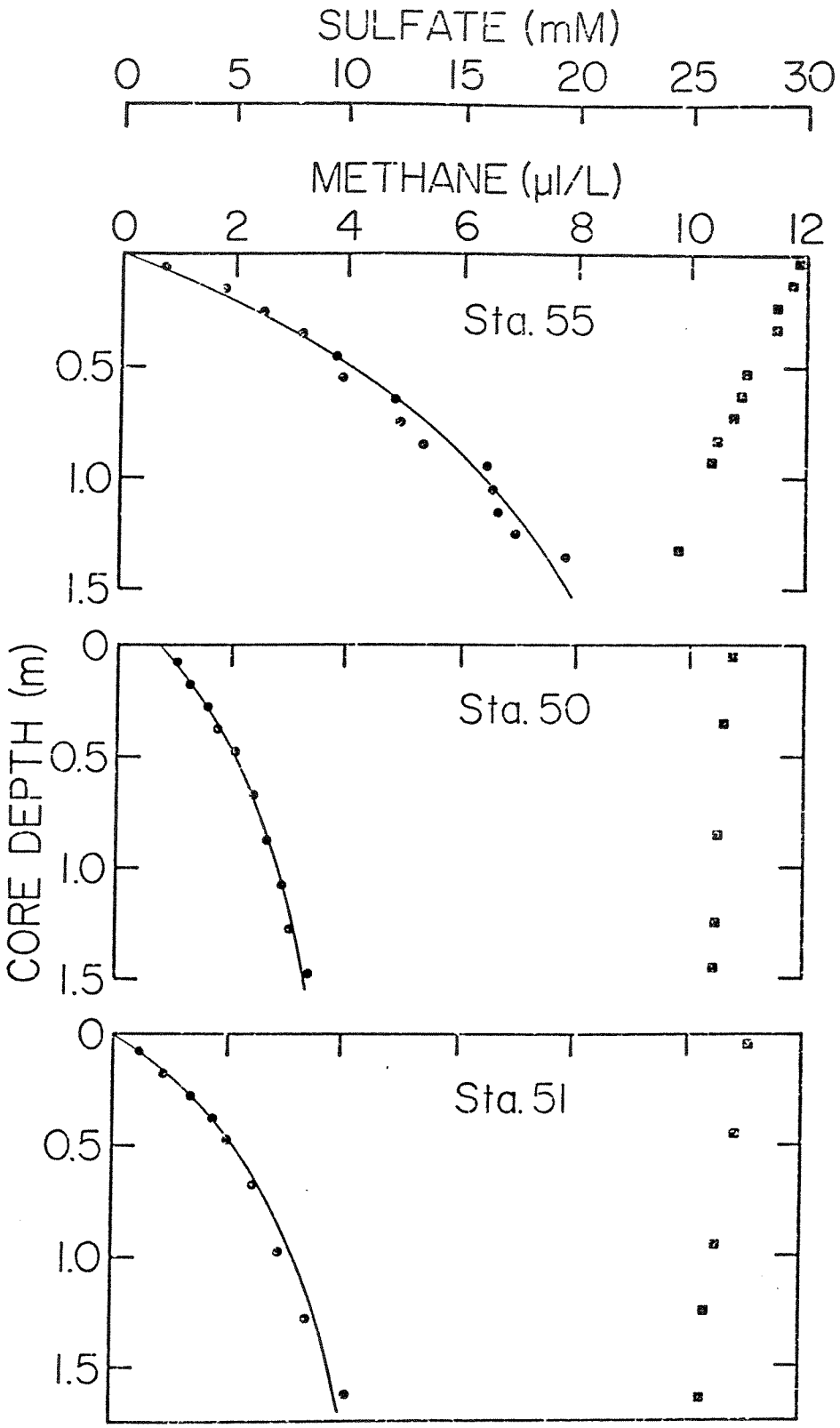

Fig. 16. Interstitial methane and sulfate at Stations 50, 51 and 55.

TABLE 6. Rates of Production and Consumption, Minimum Horizon Depth, Scale Length, and Flux of Methane

STATION	C_o (µl/L)	J x 10^{10} (µl/L-sec)	K x 10^{10} (sec^{-1})	MINIMUM Z (meters)	$(D/K)^{\frac{1}{2}}$ (meters)	FLUX (nl/cm^2yr)
50	0.75	20	5.1	14.0	0.95	5
51	0	32	7.1	12.0	0.81	8
54	0	13	1.8	28.5	0.16	7
55	0	53	5.6	12.5	0.91	15
56	0	150	14.4	6.85*	0.57	27
57	0	65	9.0	11.0	0.71	15

*apparent depth rather than a minimum value.

as described earlier. At all stations, gradual sulfate reduction is observed in the depth interval sampled. Agreement of the methane data with theoretical profiles suggests that concentrations in the top few meters of slope and abyssal Gulf sediments can be adequately described by a balance of the effects of upward diffusion, microbial consumption, and production in sulfate-free microenvironments.

Figure 17 shows interstitial methane and sulfate concentrations in a gravity core taken from an intraslope basin (Station 56). Sulfate decreases rapidly with sediment depth at Station 56, approaching one-half of the overlying water concentration at 2 meters depth. Extrapolation of the interstitial sulfate concentration to zero suggests that the depth of complete removal is about 5-7 meters. The zone of extensive emthane production and corresponding methane horizon should occur just below this depth. Methane concentrations do not approach a constant value in the first two meters, but continue to increase with depth. Upward diffusion from the zone of high methane concentration probably causes the downward-increasing methane profile of Station 56. This profile requires another solution to equation 24 to describe concentration changes. Rather than using the lower boundary condition of $C=C_x$ as $x\to\infty$, the more realistic boundaries of $C=C_o$ at $x=0$ and $C=C_x$ at $x=Z$ can be applied to equation 24, where C_x represents methane concentration at the depth of the methane horizon, Z. The solution to equation 24 using these boundaries is considerably more complex, but can be simplified using two assumptions: (1) $C_x>>J/K$ and (2) $Z>4(D/K)^{\frac{1}{2}}$. The first assumption is justifiable for methane because concentrations at the methane horizon (C_x) are generally greater than 50 ml/L, whereas

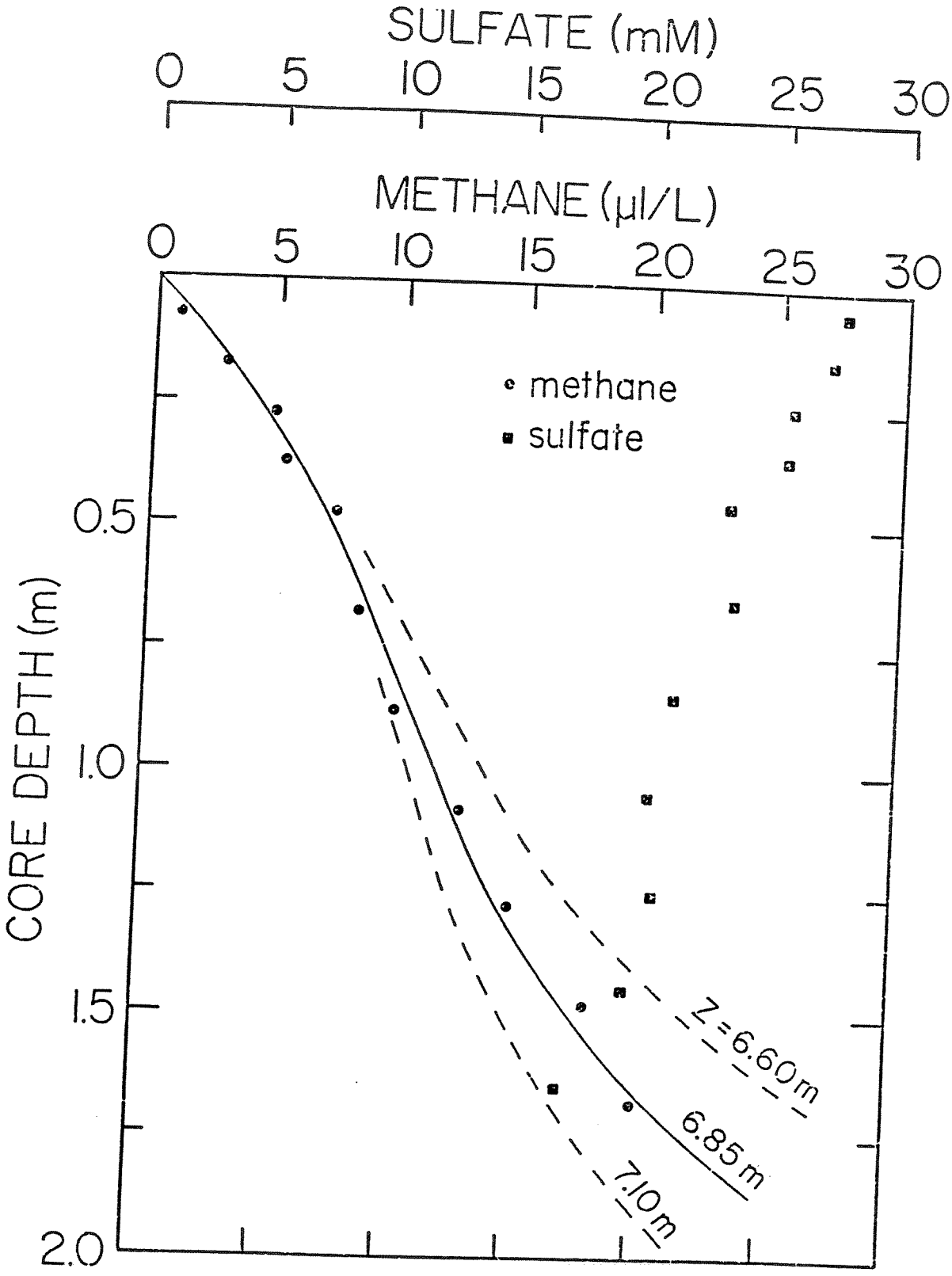

Fig. 17. Interstitial methane and sulfate at Station 56.

J/K in the sulfate-reducing zone is generally less than 10 µl/L. The second assumption requires that the depth of the methane horizon be greater than about 4 times the scale length set by diffusion and consumption (the value 4 is used because $e^{4} >> e^{-4}$). The validity of assumption 2 is not quite so apparent, but will be demonstrated later when minimum values of Z are presented.

The modified solution of equation 24 using the new boundary conditions and assumptions is given by:

$$C = A + (J/K) + B \tag{26}$$

where $$A = (C_o - J/K)\exp[-x(K/D)^{\frac{1}{2}}]$$

and $$B = C_x[\exp(x-Z)(K/D)^{\frac{1}{2}} - \exp(-x-Z)(K/D)^{\frac{1}{2}}]$$

Three observations about equation 26 should be noted:

(1) The terms (A + J/K) are identical to equation 25 and control the the distribution described by equation 26 at near-surface depths, representing the effects of diffusion out of the sediment.

(2) The value of J/K controls the methane concentration where diffusive effects are negligible between the boundary regions, representing a balance between production and consumption.

(3) The terms (J/K + B) control methane concentrations near the depth of the methane horizon (as $x \rightarrow Z$), representing the effects of upward diffusion of methane from the level of extensive production in the sulfate-free zone.

Ideally, measured methane concentrations at the horizon as well as the horizon depth are needed to produce accurate best-fit solutions to equation 26 with the methane concentration data of Station 56. these measured C_x and Z values are difficult to obtain in slope and

abyssal regions, however, since Z is generally greater than 10 meters, a depth not attainable by gravity coring and rarely obtainable by piston coring. C_x values measured in the shallow water sediments of the Mississippi Delta region range from 75-100 ml/L and are probably in the same range in slope and abyssal regions.

The methane data from Station 56 on Figure 17 agree with the theoretical profile of equation 26 (solid line) using J, K, C_x, and Z values of 1.5×10^{-8} µl/L-sec, 1.4×10^{-9} sec^{-1}, 100 ml/L, and 6.85 meters, respectively. The Z value of 6.85 meters agrees with the earlier extrapolation of decreasing interstitial sulfate to zero at 5-7 meters. The exact value of C_x is relatively unimportant since $C_x >> J/K$. The depth of the horizon (Z) is important, however, as illustrated by the effect on the Station 56 solution profile of "raising" and "lowering" the horizon only 25 centimeters, shown by the dashed lines on Figure 17. The effect can be used to predict a minimum methane horizon depth for the other stations by shifting the depth of a hypothetical horizon until its diffusive effect becomes significant at the depth were data is available, and begins to distort the theoretical profile in conflict with the observed methane distribution. As an example, methane and sulfate data measured at Station 57 are presented in Figure 18 along with solution curves using various values for the hypothetical horizon depth, Z. Values for J, K, C_o, and C_x are held constant at 6.5×10^{-9} µl/L-sec, 9.0×10^{-10} sec^{-1}, 0 µl/L, and 100 ml/L, respectively. For Z values 12 meters and greater, effects of upward diffusion from the horizon are negligible and the resulting solution curves do not change significantly within the depth range of

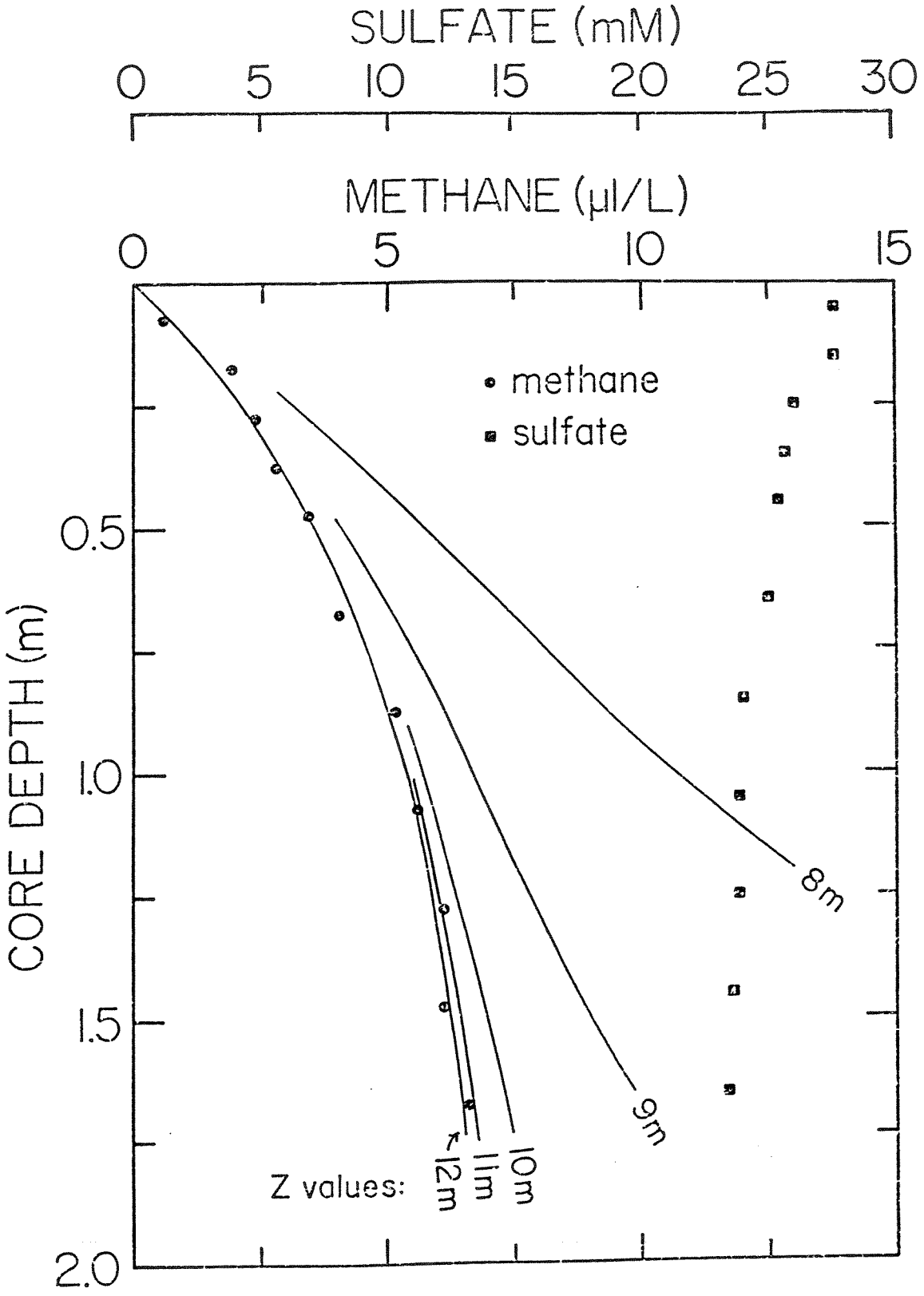

Fig. 18. Interstitial methane and sulfate at Station 57.

available data. When the hypothetical horizon is raised to 11 meters, only a very slight shift in the resulting solution curve is observed. A Z value of 10 meters produces a more significant shift, and 9 and 8 meter horizons obviously conflict with the observed data. The curves of Figure 18 demonstrate that the minimum depth at which the methane horizon could exist at Station 57 is approximately 11 meters. If a value for methane concentration at the horizon of 50 ml/L rather than 100 ml/L is used, virtually the same curves are generated if Z values of 11.5, 10.5, 9.5, 8.5, and 7.5 meters are used in place of 12, 11, 10, 9, and 8 meters, respectively. Likewise, doubling the C_x value to 200 ml/L raises the Z values corresponding to the curves of Figure 5 by 0.5 meters. Thus, if the assumed C_x is in error by a factor of 2, the minimum depth of the methane horizon is in error by only a half a meter.

Minimum values of Z can be approximated in the same manner for the other stations. Estimated values of J, K, $(D/K)^{\frac{1}{2}}$, and minimum Z, using a C_x value of 100 ml/L for all stations, are given in Table 6. Values of J and K generally vary inversely with minimum Z since the three parameters are all functions of temperature, sedimentation rate, and organic input of an area, *i.e.*, Z should increase and J and K should decrease with increasing water depth. Values of $(D/K)^{\frac{1}{2}}$ are listed to demonstrate that these values are always much less than Z/4, satisfying assumption 2 postulated earlier.

Fluxes of methane out of the sediments can be calculated from equation 26 using Fick's first law:

$$F = -D(\partial C/\partial x)\Big|_{x=0} \qquad (27)$$

In this case, the methane flux out of sediments is given by:

$$F = (J/K - C_o)(KD)^{\frac{1}{2}} \qquad (28)$$

Calculated fluxes are listed in Table 6 for each station in units of nl/cm^2yr. Although these flux magnitudes are generally related to water depth in the Gulf of Mexico, they vary from area to area and are influenced to a large degree by the local bacterial populations involved in the processes of production and consumption. These flux calculations do not take into account consumption of methane by aerobic bacteria near the sediment surface. They should be considered upper limits only. If an overall average flux of 10 nl/cm^2yr is assumed from Gulf of Mexico slope and abyssal sediments covering a total area of 10^{16} cm^2, the annual input of methane into Gulf waters is 10^8 liters. This contribution is miniscule compared to the large inputs from rivers, deltas and marshes, shelf sediments, natural gas seepage, *in situ* water column production, and underwater venting and brine discharge from petroleum production activities in the Gulf.

Highly Reducing Sediments

Reducing conditions are often observed in estuarine or coastal sediments due to the influx of labile organic matter, warm temperatures, and rapid deposition rates. These conditions are commonly observed in Mississippi Delta sediments where microorganisms have depleted interstitial oxygen: various consequences are described in detail by Shokes (1976) and Trefry (1977). Interstitial sulfate is quickly consumed near the delta and the depth of sulfate depletion varies from a few centimeters at the river mouth to a few meters on the outer delta perimeter (Shokes, 1976). At the depth of near-zero interstitial

sulfate, methane begins to accumulate and concentrations increase sederal orders of magnitude. The explanation for this phenomenon has been discussed previously in this chapter.

Interstitial sulfate and methane profiles measured from a piston core taken near the Mississippi River mouth (60 meters water depth) are illustrated in Figure 19. Sulfate decreases to near-zero between 1.5 and 2.0 meters depth and methane increases correspondingly. The profiles indicate that methane is extensively produced and accumulates at a depth were sulfate is not completely depleted but rather about 0.5 to 1.0 mM. This observation is consistent with Oremland and Taylor (1978), who found that when sulfate is no longer present in sufficient concentration to support cell growth of sulfate reducers, hydrogen becomes available to the methane producers, resulting in a slight overlap in sulfate and methane distributions.

Figure 19 supports the hypothesis that methane is consumed in the sulfate-reducing zone in two ways:

(1) If only diffusive processes controlled methane concentrations from the sediment surface to a depth of 1.5 meters, the concentration profile would simply increase linearly from near zero at the surface to some higher value at depth. Advective processes due to sediment accumulation would make the profile slightly concave upward, but the observed profile cannot be generated from these physical processes alone (Martens and Berner, 1977). Consumption must be invoked in order to explain the very striking, upward concavity.

(2) $\delta^{13}C$ values of methane plotted on the right hand side of Figure 19

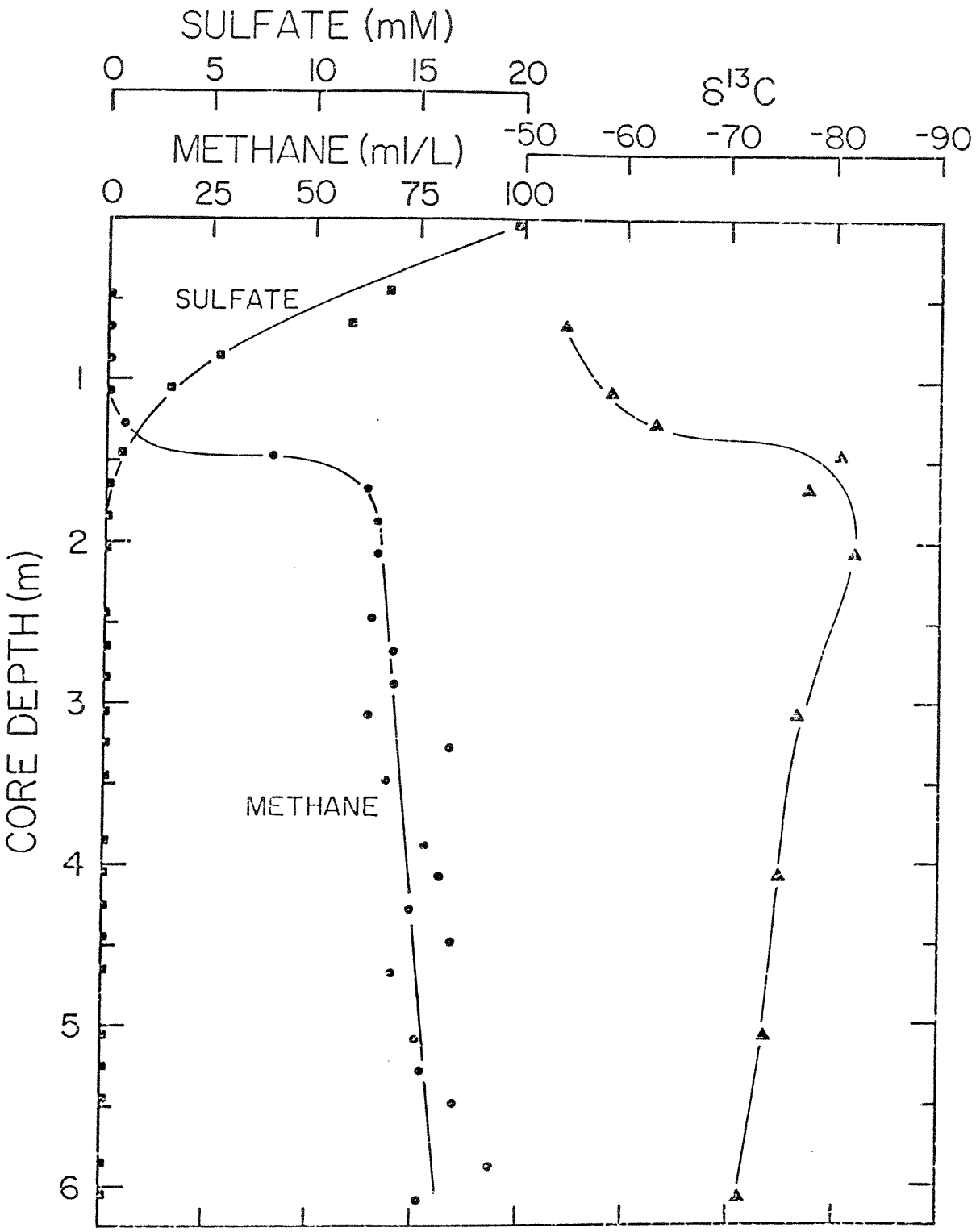

Fig. 19. Interstitial methane and sulfate at Station 58.

illustrate a marked deviation from the typical carbon isotope ratio (-80°/$_{oo}$) in samples taken the the sulfate-reducing zone. Isotopic ratios of methane increase in an upward direction to a value of -53°/$_{oo}$, indicative of a microbial process acting on the methane (physical processes cannot significantly fractionate methane over this short a distance). Microorganisms in the sulfate-reducing zone apparently selectively consume $^{12}CH_4$ over $^{13}CH_4$, thereby causing the residual methane to become isotopically heavier as it diffuses upward.

Martens and Berner (1977) observed a similar distribution of sulfate and methane in Long Island Sound sediments and were able to model the methane profile using a steady-state diagenetic equation incorporating effects of diffusion, sediment accumulation, and consumption. Using an effective diffusion coefficient of $D = 2 \times 10^{-6}$ cm^2/sec they fitted the solution of the diagenetic equation to their data assuming a consumption rate of $K = 8 \times 10^{-9}$ sec^{-1}. Similarly, the methane profile of Figure 19 can be fitted to the solution of equation 24 which incorporates the effects of diffusion, consumption, and production in the sulfate-reducing zone. The effects of sediment accumulation can be ignored again since $\omega^2/4D << K$. As described earlier, the ratio J/K represents the balance in production and consumption and can be seen as a constant concentration downward through most of the sulfate-reducing zone. This ratio can be estimated to be $\sim$500 µl/L from the concentrations at this station listed in Appendix C. The scale of Figure 19 is too large for this constant concentration from 0.5 to 1.0 meters sediment depth to be adequately illustrated,

and due to the difference in this concentration and the concentration observed at the methane horizon the observed profile could actually be modeled ignoring the effects of the relatively insignificant production, as do Martens and Berner (1977). Assuming values for D, C_o, C_x, and Z of 4.6 x 10^{-6} cm^2/sec, 500 ml/L, 66 ml/L, and 160 cm, respectively, equation 26 can be best-fit to the methane data using a consumption rate of K = 3.7 x 10^{-8} sec^{-1}. This value is comparable to the value of Martens and Berner (1977) of 0.8 x 10^{-8} sec^{-1}. If the diffusion coefficient of Martens and Berner (2 x 10^{-6} cm^2/sec) is used, even better agreement is observed. K for the profile in Figure 19 would then be 1.6 x 10^{-8} sec^{-1}.

Other Interstitial Light Hydrocarbons

Introduction

> The presentation of conclusions about production of alkanes and consumption of C_2+ alkanes by anaerobes is irresponsible and not suitable for presentation before a scientific society. It is hardly suitable for speculation in an informal discussion group.

I received this review of a presentation at a recent meeting of the Geological Society of America by an anonymous critic in the mail. It consisely expresses the current beliefs of most microbiologists on the role of microorganisms in the biogeochemistry of light alkanes. Whereas production of olefins (ethene and propene) by living organisms is commonly observed, attempts to detect microbially-produced alkanes other than methane have generally failed. Davis and Squires (1954) reported the first detection of trace amounts of ethane produced from microbial ethanol fermentation, but virtually no conclusive work since that early date has been accomplished. In summary, Coleman (1976)

states "It is now generally agreed by microbiologists that bacteria do not produce significant quantities of ethane (R. E. Kallio, pers comm)."

Reducing Sediments

Figure 20 shows methane, ethane, and propane concentrations with depth measured in a piston core taken from Mississippi Delta sediments. This core is the same sample in which methane and sulfate concentrations were measured and presented in Figure 19. Measurements illustrated by Figures 19 and 20 are tabulated in Appendix C.

Figure 20 shows the onset of extensive methane production and accumulation at about 1.5 meters. At this depth, ethane concentrations increase over an order of magnitude and remain constant with further depth. In contrast, propane increases drastically slightly below the methane horizon, then diminishes to an undetectable concentration with increasing depth. $C_1/(C_2+C_3)$ ratios above and below the methane horizon further demonstrate the improbability of the hydrocarbons originating from an oil-related source. Instead, ethane and propane are apparently microbially controlled in these highly-reducing sediments. Both hydrocarbons are most likely produced by a secondary metabolic process in conjunction with methanogenesis, with propane being subsequently consumed by the methanogens as are the larger organic molecules. The olefins were not detected in this sediment core, apparently due to their instability to decomposition in reducing environments.

Shelf and Slope Sediments

Interstitial concentrations of ethene, ethane, propene and propane

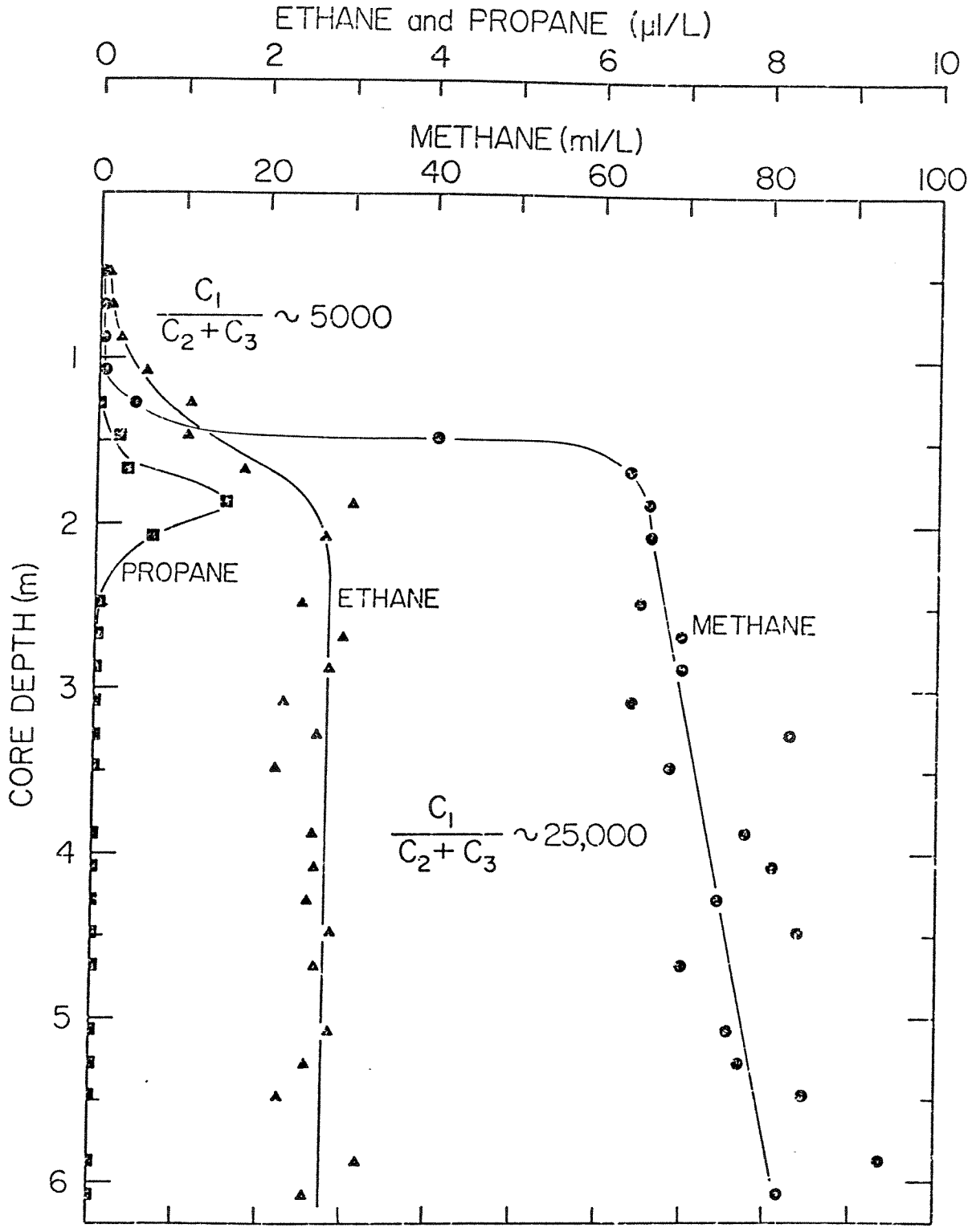

Fig. 20. Interstitial methane, ethane, and propane at Station 58.

at Station 50 are plotted against sediment depth in Figure 21. These profiles are representative of the concentrations measured in continental shelf and slope sediments and illustrate the behavior of the light hydrocarbons in the top 1.5 meters in this region.

Ethene concentrations fluctuate with depth in the cores, whereas ethane, propene, and propane are relatively constant. Ethene levels are typically twice as high as the other gases, but no trends with sediment depth are observed. Figure 22 shows average concentrations of the four hydrocarbons throughout the cores of Transect I (Figure 11) stations. The average concentration of each hydrocarbon is highest nearshore and decreases seaward until fairly uniform values are observed in the continental slope region (Station 49, 50, and 51). Average concentrations along Transect II follow the same trend although no samples were taken in the slope region for comparison.

The trends of the C_2 and C_3 hydrocarbons with distance from shore are similar to the behavior of methane. These patterns suggest that the concentrations of the C_2 and C_3 in the top few meters of shelf and slope sediments are microbially supported. Like methane, concentrations of the C_2 and C_3 hydrocarbons are probably controlled by biological oxidation and diffusion into the overlying water.

The concentrations of the hydrocarbons listed in Appendix A generally represent "baseline values" in the Texas shelf region. However, anomalous concentrations of ethane and propane were observed in one area of the shelf. Stations 4/IV, 5/IV, 2/IV, 6/IV, 3/IV, and 7/IV (in order of increasing water depth) comprise a transect progressing in a line due east of the Rio Grande River delta region

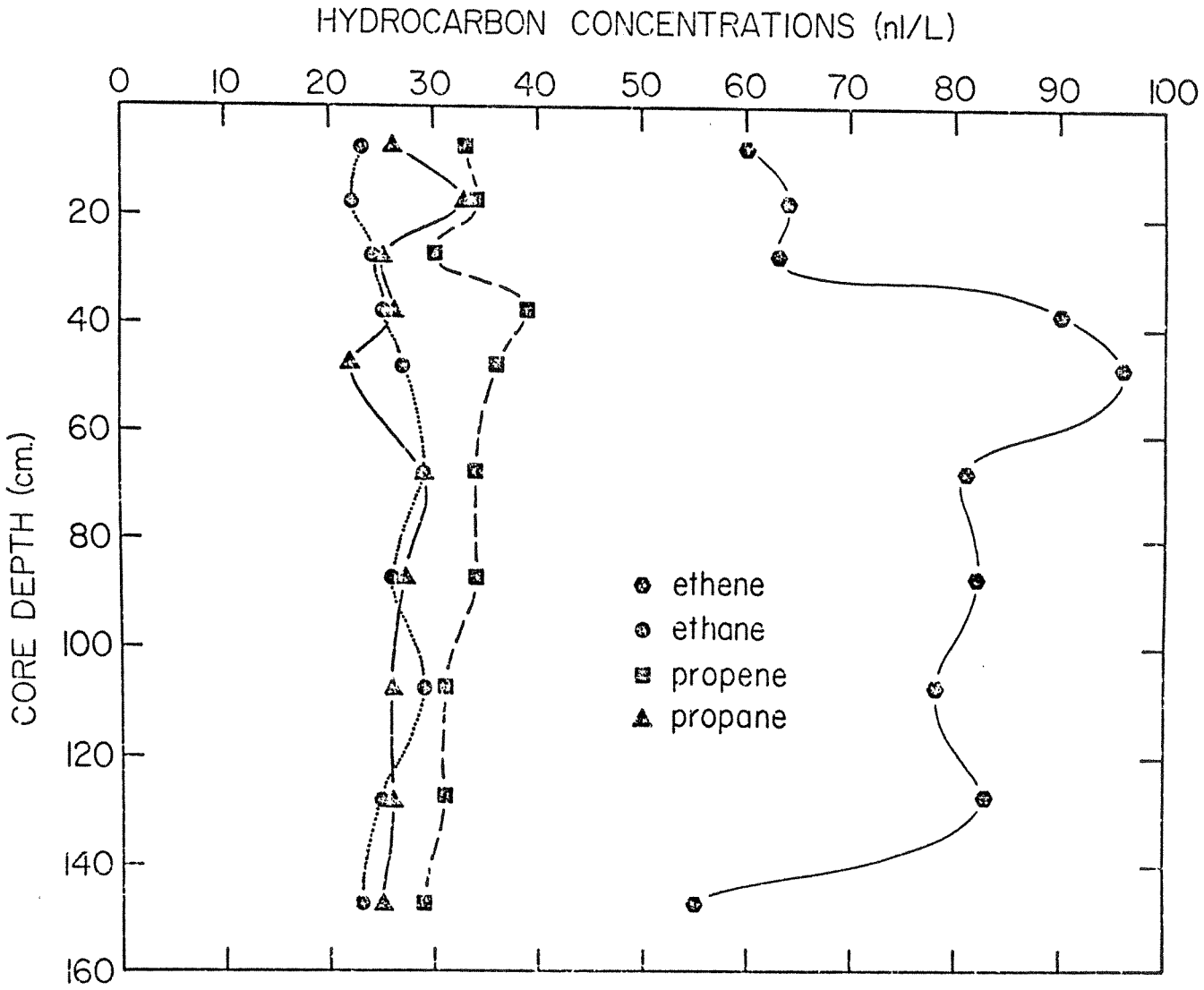

Fig. 21. Interstitial concentrations of the C_2 and C_3 hydrocarbons at Transect I stations.

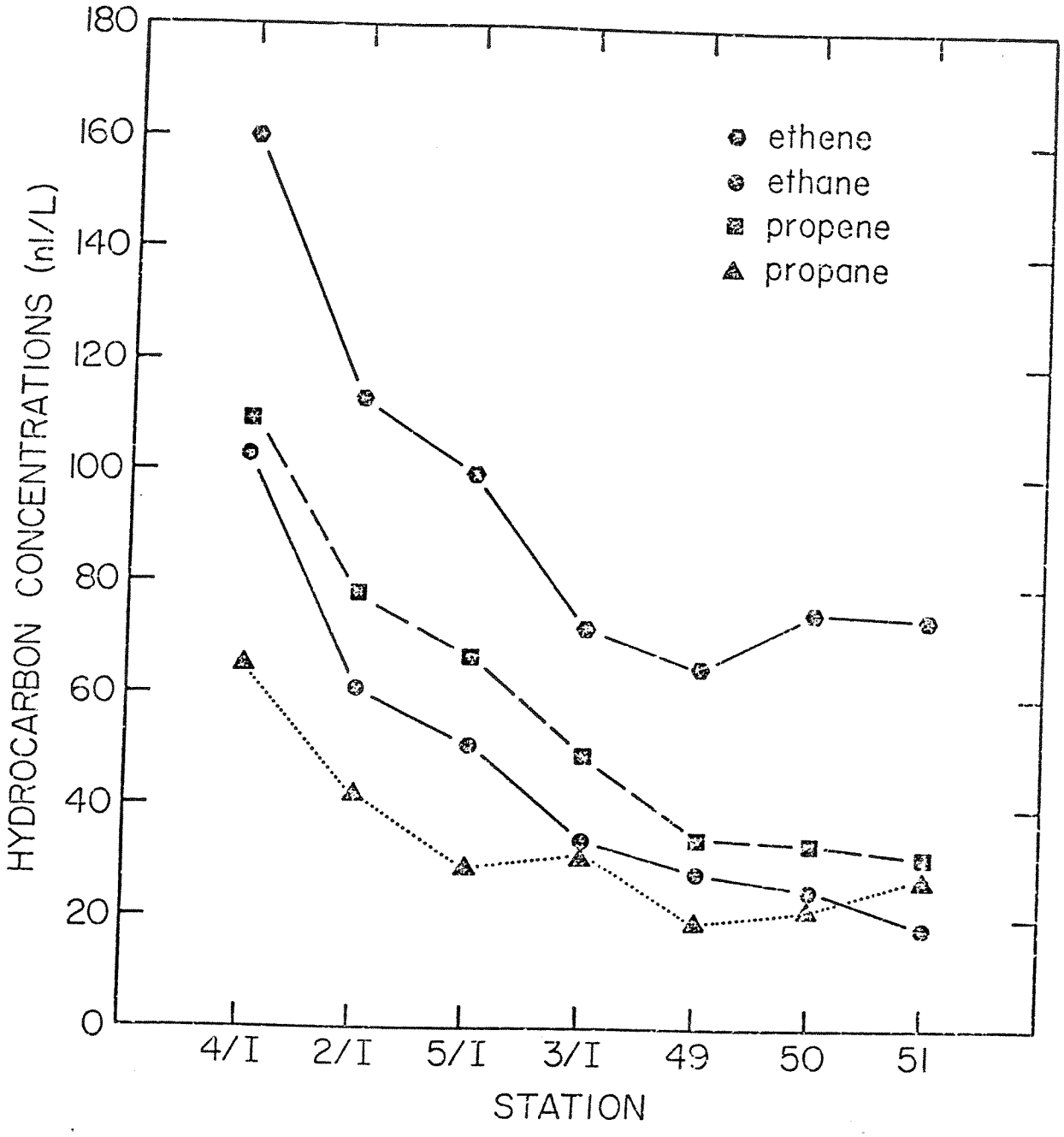

Fig. 22. Average concentrations of the C_2 and C_3 hydrocarbons at Transect I stations.

(all stations lie on latitude 26°10'N). Concentrations at the three stations nearest shore are typical of the South Texas shelf, but the outer stations 6/IV, 3/IV, and 7/IV have ethane and propane concentrations 5 to 10 times higher than normal. Corresponding $C_1/(C_2+C_3)$ ratios, normally in the hundreds or thousands, range from 15 to 100. These anomalies correlate well with dissolved hydrocarbon maxima consistently observed in the bottom waters of this region (Sackett *et al.*, 1977b) and are attributed to an input from thermocatalytic sources. Presumably, petroleum-related gas has migrated upward through natural conduits in the sediment and is dispersing in the near-surface sediments and bottom waters. Therefore, future work should include attempts to core on distinct topographic features in this region, such as faults, fractures, or bedding planes, in order to locate sites of distinct petroleum-related gas seepage.

CHAPTER IV

SUMMARY AND CONCLUSIONS

Hydrocarbon gases exist in Gulf of Mexico sediments as a product of microbial decomposition of organic substrates (microbial gas) and from thermocatalytic processes acting for millions of years at elevated temperatures and pressures on more refractory organic material. Microbial gases consist almost exclusively of methane, having $C_1/(C_2+C_3)$ hydrocarbon ratios greater than 1000 and $\delta^{13}C$ values of methane lighter than $-60°/_{oo}$. Thermocatalytic hydrocarbon gases generally have $C_1/(C_2+C_3)$ ratios smaller than 50 and isotopic ratios heavier than $-50°/_{oo}$. Since a comparison of these two parameters is diagnostic of the origin of natural gases, a simple geochemical model for the characterization of hydrocarbon gas sources can be constructed from the $C_1/(C_2+C_3)$ ratios and $\delta^{13}C$ values measured from natural gases. The hydrocarbon composition of thermocatalytic gas can apparently be altered to resemble microbial gas during migration through the sediments, and microbial gas can be isotopically altered by depletion of ^{12}C in the substrate on which the methanogenic bacteria are feeding or by microbial consumption of methane. Moreover, mixtures of gases from the two sources can retain the character of petroleum-related gas in hydrocarbon composition while appearing biogenic in isotopic composition.

Assuming that the 21 gas seep compositions reported here are representative of gas seepage in general, the use of hydrocarbon "sniffing" in offshore petroleum exploration must be reevaluated. Only one gas sample (seep 1) has isotopic and molecular compositions

unequivocally indicative of a thermocatalytic origin. Two other isotopically heavy samples (seeps 2 and 3) contain larger fractions of higher hydrocarbons than microbial degradation should produce, but if they are truly oil-related, ethane and higher hydrocarbons have been depleted before collection. High concentrations of dissolved microbial methane in near-bottom waters could be misinterpreted as the result of seepage from thermocatalytic sources. In addition, dissolved higher hydrocarbons may not be detected near existing oil-related seepage due to depletion during migration. Since the measurement of only one of the two parameters can be misleading, determination of the isotopic composition of methane from seepage and sediment gas in conjunction with molecular compositions can provide more definitive interpretation.

In the highly reducing sediments of the Mississippi Delta region, interstitial sulfate is quickly depleted and extensive microbial production of methane is observed within one or two meters of the seawater-sediment interface. This "horizon" of high methane concentration, generally greater than 50 milliliters per liter pore water, occurs progressively deeper in the sediment in an offshore direction. Carbon isotope ratios of methane generally range from $-70^{\circ}/_{\circ\circ}$ to $-90^{\circ}/_{\circ\circ}$, and $C_1/(C_2+C_3)$ ratios are typically greater than 10,000, certainly indicative of microbial production. Above, in the sulfate-reducing zone, both isotopic values of methane and $C_1/(C_2+C_3)$ ratios shift toward a pseudo-thermocatalytic composition due to microbial consumption of methane. Future work with improved analytical techniques is needed to better understand the changes in isotopic com-

position of methane in this region.

At the depth of the methane horizon, ethane and propane concentrations increase more than ten-fold but propane disappears with further sediment depth. These patterns suggest that ethane and propane are also microbially produced to some extent in recent sediments and propane is subsequently consumed. Evidence for microbial production of ethane and propane is contrary to previous microbiological investigations, but advances in analytical technology have now enabled easier detection of the gases. Future work should include an attempt to conclusively demonstrate their microbial production. Since culture experiments in the laboratory are necessarily limited to relatively short periods of time, the sediments of the Mississippi Delta would be an ideal site to investigate the minute quantities of gases produced over several hundreds or thousands of years.

Methane in the top few meters of Texas shelf sediments is generally of microbial origin, as evidenced by the existence of anomalously high methane concentrations in the top sediment layers. Apparently, bacterial production of methane is not restricted to the sulfate-free zone, but also occurs within microenvironments in sediments having near-seawater interstitial sulfate concentrations. In Texas shelf sediments, sulfate is not depleted until several meters depth and methane existing in the upper few meters of sediment cannot be explained by upward diffusive processes or inputs from overlying water. Two-meter vertical methane profiles in nearshore sediments exhibit maxima ranging from 100 to 500 microliters per liter pore water. The maxima are related to the large microbial population at

the sediment surface on the shelf, but disappear in the slope and abyssal region, presumably due to inhibited microbial activity at lower temperatures, higher pressures, and decreased input of labile organic carbon. Figure 23 is a schematic representation of interstitial methane in the upper 4 meters of sediments studied. The diagram illustrates the disappearance of the maxima as well as the trend of decreasing interstitial methane in an offshore direction. These conclusions imply that methane concentrations in near-surface shelf sediments are seasonally influenced. Warmer temperatures and increased detrital and nutrient input in the spring might enhance microbial production, so that oscillations of methane could be observed. If real, these oscillations in methane concentration could provide an excellent means of quantitating the magnitude of the effective diffusion coefficient of methane in porous sediments.

Interstitial concentrations of ethene, ethane, propene, and propane are relatively constant with depth in the upper two meters of shelf, slope, and abyssal sediments, decreasing progressively from 160, 100, 110, and 60 nanoliters per liter pore water in nearshore sediments, to fairly uniform levels of 80, 25, 30, and 25 nl/L downslope, respectively. The concentrations reported here generally represent "baseline values" of the light hydrocarbons on the Texas shelf. One area of anomalously high ethane and propane was found, however, indicating an input of thermocatalytic gas from the subsurface. This gas is apparently migrating upward through natural conduits in the sediment and dispersing in near-surface sediments and bottom waters in the region. Future sediment work as well as

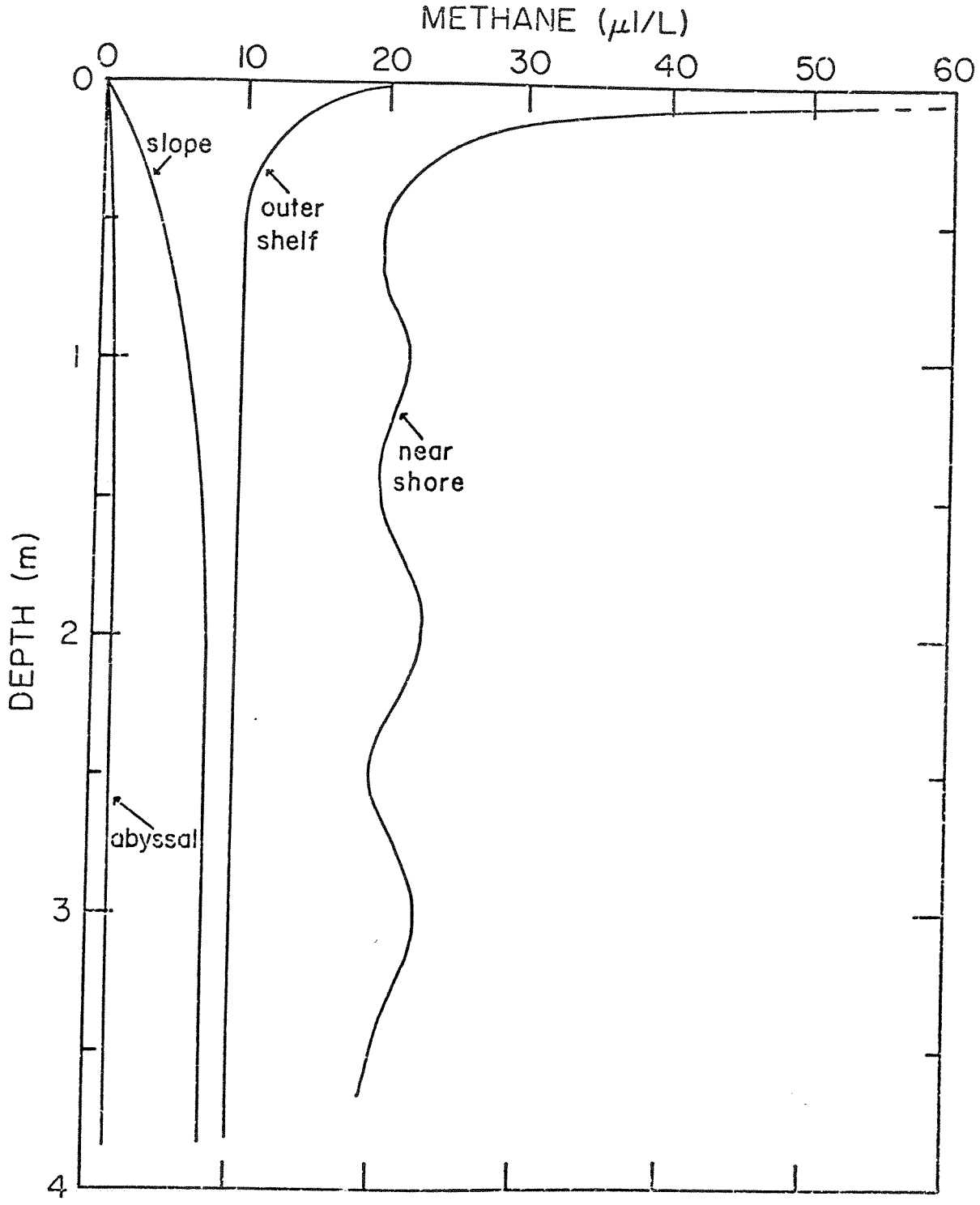

Fig. 23. Schematic diagram of methane variations in the upper 4 meters of sediment.

prospecting for reservoired hydrocarbons should include coring on or near geological features such as unconformities, faults, bedding planes, or distinct gas seepage in an effort to detect additional anomalous gas zones.

Vertical methane concentration profiles in sediments of the Gulf of Mexico can be explained mathematically by simple kinetic modeling. Relative rates of diffusion, advection, production, and consumption of methane determine solutions to a steady-state diagenetic equation. These solutions describe methane concentrations as a function of sediment depth in the sulfate-reducing zone. Correlations of the solutions to observed methane profiles and changes in isotopic ratios of methane indicate that methane is consumed by sulfate-reducing bacteria at a rate proportional to concentration. Profiles indicate that methane is also apparently produced to a minor extent throughout the sulfate-reducing zone.

Figure 24 illustrates solutions to the diagenetic equation in various sedimentary environments. The dashed line inset corresponds to the area covered by Figure 23. The primary factor controlling the theoretical profiles is the depth of sulfate disappearance. In reality, this depth is controlled by temperature, water depth, and organic input to the sediment so methane concentrations change in an offshore direction. In the highly reducing, organic-rich delta sediments, minor production of methane in the sulfate-reducing zone is negligible, and concentration profiles are controlled by methane consumption and upward diffusion from the relatively shallow methane horizon. Theoretical solutions agree well with the concave upward

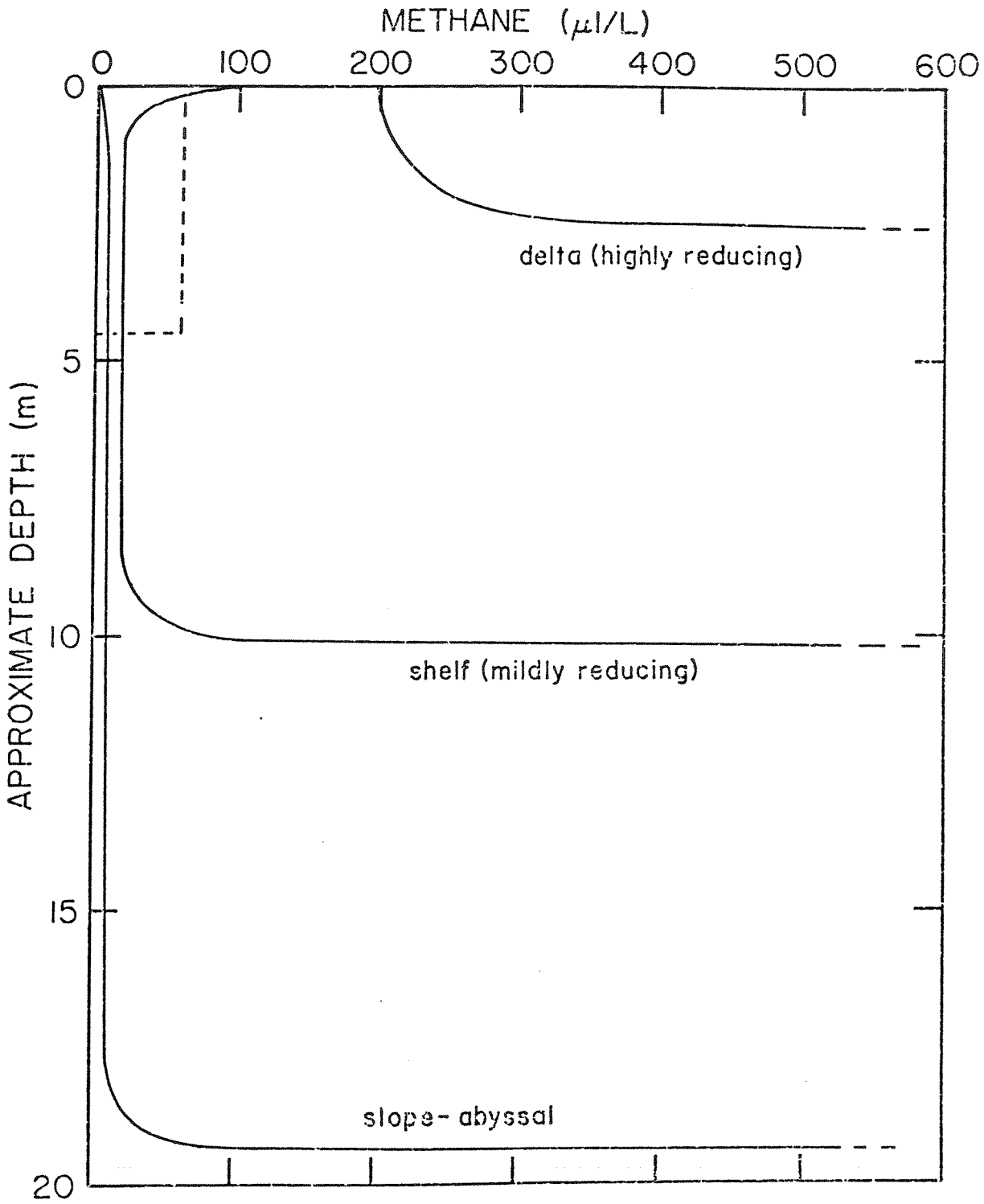

Fig. 24. Idealized methane profiles in the upper 20 meters of various sedimentary environments (inset corresponds to Fig. 23).

profiles observed in this region. In the outer shelf, slope, and abyssal region, where the depth of sulfate depletion is several meters below the surface, concentration profiles are controlled mainly by production and consumption. Diffusive effects are significant only near the sediment surface and near the depth of the methane horizon deeper in the sediment. Between these depths, the effects of production and consumption balance to form "constant" concentrations of methane with depth. Figure 24 suggests that these two processes seem to be the factors controlling interstitial methane distributions in the top few meters of open marine sediments. In these upper sediments, upward diffusion from large accumulations of methane deeper than about 10 meters is masked by the more localized production and consumption. This implies that the presence of deep gas pockets cannot be detected at the sediment surface unless conduits such as faults or fractures are present to enhance the upward migration of the gas.

Rates of methane production and consumption, as well as minimum depths of the methane horizon, vary with water depth and can be estimated from best-fit solutions to the kinetic model to the observed profiles. For example, the methane horizon depth increases from 1.5 meters at the Mississippi River mouth to greater than 28.5 meters at a downslope station at 1100 meters water depth. Similarly, the rate constant for methane consumption (K) decreases from 3.7×10^{-8} sec^{-1} to 1.8×10^{-10} sec^{-1} over this distance.

The kinetic model presented here is admittedly an oversimplified description of the processes controlling interstitial methane, but it seems to predict methane concentrations with depth surprisingly well.

Future work should include attempts to incorporate isotopic changes of methane, consumption of sulfate, and production of CO_2 into the model. The methane horizon depth should not be regarded as a boundary condition, but rather a depth at which production of methane increases.

Whereas several investigators have described the behavior of methane in restricted, highly-reducing sediments over the past decade, measurements presented in this work represent the first quantitative description of methane and the other light hydrocarbons in open shelf and slope sediments. The conclusions presented here are not limited to Gulf of Mexico sediments, but can be applied to marine sediments in general. Work in this laboratory indicates that the trends of each of the hydrocarbons from shelf to slope sediments can be extrapolated into abyssal regions, but an accurate description of the light hydrocarbons in deep-sea sediments still needs to be accomplished.

APPENDIX A. Interstitial Light Hydrocarbons and Percent Water in South Texas Shelf Sediments

STATION/LOCATION WATER DEPTH	DEPTH (cm)	METHANE (µl/L)	ETHENE (nl/L)	ETHANE (nl/L)	PROPENE (nl/L)	PROPANE (nl/L)	% WATER
1/I Feb. 77	5-10	150	151	75	67	54	33.0
28°12'N 96°27'W	15-20	33.7	165	77	112	67	33.6
18 meters	25-30	6.8	135	79	91	71	32.8
	35-40	8.3	196	93	131	80	26.7
	45-50	8.1	140	70	89	65	30.5
	65-70	10.6	235	112	154	88	28.9
	85-90	11.2	178	96	122	86	25.9
2/I Feb. 77	5-10	27.8	114	43	59	46	57.8
27°55'N 96°21'W	15-20	76.0	87	56	70	43	43.6
42 meters	25-30	19.6	107	56	70	47	47.7
	35-40	15.5	126	72	82	46	33.9
	45-50	16.5	114	60	74	37	40.5
	65-70	18.2	94	60	68	37	40.5
	85-90	19.7	68	40	55	29	45.6
	105-110	22.8	126	66	85	37	52.9
	125-130	30.8	85	57	72	42	35.9
	145-150	19.3	176	95	122	57	34.5
	165-170	19.5	149	68	104	43	32.6
3/I Feb. 77	5-10	75.5	60	24	37	34	62.2
27°34'N 96°07'W	15-20	37.7	61	32	42	35	60.2
134 meters	25-30	6.72	89	37	49	36	45.2
	35-40	3.23	80	36	47	37	53.5
	45-50	2.32	56	27	43	33	57.0
	65-70	2.57	80	37	52	36	52.0
	85-90	2.65	84	40	63	35	47.6
	105-110	3.13	61	35	52	35	56.0
	125-130	3.18	74	40	52	32	48.2

APPENDIX A. (continued)

STATION/LOCATION WATER DEPTH	DEPTH (cm)	METHANE (µl/L)	ETHENE (nl/L)	ETHANE (nl/L)	PROPENE (nl/L)	PROPANE (nl/L)	% WATER
4/I Feb. 77	5-10	393	154	87	77	51	30.8
28°14'N 96°28'W	15-20	52.1	147	87	98	57	12.0
18 meters	25-30	26.0	139	89	102	55	38.0
	35-40	9.1	130	110	102	68	26.6
	45-50	14.7	211	117	140	79	25.2
	65-70	7.5	179	109	117	68	45.9
	85-90	6.8	177	134	129	81	39.7
	105-110	7.6	139	92	104	60	24.6
5/I Feb. 77	5-10	77.6	71	33	50	36	58.7
27°45'N 96°14'W	15-20	28.5	82	48	60	30	49.3
82 meters	25-30	35.4	111	55	66	34	47.1
	35-40	19.4	137	58	84	29	45.5
	45-50	15.4	102	52	68	23	44.7
	65-70	17.6	94	46	76	27	39.8
	85-90	17.2	91	51	48	30	43.3
	105-110	15.8	93	55	67	28	41.7
	125-130	15.7	75	48	58	25	43.4
	145-150	15.7	84	55	67	25	46.5
	165-170	12.7	140	59	91	27	41.7

APPENDIX A. (continued)

STATION/LOCATION WATER DEPTH	DEPTH (cm)	METHANE (µl/L)	ETHENE (nl/L)	ETHANE (nl/L)	PROPENE (nl/L)	PROPANE (nl/L)	% WATER
6/I Feb.77	5-10	157.0	109	35	57	35	58.0
27°39'N 96°12'W	15-20	84.5	80	33	51	37	51.6
100 meters	25-30	49.7	121	44	69	32	48.1
	35-40	39.9	124	43	61	31	41.1
	45-50	27.3	124	49	66	30	47.0
	65-70	16.1	93	44	64	27	40.5
	85-90	17.9	160	64	94	40	47.1
	105-110	18.7	117	57	86	34	45.4
	125-130	21.6	104	51	74	34	53.4
	145-150	17.6	177	74	101	49	52.0
1/II July 77	5-10	104	107	39	23	32	47.3
27°40'N 96°59'W	15-20	232	159	55	53	41	42.0
22 meters	25-30	258	102	37	52	42	38.3
	35-40	212	100	31	43	35	37.8
	45-50	194	94	31	43	42	27.6
	65-70	54.9	75	25	32	32	44.1
	85-90	25.7	129	40	60	62	41.7
	105-110	19.4	88	29	39	29	46.5
2/II July 77	5-10	171	56	14	11	11	49.1
27°30'N 96°45'W	15-20	211	110	33	36	31	44.0
49 meters	25-30	70.7	99	37	44	37	46.3
	35-40	17.9	74	29	36	30	48.3
	45-50	17.0	86	31	47	37	34.2
	65-70	21.1	80	27	39	39	46.1
	85-90	20.0	107	32	49	38	43.9
	105-110	20.1	-	-	-	-	43.3
	125-130	16.9	88	19	24	16	35.9

APPENDIX A. (continued)

STATION/LOCATION WATER DEPTH	DEPTH (cm)	METHANE (µl/L)	ETHENE (nl/L)	ETHANE (nl/L)	PROPENE (nl/L)	PROPANE (nl/L)	% WATER
3/II July 77	5-10	3.22	52	12	15	32	63.2
27°18'N 96°23'W	15-20	2.65	77	22	28	30	57.8
131 meters	25-30	2.92	65	20	28	24	53.6
	35-40	2.95	71	25	37	27	54.1
	65-70	4.15	70	19	36	34	52.9
	85-90	4.96	100	27	47	37	52.5
	105-110	6.01	80	26	41	27	50.7
	125-130	5.74	82	25	43	40	49.2
4/II July 77	5-10	23.0	104	39	37	18	56.8
27°34'N 96°50'W	15-20	35.8	83	38	37	32	47.7
34 meters	25-30	42.7	104	41	41	39	41.5
	35-40	39.3	70	35	30	35	45.6
	45-50	36.5	75	32	32	33	45.0
	65-70	33.2	94	32	40	38	43.8
	85-90	30.1	99	34	47	38	54.8
	105-110	29.9	97	43	46	38	45.3
	125-130	22.6	75	27	40	43	48.9
5/II July 77	5-10	10.1	96	25	31	25	63.3
27°24'N 96°36'W	15-20	13.6	123	36	42	46	54.6
78 meters	25-30	13.1	99	36	49	41	53.3
	35-40	12.3	65	26	28	29	53.9
	45-50	13.1	71	25	35	33	51.4
	65-70	20.0	101	32	58	35	44.6
	85-90	14.8	123	30	53	35	50.8
	105-110	16.6	68	20	35	31	51.8

APPENDIX A. (continued)

STATION/LOCATION WATER DEPTH	DEPTH (cm)	METHANE (µl/L)	ETHENE (nl/L)	ETHANE (nl/L)	PROPENE (nl/L)	PROPANE (nl/L)	% WATER
6/II July 77	5-10	4.28	81	20	31	53	49.3
27°24'N 96°29'W	15-20	4.79	71	20	33	27	50.4
98 meters	25-30	4.35	71	16	36	27	52.6
	35-40	5.08	72	20	36	27	51.9
	45-50	5.23	80	24	40	31	41.9
	65-70	6.57	101	31	49	32	52.8
	85-90	7.23	73	20	28	23	48.9
	105-110	7.53	56	17	27	20	51.5
7/II July 77	5-10	2.77	60	12	15	11	62.6
27°15'N 96°19'W	15-20	1.58	46	14	23	31	55.1
183 meters	25-30	1.64	60	17	26	20	57.4
	35-40	2.05	68	18	34	28	53.6
	45-50	1.76	52	15	24	25	54.0
	65-70	1.96	64	20	33	32	50.5
	85-90	2.59	60	17	28	25	52.8
	105-110	2.85	65	20	40	41	51.7
1/III Nov. 77	5-10	10.19	92	31	37	30	51.8
26°57'N 97°11'W	15-20	21.96	115	49	61	39	44.1
27 meters	25-30	26.12	102	44	48	33	42.5
	35-40	28.80	96	34	42	24	42.4
	65-70	31.52	68	32	37	31	49.4
	105-110	30.90	75	34	42	33	42.4
	145-150	23.65	89	38	50	34	35.7

APPENDIX A. (continued)

STATION/LOCATION WATER DEPTH	DEPTH (cm)	METHANE (µl/L)	ETHENE (nl/L)	ETHANE (nl/L)	PROPENE (nl/L)	PROPANE (nl/L)	% WATER
2/III Nov. 1977	5-10	12.22	91	36	31	29	62.0
26°57'N 96°48'W	15-20	18.73	100	40	32	34	49.7
66 meters	25-30	25.71	59	27	17	22	50.6
	35-40	30.82	86	28	20	24	58.0
	45-50	30.68	66	26	23	19	55.7
	75-80	37.69	78	29	31	28	54.8
	105-110	51.51	151	48	47	51	53.5
3/III Sept. 1977	20-25	7.41	79	22	17	21	50.4
27°03'N 96°34'W	40-45	10.07	71	25	26	24	-
104 meters	60-65	10.68	60	23	29	20	53.4
	80-85	11.36	112	35	76	41	-
	100-105	15.07	107	35	60	42	54.1
	140-145	12.91	78	28	36	22	-
	170-175	18.48	64	21	32	22	53.7
4/III Sept. 1977	5-10	53.02	242	163	107	131	24.4
26°56'N 97°16'W	15-20	12.32	146	94	77	49	28.7
15 meters	25-30	12.49	116	100	68	55	23.1
	35-40	6.93	145	189	95	96	22.5
	45-50	5.55	49	53	5	10	22.9
	55-60	6.36	51	135	10	47	32.8

APPENDIX A. (continued)

STATION/LOCATION WATER DEPTH	DEPTH (cm)	METHANE (µl/L)	ETHENE (nl/L)	ETHANE (nl/L)	PROPENE (nl/L)	PROPANE (nl/L)	% WATER
5/III Nov. 1977	5-10	16.59	94	40	33	29	60.8
26°57'N 97°4'W	15-20	26.11	135	61	57	42	47.4
37 meters	25-30	32.07	83	-	40	40	45.5
	35-40	34.89	107	48	54	42	48.0
	45-50	39.66	89	41	45	37	46.8
	65-70	40.64	67	40	37	30	46.9
	105-110	25.76	87	38	48	35	41.8
6/III Sept. 1977	5-10	6.46	56	21	37	22	56.6
26°57'N 96°31'W	15-20	5.32	76	32	43	27	-
124 meters	25-30	6.44	112	36	61	38	-
	45-50	8.03	70	25	38	25	53.6
	65-70	9.03	51	19	30	22	-
	85-90	10.83	60	21	30	21	-
	105-110	11.70	75	31	42	35	53.4
1/IV Sept. 1977	TOO SANDY TO CORE						
2/IV Sept. 1977	5-10	6.53	122	47	60	46	56.2
26°10'N 96°37'W	15-20	8.28	98	39	46	40	47.8
48 meters	25-30	7.40	92	40	51	43	49.0
	35-40	8.11	91	41	57	44	-
	45-50	11.22	115	49	69	64	41.3
	65-70	15.27	95	48	59	51	-
	85-90	12.04	133	60	78	68	41.8
	105-110	11.00	72	29	38	35	-
	125-130	8.36	116	66	75	66	43.4

APPENDIX A. (continued)

STATION/LOCATION WATER DEPTH	DEPTH (cm)	METHANE (µl/L)	ETHENE (nl/L)	ETHANE (nl/L)	PROPENE (nl/L)	PROPANE (nl/L)	% WATER
3/IV Sept. 1977	5-10	49.66	407	423	257	244	33.9
26°11'N 96°23'W	15-20	66.15	147	451	41	256	28.7
90 meters	25-30	106.00	870	1464	296	758	27.7
	35-40	22.70	126	512	39	244	27.4
	45-50	16.04	191	771	73	368	25.4
4/IV Sept. 1977	5-10	24.98	52	215	9	108	24.9
26°10'N 97°07'W	15-20	23.11	48	254	6	117	23.9
15 meters							
5/IV Sept. 1977	5-10	29.92	60	28	17	16	51.2
26°10'N 96°54'W	15-20	42.70	86	40	46	33	49.4
38 meters	25-30	33.44	63	30	39	30	38.2
	35-40	36.41	72	32	43	29	44.8
	65-70	32.25	96	42	61	38	-
	85-90	35.28	122	58	79	60	43.4
	105-110	20.36	126	53	70	50	-
	145-150	9.57	169	89	88	70	32.9
6/IV Sept. 1977	5-10	8.49	129	71	67	76	39.9
26°10'N 96°30'W	15-20	7.82	146	102	66	78	40.9
62 meters	30-35	11.56	84	110	39	69	36.8
	45-50	9.28	108	98	59	57	-
	65-70	9.00	147	159	100	95	29.8
	75-80	8.61	102	157	64	96	-
	105-110	8.18	106	200	65	112	25.8

APPENDIX A. (continued)

STATION/LOCATION WATER DEPTH	DEPTH (cm)	METHANE (µl/L)	ETHENE (nl/L)	ETHANE (nl/L)	PROPENE (nl/L)	PROPANE (nl/L)	% WATER
7/IV Sept. 1977	5-10	18.53	51	33	26	41	32.4
26°10'N 96°20'W	15-20	13.97	55	27	28	32	40.8
144 meters	25-30	7.75	164	218	91	136	27.9
	35-40	7.33	179	289	104	158	-
	45-50	6.74	155	283	93	220	25.3
	65-70	6.94	193	296	157	183	-
	85-90	11.33	180	242	108	164	23.4
27 Nov. 1977	5-10	9.42	85	35	21	29	45.2
27°44'N 96°59'W	15-20	4.66	118	83	55	31	40.3
16 meters	25-30	8.59	54	25	23	17	29.0
	35-40	14.50	24	13	4	3	44.4
28 Nov. 1977	5-10	6.49	77	-	20	24	47.3
27°41'N 96°59'W	15-20	6.93	174	60	84	60	48.4
19 meters	25-30	10.04	104	48	52	36	29.9
	35-40	11.74	107	68	51	41	37.9
	45-50	7.92	168	62	52	58	39.5
	55-60	11.48	68	32	21	27	53.1
29 Sept. 1977	5-10	19.83	100	38	29	54	49.1
27°37'N 96°56'W	15-20	28.01	118	48	39	55	-
25 meters	25-30	32.39	69	40	40	32	38.0
	35-40	31.33	68	33	35	26	-
	45-50	34.95	113	57	65	43	40.3
	65-70	32.13	70	29	41	20	-
	85-90	33.42	83	45	59	36	36.7
	105-110	25.78	91	41	65	51	-
	125-130	13.28	102	49	56	34	42.4

APPENDIX A. (continued)

STATION/LOCATION WATER DEPTH	DEPTH (cm)	METHANE (µl/L)	ETHENE (nl/L)	ETHANE (nl/L)	PROPENE (nl/L)	PROPANE (nl/L)	% WATER
30 Nov. 1977	5-10	13.01	190	72	67	64	41.8
27°37'N 97°2'W	15-20	16.87	162	52	48	53	52.8
22 meters	25-30	19.84	158	67	69	46	51.8
	35-40	22.04	114	52	63	40	28.4
	45-50	27.40	83	40	39	31	44.3
	65-70	26.10	53	24	25	18	45.4
	85-90	20.14	49	25	21	18	30.5
	105-110	17.62	97	43	48	29	33.9
	145-150	13.38	101	48	48	33	28.4
31 Nov. 1977	10-15	20.83	73	34	30	35	60.4
27°32'N 97°4'W	20-25	31.46	81	40	32	38	30.4
24 meters	35-40	16.70	66	39	30	36	31.9
	45-50	10.24	99	37	48	34	40.6
	65-70	21.84	49	27	26	24	44.6
	85-90	28.25	46	20	23	19	49.5
	105-110	26.40	54	27	27	20	47.0
	165-170	15.62	41	20	21	18	40.5
32 Nov. 1977							
27°25'N 97°6'W	15-20	26.85	80	36	35	30	53.0
25 meters	25-30	39.75	44	18	19	15	61.6
	35-40	72.89	89	40	36	32	45.7
	45-50	20.34	52	22	19	20	46.8
	65-70	37.97	60	28	36	23	40.5

APPENDIX A. (continued)

STATION/LOCATION WATER DEPTH	DEPTH (cm)	METHANE (µl/L)	ETHENE (nl/L)	ETHANE (nl/L)	PROPENE (nl/L)	PROPANE (nl/L)	% WATER
33 Nov. 1977	5-10	22.09	91	32	29	35	56.9
27°21'N 97°7'W	15-20	26.81	100	41	43	39	54.4
25 meters	25-30	31.45	140	52	56	37	51.4
	35-40	32.51	122	55	50	37	43.5
	45-50	36.47	110	49	47	34	41.6
	55-60	35.72	70	29	20	12	42.4
34 Nov. 1977	5-10	15.48	126	46	38	40	59.2
27°17'N 97°9'W	15-20	15.91	120	47	50	38	54.7
25 meters	25-30	25.79	131	66	48	40	47.0
	35-40	30.20	80	38	43	28	42.7
	45-50	32.69	108	45	46	30	36.7
	65-70	26.13	48	28	10	7	35.9
35 Nov. 1977	5-10	12.73	136	45	41	38	55.7
27°13'N 97°7'W	15-20	30.38	116	49	38	38	57.1
26 meters	25-30	29.53	87	41	31	24	49.7
	35-40	30.56	76	35	33	23	49.6
	45-50	30.90	80	39	39	28	38.0
	65-70	33.28	56	28	30	20	48.7
	85-90	34.79	70	32	35	24	45.3
	105-110	18.23	93	25	30	18	45.3
	145-150	34.50	61	24	30	22	30.8

APPENDIX A. (continued)

STATION/LOCATION WATER DEPTH	DEPTH (cm)	METHANE (µl/L)	ETHENE (nl/L)	ETHANE (nl/L)	PROPENE (nl/L)	PROPANE (nl/L)	% WATER
36 Nov. 1977	5-10	13.10	87	42	34	38	46.9
27 10'N 97 11'W	15-20	19.17	85	42	33	32	50.3
26 meters	25-30	19.15	65	37	24	23	49.0
	35-40	24.84	92	44	48	32	42.8
	45-50	30.59	61	37	32	25	43.1
	65-70	36.88	52	29	28	23	41.4
	85-90	34.48	108	59	65	54	45.2
37 Nov. 1977	5-10	13.86	100	35	30	34	58.3
27°7'N 97°11'W	15-20	27.22	85	36	-	27	49.0
26 meters	25-30	21.60	115	40	29	58	46.0
	35-40	22.00	93	36	43	30	44.2
	45-50	19.44	187	89	91	49	43.9
	65-70	19.18	74	26	34	23	45.2
	85-90	17.62	103	42	50	37	47.1
	105-110	15.69	125	52	59	38	42.5
	155-160	8.60	128	51	59	51	35.1
38 Sept. 1977	25-30	11.37	136	117	80	70	27.4
27°5'N 97°15'W	35-40	8.37	211	153	121	96	30.6
18 meters	45-50	15.39	153	77	97	62	24.2
	55-60	9.52	116	77	78	53	48.6
	65-70	10.33	42	67	5	19	24.1

APPENDIX A. (continued)

STATION/LOCATION Water Depth	DEPTH (cm)	METHANE (µl/L)	ETHENE (nl/L)	ETHANE (nl/L)	PROPENE (nl/L)	PROPANE (nl/L)	% WATER
39 Nov. 1977	5-10	12.94	110	36	33	33	55.3
27°3'N 97°15'W	15-20	24.70	71	35	34	30	49.2
26 meters	25-30	23.43	115	47	43	33	30.7
	35-40	30.69	86	39	34	34	39.4
	45-50	31.72	99	47	46	40	33.9
	65-70	22.54	96	43	50	36	34.4
	85-90	23.63	115	56	56	46	41.1
	105-110	18.24	93	49	44	36	43.3
	145-150	10.57	90	39	45	36	33.1
40 Sept. 1977	5-10	7.97	122	39	36	29	52.0
27°23'N 96°51'W	15-20	12.54	109	44	41	32	-
46 meters	25-30	20.03	79	33	29	24	42.6
	45-50	19.40	59	33	32	21	43.7
	65-70	23.47	60	33	35	25	46.5
	85-90	25.64	75	36	38	26	-
	105-110	25.67	74	33	41	25	43.7
	135-140	25.36	58	21	16	8	43.7
41 Nov. 1977	5-10	8.80	97	32	28	52	61.1
27°27'N 96°36'W	15-20	12.32	128	47	49	59	52.5
75 meters	25-30	12.59	122	53	56	59	54.4
	35-40	11.45	244	65	112	78	49.0
	45-50	12.33	63	23	28	29	52.3
	65-70	10.55	76	32	35	37	51.9
	85-90	13.93	69	31	35	30	52.6
	115-120	7.05	171	43	83	47	51.3

APPENDIX A. (continued)

STATION/LOCATION WATER DEPTH	DEPTH (cm)	METHANE (µl/L)	ETHENE (nl/L)	ETHANE (nl/L)	PROPENE (nl/L)	PROPANE (nl/L)	% WATER
42 Nov. 1977	5-10	11.43	81	22	19	41	63.9
27°23'N 96°36'W	15-20	19.01	91	39	37	52	59.2
75 meters	25-30	21.50	85	38	40	62	51.4
	35-40	25.57	71	30	29	44	52.9
	55-60	25.91	88	38	44	51	53.6
	75-80	22.97	101	43	49	52	52.0
	105-110	22.84	111	44	57	59	42.3
43 Nov. 1977	5-10	9.72	84	29	24	44	60.3
27°18'N 96°37'W	15-20	15.00	46	26	15	40	47.6
77 meters	35-40	19.52	79	39	35	50	56.6
	45-50	21.24	78	36	35	50	54.0
	75-80	36.07	101	42	51	57	55.0
	115-120	19.65	87	34	43	47	57.0
44 Nov. 1977	5-10	6.98	63	24	23	36	68.2
27°15'N 96°40'W	15-20	11.24	99	36	34	58	57.0
77 meters	25-30	7.63	261	60	119	77	52.4
	35-40	13.44	82	30	33	37	55.3
	55-60	8.41	29	57	126	65	50.8
	85-90	19.45	80	28	31	35	36.9
	125-130	15.78	236	78	113	84	55.2

APPENDIX A. (continued)

STATION/LOCATION WATER DEPTH	DEPTH (cm)	METHANE (µl/L)	ETHENE (nl/L)	ETHANE (nl/L)	PROPENE (nl/L)	PROPANE (nl/L)	% WATER
45 Nov. 1977	5-10	10.52	83	21	22	33	66.3
27°12'N 96°40'W	15-20	7.79	144	39	29	48	48.6
75 meters	25-30	9.44	216	58	92	77	55.3
	35-40	18.79	89	36	29	43	53.1
	45-50	11.92	194	52	97	56	46.6
	65-70	8.72	189	55	92	53	57.1
	85-90	29.04	105	35	40	39	54.5
	130-135	15.57	63	22	29	24	53.2
46 Nov. 1977	5-10	8.74	75	29	24	39	58.4
27°9'N 96°43'W	15-20	15.52	90	38	34	47	53.7
75 meters	25-30	6.45	188	42	97	48	55.3
	35-40	10.88	269	67	119	76	54.2
	45-50	16.63	110	47	54	47	99.6
	65-70	18.92	110	43	56	37	54.9
	85-90	21.04	32	8	4	3	55.6
47 Nov. 1977	5-10	4.41	91	27	24	20	59.4
27°4'N 96°42'W	15-20	10.16	114	40	32	46	49.5
73 meters	25-30	11.16	93	37	32	47	53.1
	35-40	12.62	86	34	45	38	53.9
	55-60	15.70	52	24	27	33	54.9
	75-80	18.92	51	21	28	28	50.1
	105-110	21.91	62	25	32	27	52.3
	150-155	25.96	79	28	38	30	53.7

APPENDIX A. (continued)

STATION/LOCATION WATER DEPTH	DEPTH (cm)	METHANE (µl/L)	ETHENE (nl/L)	ETHANE (nl/L)	PROPENE (nl/L)	PROPANE (nl/L)	% WATER
48 Nov. 1977	5-10	13.24	217	63	67	64	-
27°1'N 96°46'W	15-20	16.36	133	49	50	50	52.6
70 meters	25-30	18.17	124	44	41	59	51.4
	35-40	22.45	96	35	24	29	56.4
	55-60	14.84	364	79	150	84	55.7
	75-80	21.80	113	37	40	32	52.5
	155-160	19.90	125	29	37	38	51.6
49 Feb. 1977	5-10	6.60	75	26	29	21	67.8
27°23'N 95°58'W	15-20	2.39	55	24	26	16	57.1
397 meters	25-30	2.54	58	28	34	19	60.0
	35-40	2.79	59	28	32	18	75.5
	45-50	3.25	67	29	35	19	69.2
	65-70	3.67	96	35	43	23	53.6
	85-90	3.87	103	36	40	21	51.2
	105-110	3.74	30	23	33	17	55.4
	125-130	4.00	52	26	30	17	56.6
	145-150	4.34	54	30	35	22	55.2
	165-170	3.86	61	25	33	17	66.2

APPENDIX A. (continued)

STATION/LOCATION WATER DEPTH	DEPTH (cm)	METHANE (µl/L)	ETHENE (nl/L)	ETHANE (nl/L)	PROPENE (nl/L)	PROPANE (nl/L)	% WATER
50 Feb. 1977	5-10	1.05	60	23	33	26	65.5
27°19'N 95°51'W	15-20	1.23	64	22	34	33	63.3
631 meters	25-30	1.59	63	24	30	25	57.1
	35-40	1.79	90	25	39	26	58.8
	45-50	2.08	96	27	36	22	55.9
	65-70	2.40	81	29	34	29	55.1
	85-90	2.64	82	26	34	27	66.9
	105-110	2.96	78	29	31	26	55.8
	125-130	3.08	83	25	31	26	56.4
	145-150	3.40	55	23	29	25	56.9
51 Feb. 1977	5-10	0.44	45	13	34	20	80.9
27°16'N 95°46'W	15-20	.89	64	15	32	26	61.8
874 meters	25-30	1.38	80	19	32	27	60.0
	35-40	1.78	177	20	32	30	62.2
	45-50	2.00	64	20	33	32	60.1
	65-70	2.47	51	17	28	25	59.7
	95-100	2.93	87	20	32	33	66.1
	125-130	3.43	49	19	25	29	57.1
	165-170	4.13	52	18	30	31	56.6
52 Nov. 1977	15-20	20.92	74	36	27	29	44.5
26°57'N 97°7'W	25-30	28.97	61	34	32	26	53.1
32 meters	35-40	35.20	61	31	29	26	47.0
	55-60	38.20	52	26	23	23	46.3
	85-90	26.91	56	28	28	26	49.8
	160-165	18.89	78	32	39	33	46.6

APPENDIX A. (continued)

STATION/LOCATION WATER DEPTH	DEPTH (cm)	METHANE (µl/L)	ETHENE (nl/L)	ETHANE (nl/L)	PROPENE (nl/L)	PROPANE (nl/L)	% WATER
53 Nov. 1977	5-10	12.34	103	51	37	31	57.6
26°55'N 97°0'W	15-20	10.19	49	55	21	33	49.4
44 meters	25-30	15.83	129	49	46	44	43.3
	35-40	23.70	80	41	38	30	42.2
	55-60	23.61	87	37	32	30	49.0
	75-80	26.36	64	27	25	28	49.1
	105-110	25.86	88	44	45	33	50.3
	155-160	25.50	67	24	27	30	50.7

APPENDIX B. Interstitial Methane, Sulfate, and Percent Water in Slope Sediments

STATION/LOCATION WATER DEPTH	DEPTH (cm)	METHANE (µl/L)	SULFATE (mM)	% WATER
54 76-G-10	20-25	1.4	28.7	55.5
28°29.4'N	40-45	2.1	28.7	55.8
89°01.0'W	60-65	3.2	28.0	54.1
910 meters	80-85	3.2	27.6	56.7
	100-105	3.3	27.7	56.9
	120-125	3.6	27.6	56.9
	140-145	4.1	27.2	56.1
	160-165	4.2	27.6	55.5
	180-185	4.7	27.5	53.7
	200-205	5.0	26.9	53.0
	220-225	5.7	26.9	53.8
	240-245	5.8	27.5	53.1
	260-265	5.9	27.3	51.8
	280-285	6.0	28.0	54.2
	300-305	6.1	25.5	56.1
	320-325	6.4	-	51.1
	340-345	6.7	26.9	55.0
	360-365	6.9	26.2	51.4
	380-385	7.0	26.4	52.7
	400-405	6.6	26.5	53.3
	420-425	7.3	26.6	47.1
	440-445	7.1	26.9	50.6
	460-465	7.4	26.3	51.9
	480-485	7.3	25.9	53.2
	500-505	7.6	25.9	51.5
	520-525	7.5	25.0	46.8
	540-545	6.9	25.7	45.7
	560-565	7.0	25.9	44.4
	580-585	7.5	23.8	45.6
	600-605	7.1	25.9	45.1
	620-625	7.1	25.7	44.4
	640-645	6.6	-	44.0
	660-665	6.6	26.3	42.8
	680-685	7.0	-	41.9
	700-705	7.2	-	47.9
	720-725	7.2	25.3	47.2
	740-745	7.3	25.5	41.2
	760-765	7.2	25.7	45.8
	780-785	7.8	-	45.3
	800-805	7.0	25.6	43.7
	820-825	7.6	24.2	40.7
	840-845	7.3	25.2	43.4
	860-865	7.5	-	44.1
	880-885	7.9	25.1	42.3
	900-905	7.2	-	39.9

APPENDIX B. (continued)

STATION/LOCATION WATER DEPTH	DEPTH (cm)	METHANE (µl/L)	SULFATE (mM)	% WATER
55 75-G-13	5-10	0.74	29.6	-
26°40.1'N	15-20	1.8	29.4	-
95°51.5'W	25-30	2.5	28.7	-
1372 meters	35-40	3.2	28.7	-
	45-50	3.8	28.8	-
	55-60	3.9	27.4	-
	65-70	4.8	27.2	-
	75-80	4.9	26.8	-
	85-90	5.3	26.1	-
	95-100	6.4	25.9	-
	105-110	6.5	26.6	-
	115-120	6.6	24.0	-
	125-130	6.9	26.0	-
	135-140	7.8	24.4	-
56 77-G-2	5-10	0.89	27.5	60.4
27°00.6'N	15-20	2.88	27.0	43.4
91°31.8'W	25-30	4.87	25.5	40.4
2153 meters	35-40	5.41	25.4	36.3
	45-50	6.72	23.1	66.8
	65-70	8.58	23.4	51.0
	85-90	10.1	21.1	44.5
	105-110	12.8	20.3	41.0
	125-130	14.9	20.6	40.5
	145-150	18.0	19.6	43.1
	165-170	20.0	17.1	38.8
57 77-G-2	5-10	0.54	27.6	52.3
26°57.5'N	15-20	1.91	27.6	60.9
92°03.0'W	25-30	2.36	26.0	46.4
2033 meters	35-40	2.79	25.7	61.3
	45-50	3.44	25.4	43.9
	65-70	4.03	25.0	50.1
	85-90	5.17	24.0	49.1
	105-110	5.61	23.9	42.5
	125-130	6.11	23.8	57.3
	145-150	6.13	23.6	51.2
	165-170	6.63	23.4	48.9

APPENDIX C. Interstitial Methane, Ethane, Propane, Sulfate, and Percent Water in Delta Sediments

STATION/LOCATION WATER DEPTH	DEPTH (cm)	METHANE (ml/L)	ETHANE (µl/L)	PROPANE (µl/L)	SULFATE (mM)	% WATER	$\delta^{13}C_{CH_4}$
58 76-G-10	0-5	-	-	-	19.7	54.3	-
28°50.38'N	40-45	0.57	0.082	nd*	13.6	49.7	-
89°23.42'W	60-65	0.68	0.15	nd	11.8	44.6	-54.0
60 meters	80-85	0.70	0.25	nd	5.4	47.3	-
	100-105	0.92	0.57	nd	3.0	47.4	-58.5
	120-125	4.26	1.09	nd	-	47.0	-62.7
	140-145	40.2	1.04	0.27	0.7	-	-80.5
*nd - not	160-165	63.3	1.73	0.37	0.1	46.0	-77.4
detected	180-185	65.7	3.01	1.51	nd	46.8	-
	200-205	65.9	2.70	0.69	nd	48.9	-81.9
	240-245	64.6	2.45	0.01	nd	47.9	-
	260-265	69.6	2.93	0.01	nd	44.6	-
	280-285	69.6	2.78	0.01	nd	39.3	-
	300-305	63.8	2.24	nd	nd	40.8	-76.1
	320-325	82.5	2.65	nd	nd	43.0	-
	340-345	68.3	2.16	0.01	nd	41.3	-
	380-385	77.3	2.61	nd	nd	38.9	-
	400-405	80.8	2.64	nd	nd	47.8	-74.7
	420-425	74.1	2.57	nd	nd	40.2	-
	440-445	83.7	2.83	0.01	nd	42.3	-
	460-465	69.9	2.66	0.01	nd	45.1	-
	500-505	75.5	2.80	nd	nd	36.6	-73.5
	520-525	76.9	2.55	nd	nd	40.2	-
	540-545	84.5	2.21	nd	nd	34.5	-
	580-585	93.4	3.19	0.01	nd	42.8	-
	600-605	76.7	2.54	nd	nd	36.2	-71.0

Bernie Boyd Bernard was born to Virgil William and Grace Legate Bernard on September 1, 1952 in Bryan, Texas. He attended public schools in Abilene, Texas and Austin, Texas and graduated from Austin's McCallum High School in May, 1970. He enrolled at Abilene Christian University in September, 1970 and graduated with a Bachelor of Science degree in chemistry in May, 1974. He enrolled in the graduate school of Texas A&M University in September 1974.

He currently resides with his wife, Laura, and two children, Rachael and Sara, at 3911 Glenn Oaks, Bryan, Texas.

The typist for this dissertation was Bernie B. Bernard.